A RELATION BETWEEN CREEP IN TENSION, CREEP IN BENDING AND TENSION TESTS

by
W. N. Findley and J. J. Poczatek

A Research Project of the
DEPARTMENT OF THEORETICAL AND APPLIED MECHANICS
UNIVERSITY OF ILLINOIS

ed by
ORDNANCE CORPS
)F THE ARMY
)-401, Project No. TB4-721

Illinois
1953

A RELATION BETWEEN CREEP IN TENSION, CREEP IN BENDING AND TENSION TESTS

by

W. N. Findley and J. J. Poczatek

A Research Project of the
DEPARTMENT OF THEORETICAL AND APPLIED MECHANICS
UNIVERSITY OF ILLINOIS

Sponsored by
PICATINNY ARSENAL, ORDNANCE CORPS
DEPARTMENT OF THE ARMY
Contract No. DA-11-022-ORD-401, Project No. TB4-721

Urbana, Illinois
August, 1953

INTERIM REPORT NO. 1

on a research project entitled
STUDY OF RELATIONSHIP BETWEEN
TIME SENSITIVE MECHANICAL
PROPERTIES OF PLASTICS

Project Supervisor, W. N. Findley

A RELATION BETWEEN CREEP IN TENSION, CREEP IN BENDING AND TENSION TESTS

W. N. Findley
Research Associate Professor

J. J. Poczatek
Research Assistant
(Now with International Harvester)

DEPARTMENT OF THEORETICAL AND APPLIED MECHANICS
UNIVERSITY OF ILLINOIS

Summary

A method of predicting creep in bending from data on creep in tension has been derived and applied to creep of a canvas laminate. Both creep deflections and stress distribution were derived. The deflections compared favorably with test data. It was shown that the stress distribution remained constant during creep in bending when creep in tension and compression were equal and the coefficient of the time-dependent term was equal to the time-independent term. Methods of determining creep deflections of beams having non-uniform bending moments are described.

Conclusions

The form of creep equation employed seems adequate to describe the tension creep of a grade-C canvas laminate. The close agreement between creep in bending predicted by this equation and actual data lends support to the possible usefulness of the equation. Further evidence is provided by the agreement between the stress-strain curve derived from the same creep equation and actual test data.

DISTRIBUTION LIST

INTERIM AND FINAL REPORTS

Contract No. DA-11-022-ORD-401 Project No. TB4-721

Commanding Officer
Attn: Technical Division (2)
R and D Contract Section
Picatinny Arsenal
Dover, New Jersey

Commanding Officer
Attn: Library
Picatinny Arsenal
Dover, New Jersey

Chicago Ordnance District
Attn: R and D Branch
209 West Jackson Boulevard
Chicago 6, Illinois

Chief of Ordnance
Attn: ORDTB (10)
Department of the Army
Washington 25, D. C.

Chief of Ordnance
Attn: ORDTX-AR
Department of the Army
Washington 25, D. C.

Chief of Ordnance
Attn: ORDTA
Department of the Army
Washington 25, D. C.

Chief of Ordnance
Attn: ORDTR
Department of the Army
Washington 25, D. C.

Chief of Ordnance
Attn: ORDTS
Department of the Army
Washington 25, D. C.

Chief of Ordnance
Attn: ORDTT
Department of the Army
Washington 25, D. C.

Chief of Ordnance
Attn: ORDTU
Department of the Army
Washington 25, D. C.

Chief of Ordnance
Attn: ORDIX (2)
Department of the Army
Washington 25, D. C.

Chief of Ordnance
Attn: ORDFX (2)
Department of the Army
Washington 25, D. C.

Department of the Navy
Office of Naval Research
Attn: Code 423
Washington 25, D. C.

Department of the Navy
Bureau of Aeronautics
Airborne Equipment Division
Materials Branch
Washington 25, D. C.

Signal Corps Engineering Laboratory
Squier Signal Laboratory
Materials Section
Attn: Mr. Luis Reiss
Fort Monmouth, New Jersey

Chemical Corps
Attn: Mr. T. P. Steinmetz
Technical Command
Army Chemical Center, Md.

Commanding General
U. S. Air Force (2)
Air Material Command
Engineering Division
Materials Laboratory
Attn: Mr. Robert T. Schwartz, WCRTS
Mr. Peterson, WCRTE
Wright-Patterson Air Base, Ohio

Department of the Navy
Attn: Mr. H. A. Perry
Naval Ordnance Laboratory
8050 Georgia Avenue
Silver Springs, Maryland

Director of Naval Research
Attn: Technical Information Officer
Washington 25, D.C.

Department of the Navy
Bureau of Ships (2)
Research and Development
Material Development Division
Attn: Mr. J. B. Alfors, Code 346
Mr. J. G. Kuenzel, Code 345
Washington 25, D. C.

Department of the Navy
Attn: Code Re 1
Bureau of Ordnance
Research and Development Division
Materials and Handling Branch
Washington 25, D. C.

Engineer Center
Engineer Research and Development
Laboratories
Attn: Mr. Philip Mitton
Materials Branch
Fort Belvoir, Virginia

Office of the Quartermaster General
Research and Development Division
Attn: Dr. Warren Stubblebine
Chemical and Plastics Section
Washington, D. C.

Department of Commerce
Attn: Mr. Frank W. Reinhart
National Bureau of Standards
Romm 4022, Industrial Building
Washington 25, D. C.

Department of the Navy
Attn: Mr. M. N. DeNeale
Naval Gun Factory
Metallurgical and Testing Branch
M and 8th Streets, S. E.
Washington 25, D. C.

Office of Ordnance Research
Box CM
Duke Station
Durham, North Carolina

Commanding Officer
Attn: Technical Division (2)
Detroit Arsenal
28251 Van Dyke
Centerline, Michigan

Commanding Officer
Attn: Technical Division (2)
Aberdeen Proving Ground, Md.

Commanding Officer
Attn: Technical Division
White Sands Proving Ground
Las Cruces, New Mexico

Commanding Officer
Attn: Technical Division
Redstone Arsenal
Huntsville, Alabama

Commanding Officer
Attn: Technical Division (2)
Frankford Arsenal
Bridesburgh Station
Philadelphia 37, Pennsylvania

Commanding Officer
Attn: Technical Division
Picatinny Arsenal
Dover, New Jersey

Commanding Officer
Attn: Technical Division
Rock Island Arsenal
Rock Island, Illinois

Commanding Officer
Attn: Technical Division
Springfield Armory
Springfield 1, Massachusetts

Commanding Officer
Attn: Technical Division
Watertown Arsenal
Watertown 72, Massachusetts

Commanding Officer
Attn: Technical Division
Watervliet Arsenal
Watervliet, New York

Acknowledgment

This project is conducted in the Department of Theoretical and Applied Mechanics as part of the work of the Engineering Experiment Station of the University of Illinois, in cooperation with Picatinny Arsenal, Ordnance Corps, Department of the Army.

The authors are grateful to P. N. Mathur, H. G. Russel, and E. J. Scott for checking the work and to W. A. Hagemeyer and G. E. Milum for preparing the illustrations.

STATUS OF THE PROBLEM

Tensile Creep

Numerous attempts have been made to express creep behavior by a mathematical expression either emperically or theoretically. Many investigators have assumed the time dependence of creep at constant load to be a linear function of time (1-4)[+] and have examined the rate of creep as a function of stress and temperature - usually only stress has been considered. Some of the types of equations which have been employed to describe the relationship between creep rate v and stress σ are as follows:

$$v = B\sigma \text{ (viscous)} \qquad \text{Eq. 1}$$

$$v = B\sigma^{a} \text{ (power)} \qquad \text{Eq. 2}$$

$$v = A'e^{B\sigma} \text{ or } \ln v = A + B\sigma \qquad \text{Eq. 3}$$
(exponential or logarithmic)

$$v = B \sinh \frac{\sigma}{\sigma_o} \text{ (hyperbolic sine)} \qquad \text{Eq. 4}$$

where a, A, A', B, and σ_o are constants.

Of these equations, the hyperbolic sine, Eq. 4, has been shown to have fundamental significance in terms of molecular behavior (5). It should be noted that Eqs. 1 and 3 are approximations of Eq. 4 if $\frac{\sigma}{\sigma_o}$ is either small or large respectively.

Other investigators (6-14) observing that creep was usually not a linear function of time, expressed the strain, ε, versus time, t, relation non-linearly by equations, such as the following:

$$\varepsilon = C + D \ln t + Et \qquad \text{Eq. 5}$$

See references (7, 8)

$$\varepsilon = C + D(1-e^{-bt}) + Et \qquad \text{Eq. 6}$$

See reference (14)

$$\varepsilon = \varepsilon_o + mt^{n} \qquad \text{Eq. 7}$$

See references (6, 9, 11-13)

[+] Numbers in parentheses refer to the list of references appended to this paper.

where b and n are constants and C, D, E, ε_o, and m are functions of stress.

When the coefficients ε_o and m in Eq. 7 are expressed as hyperbolic sine functions of stress, Eq. 7 becomes (13, 15):

$$\varepsilon = \varepsilon_o \sinh \frac{\sigma}{\sigma_\varepsilon} + m' t^n \left[\sinh \frac{\sigma}{\sigma_m} \right] \qquad \text{Eq. 8}$$

where ε_o', m', σ_ε, σ_m, and n are constants. From Eq. 8 the creep rate v, as obtained by differentiation, is:

$$v = m' n t^{n-1} \sinh \frac{\sigma}{\sigma_m} \qquad \text{Eq. 9}$$

and is a function of time rather than a constant as often assumed.

Bending Creep

The first analysis of creep in bending was reported by McCullough (16) in 1933. The results of his tests of lead beams were in reasonable agreement with the deflections calculated from observed minimum creep rates in tension and compression. Linearity of strain with distance from the neutral axis was demonstrated, that is, plane sections remained plane even during creep.

Tapsell and Johnson (2) also demonstrated for lead beams that the strain remained a linear function of distance from the neutral axis. It followed from this observation and was shown by the data that the strain-time curves at every position (fiber) of the beam have a similar shape.

Creep of beams of aluminum and polystyrene plastic were investigated by Marin and Zwissler (17) and Marin and Cuff (18). The observed minimum creep rates in bending were compared with bending creep rates computed from tension creep tests assuming a linear dependence of creep on time and a power relation between creep rate and stress. The theory did not permit computation of deflection. Both the tension and bending creep curves

depart considerably from the assumed linear dependence on time. In a discussion Findley (18) presented data on creep of polystyrene which indicated that the power function of stress was not satisfactory for small stresses.

Creep of an imaginary copper beam was examined by Popov (19) using several creep rate vs. stress relations. His examination indicated that the stress distribution in a beam changed with time and tended toward a steady-state distribution of a non-linear shape. An approximate summation procedure was employed to calculate the stress distribution. Deflections were calculated on an assumption of a linear variation of strain with time. Deflections were also calculated using a creep equation of the type of Eq. 7 with a linear function of stress for ε_o and an exponential function of stress for m. No experimental verification was reported, however.

In a paper by Marin, Pao, and Cuff (4), a method was described for calculating bending creep rates and deflections in a beam of material for which the creep behavior is different in tension and compression. The results were compared with data on creep of Lucite and Plexiglas. Again a linear time function was assumed which was not a close approximation to the observed behavior. Different power functions of stress were employed to describe the elastic strains and creep strains. In the analysis the elastic and creep strains were treated separately. The analysis predicted a different stress distribution and position of the neutral axis for the elastic component of strains than for the creep (time dependent) component of strains in the beam. Since these two stress distributions must exist simultaneously it does not seem possible for them to be different.

In a paper which had just become available at the time this manuscript was prepared, Pao and Marin (14) presented another analysis for bending

creep of Plexiglas in which a complex equation for creep of the form of Eq. 6 was employed. This equation did not describe the initial part of the creep curves much more closely than a linear equation. Identical creep relations in tension and compression were assumed although the authors previous data on Plexiglas showed this to be untrue. The analysis permits the stress distribution to vary with time but neglects the resulting changes in elastic strains. Other simplifications were found necessary in order to solve the problem. The resulting equation predicted a constant creep rate after about 1000 hours which did not agree with the data, which were presented to 11,000 hours, in which the creep rate decreased continuously. The paper also described methods for determining creep deflections of beams in which the bending moment varied along the beam.

DERIVATION FOR BENDING WITH EQUAL CREEP IN TENSION AND COMPRESSION AND EQUAL TIME DEPENDENT AND INDEPENDENT CONSTANTS

In previous studies (9, 11, 15) the creep curves obtained from a canvas laminate tested at different constant stresses were found to be closely described by an equation of the form

$$\varepsilon = \varepsilon_o + mt^n = (\varepsilon_o' + m't^n) \sinh \frac{\sigma}{\sigma_o} \qquad \text{Eq. 10}$$

where the symbols are the same as described above. This relation has been shown (9) to be related to the activation energy theory of creep. It has also been shown previously (15) that an equation for the stress-strain curve obtained from a constant strain rate tension test could be derived from Eq. 10 and that the resulting equation was in close agreement with the experimental data.

Fortunately, bending creep data were also obtained for material of identical composition made by the same manufacturer at about the same time. These data were obtained by Marin (20). While Marin also obtained tension creep curves on this material which agreed in general with the tension creep curves in reference (9), they did not have sufficient self consistency to permit evaluating the constants in Eq. 10.

Dr. Marin in a private communcation provided compression creep curves of a canvas laminate which show a greater creep for a given stress than the tension creep data. However, the instantaneous strains were also 50 percent greater, whereas the stress-strain curves of this material in tension and compression were nearly the same for the stresses involved in the creep tests (12). In view of this observation, the following derivation has been prepared on the assumption that creep in tension and compression was identical for the canvas laminate.

Eq. 10 accurately represents the creep data under conditions of constant stress. It probably does not, however, accurately describe creep under varying stress. Thus, if the stress distribution in the beam changed during creep, as described by Popov (19), some inaccuracy might be introduced by the use of this equation unless the material obeys the time-hardening law (21), which is probably not the case.

To determine the bending creep relation the conditions of equilibrium and geometry must be satisfied. From the geometry of a beam in pure bending, or one in which the distortion due to shear is negligible, the following well-known geometrical relation applies:

$$\varepsilon = \frac{y}{\rho} \qquad \text{Eq. 11}$$

where ε is the strain at a distance y measured perpendicularly from the neutral axis and ρ is the radius of curvature of the centroidal axis. This

relation is equivalent to assuming that plane sections remain plane - a fact which has been demonstrated for plastically bent beams by Nadai (22) and for creep of lead beams by MacCullough (16). Also, consideration of compatability of strains in the different "fibers" of a beam of great length, bent by a constant bending moment into the arc of a circle, suggests that plane sections must remain plane at all points along the beam which are remote from the ends.

The conditions of equilibrium for a beam are expressed by the following equations when the accelerations involved in the creep are so small as to be negligible - which is usually the case:

$$\int_{c-h}^{c} \sigma y(dA) = M \qquad \text{Eq. 12}$$

$$\int_{c-h}^{c} \sigma(dA) = 0 \qquad \text{Eq. 13}$$

where A is the cross-sectional area of the beam, h is the depth of the beam, and c is the distance from the neutral axis to the tension face of the beam.

Substituting Eq. 11 for ε in Eq. 10 and solving for the stress σ the following is obtained:

$$\sigma = \sigma_o \sinh^{-1}\left[\frac{y}{\rho(\varepsilon_o' + m't^n)}\right] = \sigma_o \sinh^{-1}(Ny) \qquad \text{Eq. 14}$$

where the symbol

$$N = \frac{1}{\rho(\varepsilon_o' + m't^n)} \qquad \text{Eq. 15}$$

has been introduced.

For a beam of rectangular cross-section of width b, $(dA) = b(dy)$, in Eq. 12 and 13. Making this substitution and introducing Eq. 14 for σ in Eq. 13, the following results:

$$b\int_{c-h}^{c} \sigma(dy) = b\sigma_o \int_{c-h}^{c} \sinh^{-1}(Ny)(dy) \qquad \text{Eq. 16}$$

Upon integration, assuming identical creep relations for tension and compression, Eq. 16 shows that $c = \frac{h}{2}$, i.e., the neutral axis is at the center of the beam and does not change position with time under load.

Making the same substitutions in Eq. 12 and changing the limits in accordance with the previous paragraph yields:

$$M = b\int_{-c}^{c} \sigma y(dy) = b\sigma_o \int_{-c}^{c} y \sinh^{-1}(Ny)\,(dy) \qquad \text{Eq. 17}$$

After integrating and rearranging terms this becomes

$$\frac{2M}{\sigma_o bc^2} = (Nc)^{-2}\left\{\left[2(Nc)^2 + 1\right] \sinh^{-1}(Nc) - (Nc)\sqrt{1+(Nc)^2}\right\} \qquad \text{Eq. 18}$$

which for convenience in computations may be written

$$\frac{2M}{\sigma_o bc^2} = \frac{2\theta \operatorname{Cosh} 2\theta - \operatorname{Sinh} 2\theta}{\operatorname{Cosh} 2\theta - 1}$$

where $\theta = \operatorname{Sinh}^{-1} Nc$.

Eq. 18 shows that the bending moment M is a function of N for a beam of given size and material. Thus, for a constant bending moment M, N must be a constant. Hence, from Eq. 15 it is observed that the curvature $\frac{1}{\rho}$ of the beam under a constant bending moment varies with time in accordance

with the same time function as strain varies in a tension creep test. That is,

$$\frac{1}{\rho} = N(\varepsilon_o' + m't^n) \qquad \text{Eq. 19}$$

In this equation N is the function of bending moment, M, given by Eq. 18. The most convenient way of determining N from Eq. 18 is by means of a diagram of $\frac{2M}{\sigma_o bc^2}$ versus Nc, which is easily constructed from the second form of Eq. 18 as shown in Fig. 1.

From Eq. 14 the stress distribution

$$y = \frac{1}{N} \sinh \frac{\sigma}{\sigma_o} \qquad \text{Eq. 20}$$

is obtained. Since N is a function of the bending moment, size and material of the beam and independent of time (according to Eq. 18), it follows that the stress distribution does not change with time during creep under a constant bending moment.

APPLICATION TO CREEP OF CANVAS LAMINATE IN PURE BENDING

Deflections

Numerical values of the constants in Eq. 10 which were determined from tension creep data (9) are as follows:

$$\varepsilon_o' = m' = 0.001875 \text{ in per in.}$$

$$n = 0.1183$$

$$\sigma_o = 4000 \text{ psi.}$$

The values differ from the values determined for this laminate in a previous study (15) in which m' was 0.0029 and σ was 5230. The agreement between the tension creep test data and Eq. 10 using the present constants is shown in Fig. 2

The agreement is excellent except for the highest stresses of 5700 and 6650 psi. Since the specimen at the latter stress fractured at 550 hours, it is possible that the fracturing mechanism may have influenced the creep results at the highest stress. It is also always possible that specimens may have been slightly overstrained during loading, although great care was exercised in this respect. It has been shown (23) that such overstraining alters the shape of the creep curve. The short horizontal lines at the left border of Fig. 2 indicate the first test points for each test.

To calculate the deflection-time curves for a beam of the dimensions employed by Marin (20), values of N were determined from Fig. 1, corresponding to the desired bending moments. These values were substituted into Eq. 19 together with the values of the constants given above and the curvature $\frac{1}{\rho}$ was determined for various values of time t. Then the deflection ω at midspan of a beam of length ℓ subjected to a uniform bending moment was calculated for each curvature from the well known geometrical relation

$$\omega = \frac{\ell^2}{8\rho} \qquad \text{Eq. 21}$$

The resulting theoretical bending creep curves are shown in Fig. 3 together with the experimental data reported by Marin (20) for a grade C canvas laminate. In Fig. 3 the solid lines show the bending creep predicted by Eq. 19 using the constants employed in computing the solid lines shown in Fig. 2. The black dots in Fig. 3 represent the creep that would have been predicted by using the constants previously employed to fit Eq. 10 to the data of Fig. 2.

The short horizontal lines at the left border of Fig. 3 indicate the deflection predicted at zero time if the load could have been applied instantaneously without shock.

The agreement between the theory given by the solid lines of Fig. 3 and experimental data is reasonably good. Some of the discrepancies which do exist may be explained as follows: For the curve at a bending moment of 624 lb.-in. the experimental data indicate a constant deflection between 200 and 900 hours. Since curves for higher and lower moments showed a continuously increasing deflection, it seems likely that experimental difficulties, such as the sticking of a dial, may have been responsible for the constant deflection.

The divergence in the early part of the test at a bending moment of 767 lb.-in. may have been caused by overstraining during load application. This possible explanation seems to be supported by the fact that the difference between experimental and theoretical data at this load decreases as the time increases. This trend is in accord with the observations of Everett (23) and MacCullough (16) on the effect of overstraining while loading.

The experimental data for bending moments of 917 lb.-in. and 932 lb.-in. show a difference that seems too large for the small change in bending moment. There is no way of knowing which of the two curves is more nearly correct.

Stresses

The stress distribution in the beam under a bending moment of 679 lb.-in. was computed from Eq. 20 and is shown in Fig. 4. The maximum stresses in the beams were also computed for the several beams for which data are reported in Fig. 3. These stresses, in order of increasing bending moments, were 4920, 5640, 6060, 6740, 7940, 8,000 psi. respectively. It was observed that the two highest stresses are very near the stress in the tension test,

Fig. 5, at which the strain increased rapidly with small increases in stress. This may account in part for the large difference between the creep of the two beams having the highest loads, see Fig. 3.

RELATION TO TENSION TEST OF CANVAS LAMINATE

In a prior paper (15) an equation for the stress-strain relation in a tension test was derived from a creep equation of the form of Eq. 10. The resulting stress-strain equation was:

$$\varepsilon = \varepsilon_o \sinh \frac{\sigma}{\sigma_o} \left[1 + \left(\frac{\varepsilon_o n}{\dot{\varepsilon} t_o} \sinh \frac{\sigma}{\sigma_o} \right)^{\frac{n}{1-n}} \right] \qquad \text{Eq. 22}$$

where $\dot{\varepsilon}$ is the strain rate.

Excellent agreement was found between the stress-strain curve computed from the creep data for the canvas laminate used in the above study and the data from a tension test. Since the constants in the creep equation as employed in the present analysis differ from those used in the previous paper, the stress-strain relation has been recomputed from Eq. 22 using the new constants. The theoretical and experimental curves are compared in Fig. 5. The agreement is close but not as satisfactory as for the previous set of constants (15).

NON-UNIFORM BENDING MOMENT

If the bending moment M in the beam varies with distance x along the beam, then M may be expressed in terms of x as $M = f(x)$. Hence from Eq. 18 N is a function of x, $N = g(x)$. If in Eq. 19 $g(x)$ is substituted for N and

$$\frac{1}{\rho} = \frac{\frac{d^2\omega}{dx^2}}{\left[1 + \left(\frac{d\omega}{dx}\right)^2\right]^{\frac{3}{2}}} \simeq \frac{d^2\omega}{dx^2} \text{ (for small deflections)} \qquad \text{Eq. 23}$$

is substituted for the curvature the differential equation

$$\frac{d^2\omega}{dx^2} = g(x)\ (\varepsilon_o' + m't^n) \qquad \text{Eq. 24}$$

is obtained which may be solved for the deflection of the beam.

Example 1. Let $g(x) = Qx$ where Q is a constant. This corresponds to a beam having a bending moment M which varies with distance x according to the equation obtained from Eq. 18 by substituting Qx for N. The shape of this bending moment diagram is the same as the curve shown in Fig. 1 since the ordinate is proportional to the bending moment and the abscissa is proportional to x. Within the range of Nc shown, Fig. 1 has approximately the shape bending moment diagram which would be produced in a cantilever beam loaded with its own weight and having an upward force at the free end. At a given time t_1 the deflection of the beam may be determined in a manner identical to that employed for elastic beams. From Eq. 24

$$\frac{d^2\omega}{dx^2} = Qx(\varepsilon_o' + m't_1^n) = QT\,x \qquad \text{Eq. 25}$$

where $T = \varepsilon_o' + m't_1^n$

Integrating once

$$\frac{d\omega}{dx} = QT\frac{x^2}{2} + C$$

If the beam is rigidly clamped at x = L, then

$$\frac{d\omega}{dx} = 0$$

at x = L

and $C = -QT\frac{L^2}{2}$

Integrating again

$$\omega = QT\frac{x^3}{6} - QT\frac{L^2}{2}x + C_1$$

But $\omega = 0$ at $x = L$ so $C_1 = \frac{QTL^3}{3}$, hence, $\omega = QT\frac{x^3}{6} - QTL^2\frac{x}{2} + \frac{QTL^3}{3}$ which is the deflection curve of the beam for small deflections. At $x = 0$ the deflection ω is

$$\omega = \frac{QTL^3}{3} = \frac{QL^3}{3}(\varepsilon_o' + m't_1^n) \qquad \text{Eq. 26}$$

When the bending moment varies with distance x then the stress distribution will vary also with x in accordance with the expression obtained by substituting g(x) for N in Eq. 20.

$$y = \frac{1}{g(x)} \sinh \frac{\sigma}{\sigma_o} \qquad \text{Eq. 27}$$

Example 2. Eq. 18 usually cannot be solved for N as an explicit function of x. Thus, Eq. 24 cannot usually be evaluated by integration. A somewhat different approach is described below:

Consider a cantilever beam of length L subjected to a concentrated load P at the end. Let the depth be 2c, and the beam width b. Measuring distance x along the beam from the free end, the bending moment M is

$$M = Px \qquad \text{Eq. 28}$$

Differentiating with respect to x

$$dM = Pdx \qquad \text{Eq. 29}$$

Eq. 14 may be written for the stress σ_1 in the extreme "fiber" as

$$Nc = \sinh \frac{\sigma_1}{\sigma_o} = \sinh S \qquad \text{Eq. 30}$$

where $S = \frac{\sigma_1}{\sigma_o}$, and S is a function of x since N is a function of x. Eq. 18 can be rewritten as follows by substituting Eq. 30 and cancelling terms

$$M = \frac{\sigma_o bc^2}{2}\left[S(2 + \operatorname{csch}^2 S) - \coth S\right] \qquad \text{Eq. 31}$$

Substituting for M from Eq. 28 and differentiating, the following is obtained

$$dx = \frac{\sigma_o bc^2}{P} \left[\coth^2 S - S \coth S \operatorname{csch}^2 S \right] dS \qquad \text{Eq. 32}$$

From Eq. 10 and 11, the following may be written for the extreme fiber

$$\frac{1}{\rho} = \frac{\varepsilon_1}{c} = \frac{(\varepsilon_o' + m't^n) \sinh S}{c} \qquad \text{Eq. 33}$$

After eliminating $\frac{1}{\rho}$ between Eq. 23 and 33, the following integral can be formed in terms of S and x

$$\frac{d\omega}{dx} = \int \frac{(\varepsilon_o' + m't^n) \sinh S}{c} dx \qquad \text{Eq. 34}$$

Substituting dx from Eq. 32 into Eq. 34 and integrating, an equation for the slope, $\frac{d\omega}{dx}$, of the beam is obtained

$$\frac{d\omega}{dx} = \frac{\sigma_o bc}{P} (\varepsilon_o' + m't^n)(\cosh S + S \operatorname{csch} S + C_1) \qquad \text{Eq. 35}$$

where C_1 is a constant to be determined from boundary conditions.

The deflection, ω, of the beam may be found by multiplying Eq. 35 by dx, substituting for dx from Eq. 32 and forming the integral. After expanding and collecting terms, the expression becomes

$$\omega = \frac{\sigma_o^2 b^2 c^3}{P^2} (\varepsilon_o' + m't^n) \int (\coth^2 S \cosh S - S^2 \coth S \operatorname{csch}^3 S + C_1 \coth^2 S - C_1 S \coth S \operatorname{csch}^2 S) dS \qquad \text{Eq. 36}$$

The indicated integration may be evaluated with the following result

$$\omega = \frac{\sigma_o^2 b^2 c^3}{P^2}(\varepsilon_o' + m't^n)\left[\sinh S + \frac{S^2}{3\sinh^3 S} + \frac{S\cosh S}{3\sinh^2 S}\right.$$

$$- \frac{2}{3\sinh S} + \frac{S}{3} + \frac{1}{3}\sum_{p=1,2\ldots}^{r} \frac{(-1)^p\, 2\,(2^{2p-1}-1)}{(2p-1)!} B_p S^{2p-1}$$

$$\left. + C_1\left(S - \frac{1}{2}\frac{\cosh S}{\sinh S} + \frac{S}{2\sinh^2 S}\right) + C_2\right] \qquad \text{Eq. 37}$$

where $S = \frac{\sigma_1}{\sigma_o}$, σ_1 is the stress on the extreme fiber of the beam at the position for which the deflection ω is to be determined, B_p are Bernoulli numbers, and C_1 and C_2 are constants to be determined from boundary conditions. The series appearing in Eq. 37 converges for $S^2 < \pi$.

For the cantilever beam of length L the slope is zero at x = L. Thus from Eq. 35

$$C_1 = -\cosh S_L - S\,\mathrm{csch}\, S_L \qquad \text{Eq. 38}$$

where S_L is the value of S at the position x = L. The value of S_L may be determined from Eq. 31 by substituting PL for M and solving for S_L by trial, in a numerical example.

Since the deflection of the cantilever beam is zero at x = L, the value of C_2 may be determined from Eq. 37 by setting $\omega = 0$ and S equal the same value S_L as above.

To obtain the deflection ω_x at location x along the beam, substitute the bending moment Px for M in Eq. 31 and solve for the corresponding value of S, S_x, by trial. Substitute S_x in Eq. 37 together with C_1 and C_2 and compute the deflection ω_x.

It can be shown by application of L'Hospital's rule to Eq. 31 that S = 0 when M = Px = 0. Thus the deflection, ω_o, of the free end of the beam may be obtained by substituting S = 0 in Eq. 37

$$\omega_o = \frac{\sigma_o^2 b^2 c^3}{P^2} (\varepsilon_o' + m't^n) C_2 \qquad \text{Eq. 39}$$

The above solutions are valid only when $S^2 < \pi$ as noted above.

For values of $|S|$ greater than about 5 the hyperbolic functions may be approximated by exponential functions to obtain a solution. Eq. 31 then becomes approximately

$$M = \frac{\sigma_o b c^2}{2} (2S - 1) \qquad \text{Eq. 40}$$

Differentiating and substituting Eq. 29

$$dM = Pdx = \sigma_o b c^2 dS \qquad \text{Eq. 41}$$

Substituting Eq. 41 into Eq. 34 and integrating; the equation for slope of the beam is obtained

$$\frac{d\omega}{dx} = \frac{\sigma_o bc}{2P} (\varepsilon_o' + m't^n)(e^S + C_1) \qquad \text{Eq. 42}$$

The deflection equation is obtained by substituting for dx from Eq. 41 into Eq. 42 and integrating

$$\omega = \frac{\sigma_o^2 b^2 c^3}{2P^2} (\varepsilon_o' + m't^n)(e^S + C_1 S + C_2) \qquad \text{Eq. 43}$$

where the symbols are the same as before.

This solution also involves determining S as a function of x through Eq. 28 and 40. The above expression will be a good approximation to Eq. 37 when the value of S is greater than 5 throughout most of the depth of the beam and throughout most of the length of the beam. Inaccuracies will always be found in the vicinity of the neutral axis and in a region near zero bending moment as at the end of the cantilever beam.

EFFECT OF LIMITING VALUES OF THE CREEP CONSTANTS

Examination of Eq. 10 shows that as n approaches unity the creep curve approaches nearer to a linear curve (constant creep rate) which is the behavior expected from a purely viscous material. Also as σ_o becomes large so that $\frac{\sigma}{\sigma_o}$ is small, the stress function becomes nearer a linear relation. This again is what would be expected from viscous behavior.

As n becomes smaller the resulting creep curve tends to rise sharply and then level off to an apparently constant value - which is not actually constant. For small values of σ_o, such that $\frac{\sigma}{\sigma_o}$ is large, the hyperbolic sine term may be replaced by an exponential one.

It should be pointed out that erroneous results are obtained by substituting $\frac{\sigma}{\sigma_o}$ for $\sinh \frac{\sigma}{\sigma_o}$ in the expressions calculated for bending creep, Eq. 14 and 18. This does not indicate an error in the equations but simply indicates that the simplifying assumption for small stresses cannot be utilized in equations which include a difference of two terms of like magnitude, as the error in making the simplification may be larger than the value of the difference of the two terms.

REFERENCES

1. R. W. Bailey, "Utilization of Creep Test Data in Engineering Design", Inst. of Mechanical Engineers, Vol. 131, 1935, p. 131.

2. H. J. Tapsell and A. E. Johnson, "An Investigation of the Nature of Creep Under Stresses Produced by Pure Flexure", Inst. of Metals Journal, Vol. 57, Aug. 1935.

3. C. C. Davenport, "Correlation of Creep and Relaxation Properties of Copper", ASME Trans., Vol. 60, 1938, p. A-55.

4. J. Marin, Y. H. Pao, and G. E. Cuff, "Creep Properties of Lucite and Plexiglas for Tension, Compression, Bending, and Torsion", Trans. ASME, Vol. 73, 1951, p. 705-719.

5. W. Kauzmann, "Flow of Solid Metals from the Standpoint of the Chemical Rate Theory", Trans. American Inst. of Mining and Metallurgical Engineering, Institute of Metals Division, Vol. 143, 1941, p. 57.

6. R. G. Sturm, C. Dumont, and F. M. Howell, "A Method of Analyzing Creep Data", Journal of Applied Mechanics, Vol. 3, No. 2, June 1936, p. A62.

7. H. Leaderman, "Creep, Elastic Hysteresis, and Damping in Bakelite under Torsion", Journal of Applied Mechanics, Vol. 61, June 1939, p. A79.

8. D. Telfair, T. S. Carswell, and H. K. Nason, "Creep Properties of Molded Phenolic Plastics", Modern Plastics, Vol. 21, p. 137, Feb., 1944

9. W. N. Findley, "Creep Characteristics of Plastics", 1944 Symposium on Plastics, ASTM, 1944, p. 18.

10. E. P. Popov, "Correlation of Tension Creep Tests with Relaxation Tests", Journal of Applied Mechanics, Vol. 69, June 1947, p. A135.

11. W. N. Findley, C. H. Adams, and W. J. Worley, "The Effect of the Creep of Two Laminated Plastics as Interpreted by the Hyperbolic - Sine Law and Activation Energy Theory", Proceedings, ASTM, Vol. 48, 1948, p. 1217.

12. W. N. Findley and W. J. Worley, "Mechanical Properties of Five Laminated Plastics", NACA, Tech. Note 1560, August 1948.

13. W. J. Worley and W. N. Findley, "The Effect of Temperature on the Creep and Recovery of a Melamine-Glass Fabric Laminate", Proceedings, ASTM, Vol. 50, 1950.

14. Y. Pao and J. Marin, "Deflections and Stresses in Beams Subjected to Bending and Creep", Applied Mech. Division, ASME Paper No. 52-APM-34, Presented June 1952.

15. W. N. Findley, "Derivation of a Stress-Strain Equation from Creep Data for Plastics", Proc. First U. S. National Congress of Applied Mechanics, June 11-16, 1951, p. 595.

16. G. H. MacCullough, "An Experimental and Analytical Investigation of Creep in Bending", Trans. ASME, Vol. 55, 1933, p. APM 55-9-55.

17. J. Marin and L. E. Zwissler, "Creep of Aluminum Subjected to Bending at Normal Temperatures", Proc. ASTM, Vol. 40, 1940, p. 937.

18. J. Marin and G. Cuff, "Creep-Time Relations for Polystyrene under Tension, Bending, and Torsion", Proceedings ASTM, Vol. 49, 1949, p. 1158-1174.

19. E. P. Popov, "Bending of Beams with Creep", Jour. of App. Physics, Vol. 20, 1949, p. 251-256.

20. J. Marin, "Static and Dynamic Creep Properties of Laminated Plastics for Various Types of Stress", NACA, Tech. Note 1105, Feb. 1947.

21. I. Roberts,"Prediction of Relaxation of Metals from Creep Data", Proceedings ASTM, Vol. 51, 1951, p. 811.

22. A. Nadai, "Plasticity", The McGraw Hill Book Co., Inc., 1935, p. 121.

23. F. L. Everett, "Strength of Materials Subjected to Shear at High Temperatures", Trans. ASME, Vol. 53, 1931, p. 126.

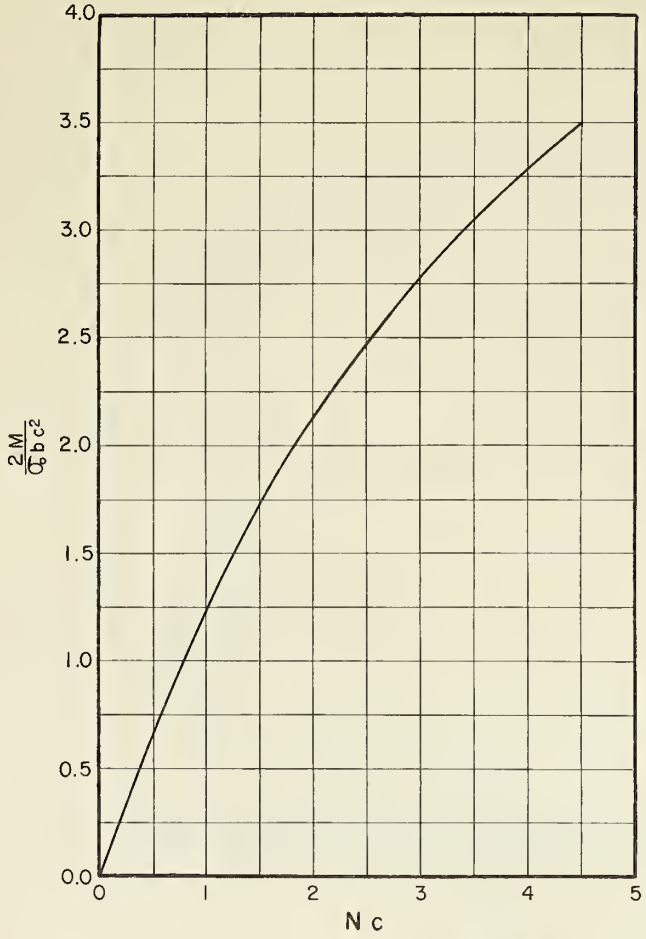

FIG. 1 Nc vs. $\frac{2M}{\sigma_0 b c^2}$, FROM EQUATION 18

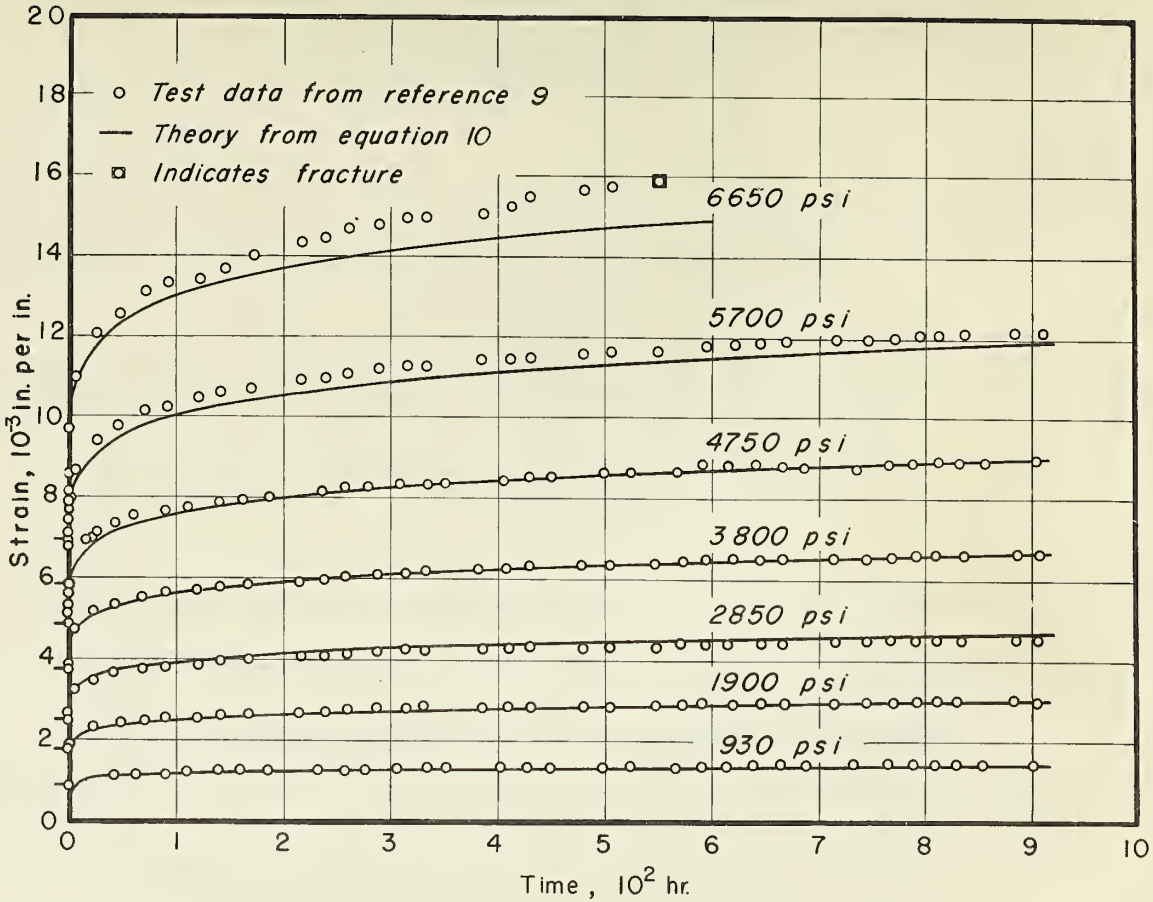

FIG. 2 CREEP TESTS IN TENSION AT DIFFERENT STRESSES FOR GRADE-C CANVAS LAMINATE TESTED AT 77°F.

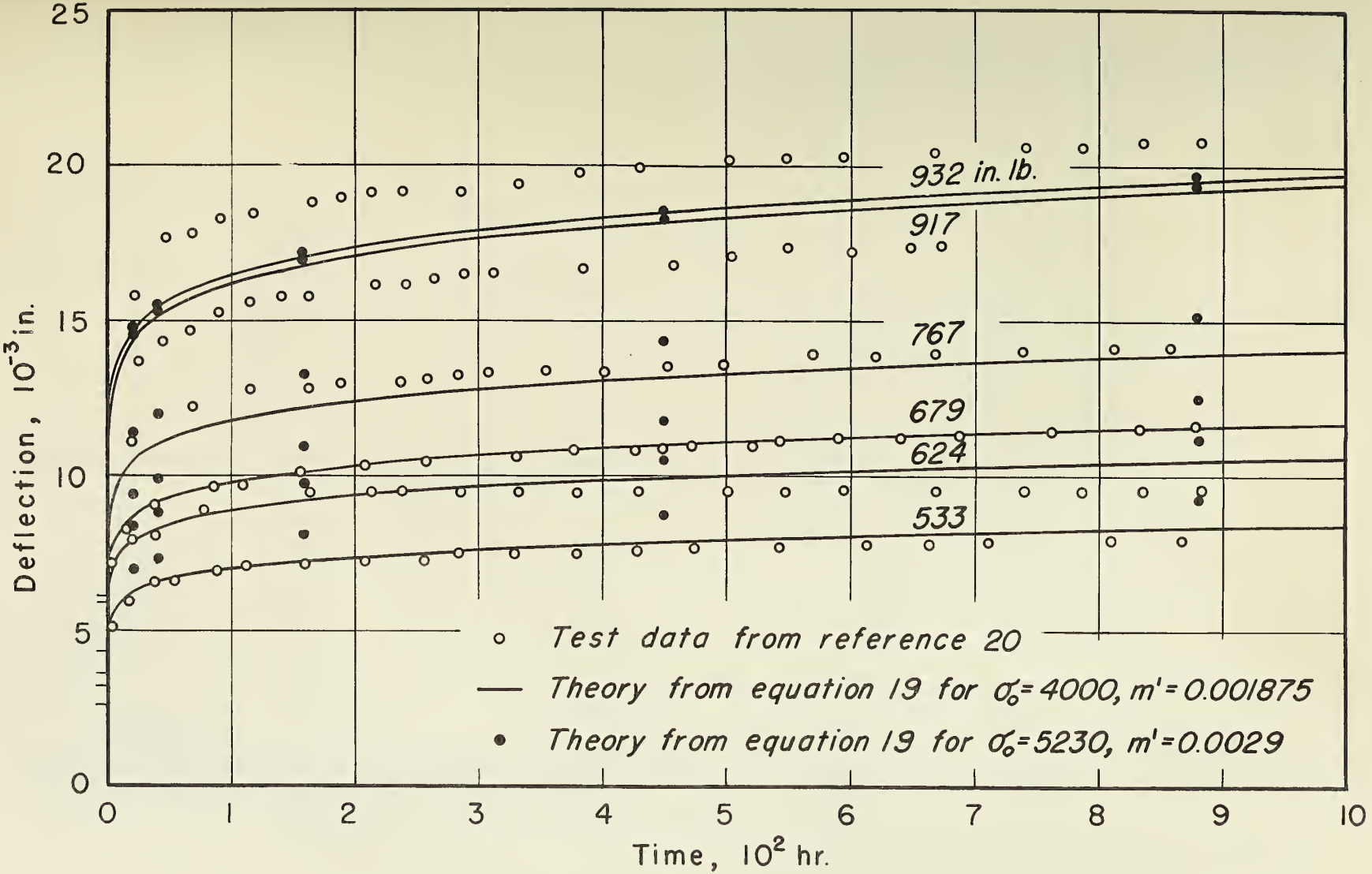

FIG. 3 CREEP TESTS IN BENDING AT DIFFERENT BENDING MOMENTS FOR GRADE-C CANVAS LAMINATE TESTED AT 77° F.

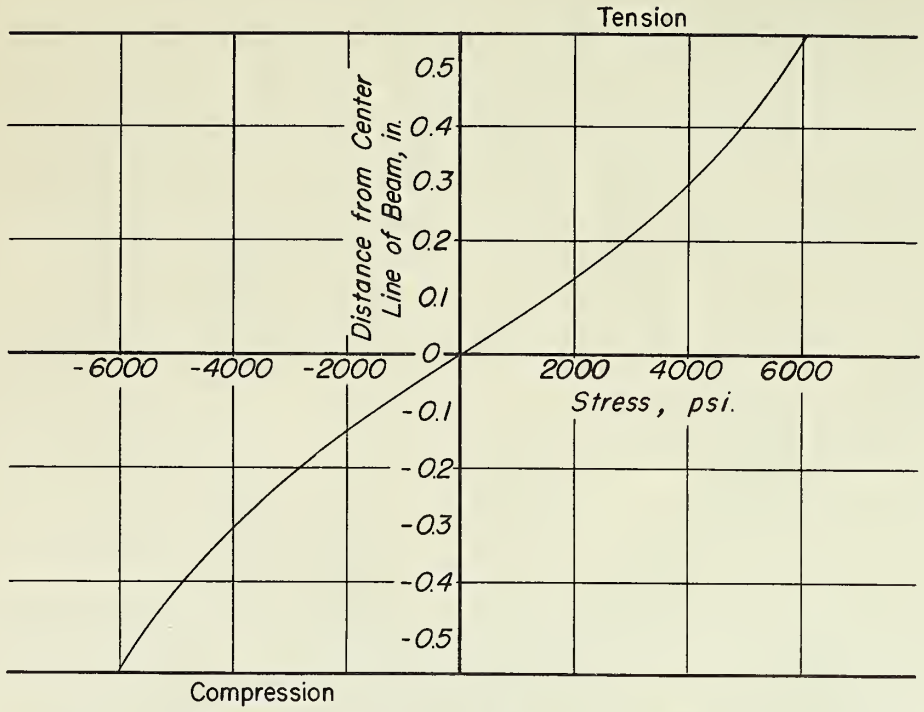

FIG. 4 STRESS DISTRIBUTION IN BEAM DURING CREEP, FOR GRADE C-CANVAS LAMINATE (BENDING MOMENT 679 IN-LB)

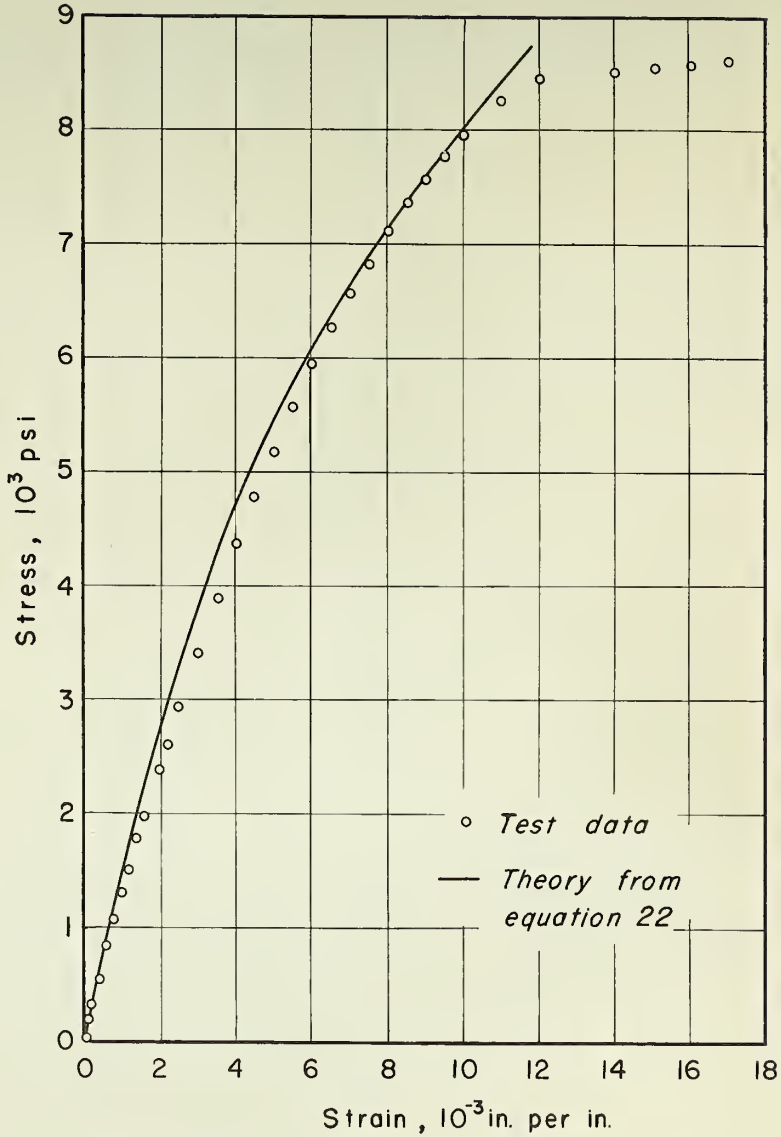

FIG. 5 STATIC STRESS-STRAIN CURVES FOR GRADE-C CANVAS LAMINATE AT 77°F.

PRELIMINARY CONSIDERATION OF LINEAR AND NONLINEAR MECHANICAL MODELS FOR CREEP OF PLASTICS

by
E. J. Scott and W. N. Findley

A Research Project of the
DEPARTMENT OF THEORETICAL AND APPLIED MECHANICS
UNIVERSITY OF ILLINOIS

Sponsored by
PICATINNY ARSENAL, ORDNANCE CORPS
DEPARTMENT OF THE ARMY

Interim Report No. 2
on
The Relationship Between Time Sensitive
Mechanical Properties of Plastics
Contract No. DA-11-022-ORD-401, Project No. TB4-721

Urbana, Illinois
January, 1954

Interim Report No. 2
on a research project entitled
Study of Relationships Between
Time Sensitive Mechanical
Properties of Plastics

Project Supervisor, W. N. Findley

PRELIMINARY CONSIDERATION ON LINEAR AND NONLINEAR MECHANICAL MODELS FOR CREEP OF PLASTICS

E. J. Scott
Associate Professor of Applied
Mechanics, Kansas State College
(formerly University of Illinois

W. N. Findley
Research Associate Professor of
Theoretical and Applied Mechanics
University of Illinois

Department of Theoretical and Applied Mechanics
University of Illinois

SUMMARY

A preliminary analysis is presented for three four-element models: (a) linear Maxwell and Voigt units in series with two masses, (b) two nonlinear Maxwell units in parallel, coupled by a mass, and (e) nonlinear Maxwell and Voigt units in series with two masses.

The equations of motion were derived in each case and the solutions of the resulting differential equations were indicated. Complete solutions for particular problems have not been included.

CONCLUSIONS

The solution of mathematical expressions describing the behavior of mechanical models composed of nonlinear elements is possible, although involved. Since these models may describe the behavior of plastics more closely than models composed of linear elements they may permit more accurate prediction of the time sensitive behavior of plastics under different loading conditions. Hence, further study of such models seems warranted and a comparison of the predicted behaviors with actual material performance is desirable.

DISTRIBUTION LIST

INTERIM AND FINAL REPORTS

Contract No. DA-11-022-ORD-401 Project No. TB4-721

Commanding Officer
Attn: Technical Division (2)
R and D Contract Section
Picatinny Arsenal
Dover, New Jersey

Commanding Officer
Attn: Library
Picatinny Arsenal
Dover, New Jersey

Chicago Ordnance District
Attn: R and D Branch
209 West Jackson Boulevard
Chicago 6, Illinois

Chief of Ordnance
Attn: ORDTB (10)
Department of the Army
Washington 25, D. C.

Chief of Ordnance
Attn: ORDTX-AR
Department of the Army
Washington 25, D. C.

Chief of Ordnance
Attn: ORDTA
Department of the Army
Washington 25, D. C.

Chief of Ordnance
Attn: ORDTR
Department of the Army
Washington 25, D. C.

Chief of Ordnance
Attn: ORDTS
Department of the Army
Washington 25, D. C.

Chief of Ordnance
Attn: ORDTT
Department of the Army
Washington 25, D. C.

Chief of Ordnance
Attn: ORDTU
Department of the Army
Washington 25, D. C.

Chief of Ordnance
Attn: ORDIX (2)
Department of the Army
Washington 25, D. C.

Chief of Ordnance
Attn: ORDFX (2)
Department of the Army
Washington 25, D. C.

Department of the Navy
Office of Naval Research
Attn: Code 423
Washington 25, D. C.

Department of the Navy
Bureau of Aeronautics
Airborne Equipment Division
Materials Branch
Washington 25, D. C.

Signal Corps Engineering Laboratory
Squier Signal Laboratory
Materials Section
Attn: Mr. Luis Reiss
Fort Monmouth, New Jersey

Chemical Corps
Attn: Mr. T. P. Steinmetz
Technical Command
Army Chemical Center, Md.

Commanding General
U. S. Air Force (2)
Air Material Command
Engineering Division
Materials Laboratory
Attn: Mr. Robert T. Schwartz, WCRTS
Mr. Peterson, WCRTE
Wright-Patterson Air Base, Ohio

Department of the Navy
Attn: Mr. H. A. Perry
Naval Ordnance Laboratory
8050 Georgia Avenue
Silver Springs, Maryland

Director of Naval Research
Attn: Technical Information Officer
Washington 25, D.C.

Department of the Navy
Bureau of Ships (2)
Research and Development
Material Development Division
Attn: Mr. J. B. Alfors, Code 346
Mr. J. G. Kuenzel, Code 345
Washington 25, D. C.

Department of the Navy
Attn: Code Re 1
Bureau of Ordnance
Research and Development Division
Materials and Handling Branch
Washington 25, D. C.

Engineer Center
Engineer Research and Development
Laboratories
Attn: Mr. Philip Mitton
Materials Branch
Fort Belvoir, Virginia

Office of the Quartermaster General
Research and Development Division
Attn: Dr. Warren Stubblebine
Chemical and Plastics Section
Washington, D. C.

Department of Commerce
Attn: Mr. Frank W. Reinhart
National Bureau of Standards
Romm 4022, Industrial Building
Washington 25, D. C.

Department of the Navy
Attn: Mr. M. N. DeNeale
Naval Gun Factory
Metallurgical and Testing Branch
M and 8th Streets, S. E.
Washington 25, D. C.

Office of Ordnance Research
Box CM
Duke Station
Durham, North Carolina

Commanding Officer
Attn: Technical Division (2)
Detroit Arsenal
28251 Van Dyke
Centerline, Michigan

Commanding Officer
Attn: Technical Division (2)
Aberdeen Proving Ground, Md.

Commanding Officer
Attn: Technical Division
White Sands Proving Ground
Las Cruces, New Mexico

Commanding Officer
Attn: Technical Division
Redstone Arsenal
Huntsville, Alabama

Commanding Officer
Attn: Technical Division (2)
Frankford Arsenal
Bridesburgh Station
Philadelphia 37, Pennsylvania

Commanding Officer
Attn: Technical Division
Picatinny Arsenal
Dover, New Jersey

Commanding Officer
Attn: Technical Division
Rock Island Arsenal
Rock Island, Illinois

Commanding Officer
Attn: Technical Division
Springfield Armory
Springfield 1, Massachusetts

Commanding Officer
Attn: Technical Division
Watertown Arsenal
Watertown 72, Massachusetts

Commanding Officer
Attn: Technical Division
Watervliet Arsenal
Watervliet, New York

Aerojet Engineering Corp.
Azusa, California
Attn: Dr. Paul J. Blatz

Allegany Ballistics Lab.
Cumberland, Maryland
Attn: Mr. Harry Winnerling

Naval Ordnance Test Station
Code 4021
Inyokern, China Lake, Calif.
Attn: Mr. D. D. Ordahl

Naval Powder Factory
Indian Head, Maryland
Attn: Mr. A. S. Johnson

Thiokol Corp., Redstone Div.
Huntsville, Alabama
Attn: Mr. W. I. Dale, Jr.

Chief Superintendent
C.A.R.D.E. N-8-3-5
P.O. Box 1427
Quebec, Que, Canada
Attn: Mr. I. R. Cameron

ACKNOWLEDGMENT

This project was conducted in the Department of Theoretical and Applied Mechanics as a part of the work of the Engineering Experiment Station of the University of Illinois, in cooperation with Picatinny Arsenal, Ordnance Corps, Department of the Army.

The authors wish to acknowledge the helpful suggestions of Professor W. J. Worley.

Various types of mechanical models have been proposed in the past for describing the time-sensitive behavior of material. These have been composed of various combinations of linear springs and linear dash pots, that is, viscous elements whose resistance is proportional to the velocity of separation imposed on the dash pot. Recently nonlinear dash pots were studied.

These models admittedly do not in any way represent the actual construction of molecular materials. In fact, models previously considered neglect the mass of the material. The mechanical behavior of these models, however, can be made to approximate some of the observed behavior of polymers and in fact analysis of these models has permitted prediction of mechanical behavior of polymers. The use of these models consisting of elastic and viscous elements has led to the description of a class of material having characteristics describable by these models as "visco - elastic" materials.

It has been found difficult to accurately describe behavior of many materials by a single element composed of a small number of units. So a large number of elements identical in form but having different constants has often been postulated. This has the effect of making possible a distribution of "relaxation times".

It may be that the multiplicity of linear elements may be replaceable by a single non-linear element. For this reason the following studies have been undertaken.

In the present report a preliminary analysis is presented for three four-element models: (a) linear Maxwell and Voigt units in series with two masses, (b) two non-linear Maxwell

units in parallel, coupled by a mass, and (c) non-linear Maxwell and Voigt units in series with two masses.

Linear Maxwell and Voigt Units in Series with Two Masses

A model consisting of a Maxwell unit (spring and dashpot in series) and a Voigt unit (spring and dashpot in parallel) in series with a mass m at either end of the Voigt unit is diagrammed in Fig. 1. This type model is particularly interesting since it predicts in a general way not only creep but recovery on removal of load.

In this section the differential equations of motion of this model are derived and solved for the case of linear springs, k, and dashpots, c. Two forcing functions F(t) of practical interest are considered.

From the free body diagrams of three portions of the model. the following equations of motion may be written:

$$k_1 X_1(t) = c_1\left[\dot{X}_2(t) - \dot{X}_1(t)\right] , \tag{1}$$

$$m_1\ddot{X}_2(t) = k_2\left[X_3(t) - X_2(t)\right] + c_2\left[\dot{X}_3(t) - \dot{X}_2(t)\right] - c_1\left[\dot{X}_2(t) - \dot{X}_1(t)\right] , \tag{2}$$

$$m_2\ddot{X}_3(t) = F(t) - k_2\left[X_3(t) - X_2(t)\right] - c_2\left[\dot{X}_3(t) - \dot{X}_2(t)\right] \tag{3}$$

Solving equation (1) for $X_1(t)$ in terms of $\dot{X}_2(t)$, we obtain

$$X_1(t = e^{-\frac{k_1}{c_1}t}\int_o^t e^{\frac{k_1}{c_1}\tau}\dot{X}_2(\tau)d\tau . \tag{4}$$

Also, using integration by parts, we have

$$\int_o^t e^{\frac{k_1}{c_1}\tau}\dot{X}_2(\tau)d\tau = X_2(t)e^{\frac{k_1}{c_1}t} - X_2(0) - \frac{k_1}{c_1}\int_o^t e^{\frac{k_1}{c_1}\tau} X_2(\tau)d\tau. \tag{5}$$

Therefore, from (4) and (5)

$$X_1(t) = X_2(t) - e^{-\frac{k_1}{c_1}t} X_2(0) - \frac{k_1}{c_1} e^{-\frac{k_1}{c_1}t} \int_0^t e^{\frac{k_1}{c_1}\tau} X_2(\tau)d\tau. \quad (6)$$

Now, from (1) and (6), we have

$$\dot{X}_2(t) - \dot{X}_1(t) = \frac{k_1}{c_1} X_1(t) = \frac{k_1}{c_1} X_2(t) - \frac{k_1}{c_1} e^{-\frac{k_1}{c_1}t} X_2(0)$$

$$- \frac{k_1^2}{c_1^2} \int_0^t e^{-\frac{k_1}{c_1}(t - \tau)} X_2(\tau)d\tau. \quad (7)$$

Substituting this result in (2), we get

$$m_1\ddot{X}_2 = k_2(X_3 - X_2) + c_2(\dot{X}_3 - \dot{X}_2) - k_1X_2 + k_1e^{-\frac{k_1}{c_1}t} X_2(0)$$

$$+ \frac{k_1^2}{c_1} \int_0^t e^{-\frac{k_1}{c_1}(t - \tau)} X_2(\tau)d\tau. \quad (8)$$

We now make use of the Laplace transform method. To that end, let $L\left\{X_1(t)\right\} = x_1(p)$, $L\left\{X_2(t)\right\} = x_2(p)$ and $L\left\{F(t)\right\} = f(p)$. Then the Laplace transforms of (8) and (3) are

$$m_1\left[p^2x_2(p) - pX_2(0) - \dot{X}_2(0)\right] = k_2\left[x_3(p) - x_2(p)\right]$$

$$+ c_2\left[p\,x_3(p) - X_3(0) - px_2(p) + X_2(0)\right] - k_1x_2(p)$$

$$+ \frac{k_1X_2(0)}{p + \frac{k_1}{c_1}} + \frac{k_1^2}{c_1} \frac{x_2(p)}{p + \frac{k_1}{c_1}}, \quad (9)$$

and

$$m_2\left[p^2x_3(p) - pX_3(0) - \dot{X}_3(0)\right] = f(p) - k_2\left[x_3(p) - x_2(p)\right] - c_2\left[px_3(p) - X_3(0) - px_2(p) + X_2(0)\right]. \quad (10)$$

Rearranging the terms of equations (9) and (10), we have

$$\left[m_1p^2 + c_2p + (k_1 + k_2) - \frac{k_1^2}{c_1}\frac{1}{p + \frac{k_1}{c_1}}\right] x_2(p) - (c_2p + k_2)x_3(p) = m_1pX_2(0) + m_1\dot{X}_2(0) - c_2X_3(0) + c_2X_2(0) + \frac{k_1X_2(0)}{p + \frac{k_1}{c_1}}, \quad (11)$$

$$-(c_2p + k_2)x_2(p) + \left[m_2p^2 + c_2p + k_2\right] x_3(p) = m_2pX_3(0) + m_2\dot{X}_3(0) + c_2X_3(0) - c_2X_2(0) + f(p). \quad (12)$$

Equation (12) when solved for $x_3(p)$ yields the result

$$x_3(p) = \frac{(c_2p + k_2)x_2(p)}{m_2p^2 + c_2p + k_2} + \frac{m_2pX_3(0) + m_2\dot{X}_3(0) + c_2X_3(0) - c_2X_2(0) + f(p)}{m_2p^2 + c_2p + k_2} \quad (13)$$

This result when substituted in (11) and simplified gives:

$$x_2(p) = \frac{(c_1p + k_1)(c_2p + k_2)(m_2pX_3(0) + m_2\dot{X}_3(0) - c_2X_2(0) + f(p))}{pD(p)} + \frac{(c_1p + k_1)(m_2p^2 + c_2p + k_2)(m_1pX_2(0) + m_1\dot{X}_2(0) - c_2X_3(0) + c_2X_2(0))}{pD(p)} + \frac{c_1k_1X_2(0)(m_2p^2 + c_2p + k_2)}{pD(p)}, \quad (14)$$

where

$$D(p) = \Big[c_1m_1m_2p^4 + (m_1m_2k_1 + c_1c_2m_2 + c_1c_2m_1)p^3$$

$$+ (m_2k_1c_1 + m_2k_1c_2 + m_2c_1k_2 + m_1k_1c_2 + m_1c_1k_2)p^2$$

$$+ (k_1k_2m_2 + k_1c_1c_2 + m_1k_1k_2)p + c_1k_1k_2\Big] . \qquad (15)$$

Substituting this result in (13), we have

$$x_3(p) = \frac{(c_1p+k_1)(c_2p+k_2)^2(m_2pX_3(0)+m_2\dot{X}_3(0)+c_2X_3(0)-c_2X_2(0)+f(p))}{p(m_2p^2 + c_2p + k_2)D(p)}$$

$$+ \frac{(c_1p+k_1)(c_2p+k_2)(m_1pX_2(0)+m_1\dot{X}_2(0)-c_2X_3(0)+c_2X_2(0))}{pD(p)}$$

$$+ \frac{c_1k_1X_2(0)(c_2p+k_2)}{pD(p)} + \frac{m_2pX_3(0)+m_2\dot{X}_3(0)+c_2X_3(0)-c_2X_2(0)+f(p)}{m_2p^2 + c_2p + k_2} \qquad (16)$$

Making use of the Complex Inversion Integral we find that

$$X_2(t) =$$

$$\frac{1}{2\pi i}\int_{c-i\infty}^{c+i\infty} \frac{(c_1p+k_1)(c_2p+k_2)(m_2pX_3(0)+m_2\dot{X}_3(0)+c_2X_3(0)-c_2X_2(0)+f(p))}{pD(p)} e^{pt}\, dp$$

$$+ \frac{1}{2\pi i}\int_{c-i\infty}^{c+i\infty} \frac{(c_1p+k_1)(m_2p^2+c_2p+k_2)(m_1pX_2(0)+m_1\dot{X}_2(0)-c_2X_3(0)+c_2X_2(0))}{pD(p)} e^{pt}dp$$

$$+ \frac{1}{2\pi i}\int_{c-i\infty}^{c+i\infty} \frac{c_1k_1X_2(0)(m_2p^2+c_2p+k_2)}{pD(p)} e^{pt}\, dp, \qquad (17)$$

$$X_3(t) =$$

$$\frac{1}{2\pi i}\int_{c-i\infty}^{c+i\infty} \frac{(c_1p+k_1)(c_2p+k_2)^2(m_2pX_3(0)+m_2\dot{X}_3(0)+c_2X_3(0)-c_2X_2(0)+f(p))}{p(m_2p^2+c_2p+k_2)D(p)} e^{pt}dp$$

$$+\frac{1}{2\pi i}\int_{c-i\infty}^{c+i\infty} \frac{(c_1p+k_1)(c_2p+k_2)(m_1pX_2(0)+m_1\dot{X}_2(0)-c_2X_3(0)+c_2X_2(0))}{pD(p)} e^{pt}\,dp$$

$$+\frac{1}{2\pi i}\int_{c-i\infty}^{c+i\infty} \frac{c_1k_1X_2(0)(c_2p+k_2)}{pD(p)} e^{pt}\,dp$$

$$+\frac{1}{2\pi i}\int_{c-i\infty}^{c+i\infty} \frac{m_2pX_3(0)+m_2\dot{X}_3(0)+c_2X_3(0)-c_2X_2(0)+f(p)}{m_2p^2+c_2p+k_2} e^{pt}\,dp \qquad (18)$$

The form of the solution will depend on the function $f(p)$ and on the nature of the roots of $D(p) = 0$ and $m_2p^2 + c_2p + k_2 = 0$. Once these are known the residues of the above integrands may be computed at those roots which are the poles of the integrands.

The nature of the roots of $D(p) = 0$ can be determined by studying its discriminant which is

$$\Delta = I^3 - 27J^2, \qquad (19)$$

where

$$I = c_1^2m_1m_2k_1k_2 - \frac{(m_1m_2k_1+c_1c_2m_2+c_1c_2m_1)(k_1k_2m_2+k_1c_1c_2+m_1k_1k_2)}{4}$$

$$+ \frac{(m_2k_1c_1 + m_2k_1c_2 + m_2c_1k_2 + m_1k_1c_2 + m_1c_1k_2)^2}{12}, \qquad (20)$$

and

$$J = \frac{c_1^2 m_1 m_2 k_1 k_2}{6}(m_2k_1c_1+m_2k_1c_2+m_2c_1k_2+m_1k_1c_2+m_1c_1k_2)$$

$$+ \frac{1}{48}(m_1m_2k_1+c_1c_2m_2+c_1c_2m_1)(k_1k_2m_2+k_1c_1c_2+m_1k_1k_2)(m_2k_1c_1+m_2k_1c_2$$

$$+ m_2c_1k_2 + m_1k_1c_2+m_1c_1k_2) - \frac{1}{16}c_1m_1m_2(k_1k_2m_2+k_1c_1c_2+m_1k_1k_2)^2$$

$$- \frac{1}{216}(m_2k_1c_1+m_2k_1c_2+m_2c_1k_2+m_1k_1c_2+m_1c_1k_2)^3$$

$$- \frac{c_1k_1k_2}{16}(m_1m_2k_1+c_1c_2m_2+c_1c_2m_1)^2. \qquad (21)$$

We now have the following cases:

(1) If two roots are equal $\Delta = 0$,

(2) If $\Delta < 0$, two roots are real and two imaginary

(3) If $\Delta > 0$, the roots are all real or all imaginary.

In order to apply this solution to creep, $F(t)$ is made equal to a constant F_o for $t > 0$ and $X_3(t)$ is determined. Values of the constants m_1, m_2, e_1, e_2, k, and k_2 must be selected to fit the characteristics of the material under consideration. Also the following initial conditions must obtain:

$$X_1(0) = X_2(0) = X_3(0) = F_o/k_1 \text{ and } \dot{X}_2(0) = \dot{X}_3(0) = 0 \qquad (22)$$

For stress relaxation $X_3(t)$ is made equal to a constant X_{30} for $t > 0$ and $F(t)$ is determined for the same values of the constants and the following initial conditions: $X_1(0) = X_2(0) = X_{30}$, $F(0) = X_{30}k_1$, $\dot{X}_2(0) = 0$.

The solution has not yet been evaluated for a specific problem.

Two Non-linear Maxwell Units in Parallel, Coupled by a Mass

Figure 2 illustrates the model considered in this section. Models such as this composed of linear units have been used to describe creep behavior. A model of this type is also capable of representing recovery. This may be explained as follows. If the springs and dashpots have unequal constants, then the deflection of the two springs after a time interval under load will be unequal. Thus, when the load is released one spring will have a residual tension--the other a residual compression. These residual internal forces will operate on the dashpots so as to relieve these forces and in so doing will produce the motion of recovery.

As far as is known the non-linear model of Fig. 2 has not been considered. Since the behavior of plastics appears to be non-linear in character it may be that properly chosen non-linear elements will permit a more accurate description of the observed behavior and hence a more accurate prediction of behavior under other circumstances.

In a previous paper [1] a stress-strain equation was derived which was in good agreement with experimental data from a canvas laminate. The time-independent portion of this equation was a hyperbolic sine function. Hence, it seems reasonable to express the deflection X of the non-linear springs as hyperbolic sine functions of force f:

$$X_1 = b_1 \sinh f_1/a_1 \text{ for spring 1,} \tag{23}$$

$$X_2 = b_2 \sinh f_2/a_2 \text{ for spring 2.} \tag{24}$$

where a_1, a_2, b_1, b_2 are constants of the springs.

Also creep data on plastics have been found to be in accord with the stress dependence predicted by the activation energy theory of creep[2]. This stress dependence is a hyperbolic sine of stress. Thus it seems reasonable to express the velocity of flow, $\dot{X}_a - \dot{X}_b$, of the time sensitive elements of the model by hyperbolic sine functions of force, f:

$$\dot{X} - \dot{X}_1 = K_1 \sinh f_3/\beta_1 \text{ for dashpot 1} \tag{25}$$

$$\dot{X} - \dot{X}_2 = K_2 \sinh f_4/\beta_2 \text{ for dashpot 2,} \tag{26}$$

where K_1, K_2, β_1, β_2 are the constants of the dashpots.

By forming the inverse of equations (23-26) so as to solve for the forces, and applying these forces to free body diagrams of portions of the model the following equations of motion of the system are found:

$$\beta_1 \sinh^{-1}(\dot{X} - \dot{X}_1)/K_1 - a_1 \sinh^{-1} X_1/b_1 = 0 \tag{27}$$

$$\beta_2 \sinh^{-1}(\dot{X} - \dot{X}_2)/K_2 - a_2 \sinh^{-1} X_2/b_2 = 0 \tag{28}$$

$$F(t) - \beta_1 \sinh^{-1}(\dot{X} - \dot{X}_1)/K_1 - \beta_2 \sinh^{-1}(\dot{X}-\dot{X}_2)/K_2 = m\ddot{X} \tag{29}$$

These equations will be solved for the special case that the springs are linear, m = 0 and F(t) = F_o (a constant) i.e., for constant load creep. If the springs are linear Eq. (23) and (24) become

$$X_1 = b_1 f_1/a_1 = f_1/k_1 \tag{30}$$

$$X_2 = b_2 f_2/a_2 = f_2/k_2 \tag{31}$$

where $k_1 = a_1/b_1$, $k_2 = a_2/b_2$, Equations (27-29) may then be written

$$\beta_1 \sinh^{-1}(\dot{X} - \dot{X}_1)/K_1 - k_1 X_1 = 0 \tag{32}$$

$$\beta_2 \sinh^{-1}(\dot{X} - \dot{X}_2)/K_2 - k_2 X_2 = 0 \tag{33}$$

$$F_o - k_1 X_1 - k_2 X_2 = 0 \tag{34}$$

Inverting Eq. (32) and (33) and substituting Eq. (34) for X_2 Eq. (32) and (33) become

$$\dot{X} - \dot{X}_1 = K_1 \sinh k_1 X_1/\beta_1 \tag{35}$$

$$\dot{X} - \dot{X}_2 + K_2 \sinh (F_o - k_1 X_1)/\beta. \tag{36}$$

Differentiating Eq. (34) yields

$$k_1 \dot{X}_1 + k_2 \dot{X}_2 = 0 \tag{37}$$

Substituting Eq. (37) in Eq. (36) and eliminating $\dot{X}$ between Eq. (35) and (36) gives

$$\dot{X}_1 = \frac{K_2 k_2}{k_1+k_2} \sinh (F_o - k_1 X_1)/\beta_1 - \frac{K_1 k_2}{k_1+k_2} \sinh k_1 X_1/\beta_1 \tag{38}$$

Expanding the first hyperbolic sine in Eq. (38) and collecting terms

$$\dot{X}_1 = \frac{K_2 k_2}{k_1+k_2} \sinh F_o/\beta_1 \cosh k_1 X_1/\beta_1 - \frac{k_2}{k_1+k_2}(K_1 + K_2 \cosh F_o/\beta_1) \sinh k_1 X_1/\beta_1 \tag{39}$$

or

$$\dot{X}_1 = \mu_1 \cosh \alpha_1 X_1 + \mu_2 \sinh \alpha_1 X_1 \tag{40}$$

where [illegible] equations [illegible] may then be written

$$[illegible] \qquad (53)$$

$$[illegible] \qquad (54)$$

$$[illegible] = 0 \qquad (55)$$

[illegible] (53) and (54) and substituting [illegible] Eq. (56) and (57) [illegible]

$$[illegible] \qquad (56)$$

$$[illegible] \qquad (57)$$

Differentiating Eq. [illegible] yields

$$[illegible] = 0 \qquad (57)$$

Substituting Eq. (57) in Eq. (54) and eliminating X between Eq. (55) and (56) gives

$$[illegible] \qquad (58)$$

Expanding the third transcendental sine in Eq. (58) and collecting terms

$$[illegible] \qquad (59)$$

or

$$[illegible] \qquad (60)$$

where $\mu_1 = \frac{K_2 k_2}{k_1+k_2} \sinh F_o/\beta_1$, $\mu_2 = -\frac{k_2}{k_1+k_2}(K_1 + K_2 \cosh F_o/\beta_1)$,

and $\alpha_1 = k_1/\beta_1$.

In order to solve the non-linear equation, Eq. (40) the reversion method[3] may be employed. Then after solving Eq. (40), X_1 and $\dot{X}_1$ as functions of time may be substituted in Eq. (35) and X may be determined by integration.

The reversion method requires the series expansion of the functions on the right hand side of the equality sign of Eq. (40) as follows:

$$\mu_1 \cosh \alpha_1 X_1 = \mu_1\left(1 + \frac{\alpha_1^2 X_1^2}{2!} + \frac{\alpha_1^2 X_1^4}{4!} + \frac{\alpha_1^6 X_1^6}{6!} + \ldots\right)$$

and

$$\mu_2 \sinh \alpha_1 X_1 = \mu_2\left(\alpha_1 X_1 + \frac{\alpha_1^3 X_1^3}{3!} + \frac{\alpha_1^5 X_1^5}{5!} + \frac{\alpha_1^7 X_1^7}{7!} + \ldots\right).$$

Consequently substituting in Eq. (40) yields

$$\dot{X}_1 = \mu_1 + \mu_2\alpha_1 X_1 + \frac{\mu_1}{2!}\alpha_1^2 X_1^2 + \frac{\mu_2}{3!}\alpha_1^3 X_1^3 + \frac{\mu_1}{4!}\alpha_1^4 X_1^4 + \frac{\mu_2}{5!}\alpha_1^5 X_1^5$$

$$+ \frac{\mu_1}{6!}\alpha_1^6 X_1^6 + \frac{\mu_1}{6!}\alpha_1^6 X_1^6 + \frac{\mu_2}{7!}\alpha_1^7 X_1^7 + \ldots, \qquad (41)$$

or, for the purpose of the method at hand,

$$\left(\frac{d}{dt} - \mu_2\alpha_1\right)X_1 - \frac{\mu_1}{2!}\alpha_1^2 X_1^2 - \frac{\mu_2}{3!}\alpha_1^3 X_1^3 - \frac{\mu_1}{4!}\alpha_1^4 X_1^4 - \frac{\mu_2}{5!}\alpha_1^5 X_1^5 - \ldots = \mu_1 \qquad (42)$$

The reversion method obtains closer and closer approximations to the solution of the non-linear equation by solving the following series of linear equations

$$\left(\frac{d}{dt} - \mu_2\alpha_1\right)X_{11} = \mu_1, \qquad (43)$$

[illegible]

$$(\frac{d}{dt} - \mu_2\alpha_1)X_{12} = \frac{\mu_1}{2!}\alpha_1^2X_{11}^2, \tag{44}$$

$$(\frac{d}{dt} - \mu_2\alpha_1)X_{13} = \frac{\mu_1}{3!}\alpha_1^3X_{11}^3 + \mu_1\alpha_1^2X_{11}X_{12}, \tag{45}$$

$$(\frac{d}{dt} - \mu_2\alpha_1)X_{14} = \frac{\mu_1}{4!}\alpha_1^4X_{11}^4 + \frac{\mu_2}{2!}\alpha_1^3X_{11}^2X_{12} + \frac{\mu_1}{2!}\alpha_1^2(2X_{11}X_{13} + X_{12}^2),$$

etc. (46)

where the solution to Eq. (42) is given by

$$X_1(t) = X_{11}(t) + X_{12}(t) + X_{13}(t) + X_{14}(t) + \ldots \tag{47}$$

The work involved in this method is great so the present example will be carried on far enough so that the procedure is clear. Further approximations can be found by using additional formulas given in the reference[3].

The solution of Eq.(43) is

$$X_{11}(t) = c_1e^{\mu_2\alpha_1t} - \frac{\mu_1}{\mu_2\alpha_1}, \tag{48}$$

If the initial conditions are $X_1(0) = X_{11}(0) = 0.$, then $c_1 = \frac{\mu_1}{\mu_2\alpha_1}$ and therefore

$$X_{11}(t) = \mu_5(1 - e^{\mu_4t}), \tag{49}$$

where $\mu_4 = \mu_2\alpha_1$ and $\mu_5 = \mu_1/\mu_4$.

Equation (49) constitutes the <u>first</u> approximation to the solution of Eq. (40). The second approximation is obtained by solving the equation

$$(\frac{d}{dt} - \mu_4)X_{12}(t) = \frac{\mu_1\alpha_1^2}{2!}\mu_5^2(1 - e^{\mu_4t})^2, \tag{50}$$

which is obtained from equation (44). The solution of Eq. (50) is

$$X_{12}(t) = -\frac{\mu_1\alpha_1^2}{2!}\mu_5^2\left(\frac{1}{\mu_4} + 2te^{\mu_4 t} - \frac{1}{\mu_4}e^{2\mu_4 t}\right) + c_2 e^{\mu_4 t}.$$

If the initial condition is $X_{12}(0) = 0$, then $c_2 = 0$ so that

$$X_{12}(t) = -\frac{\mu_1\alpha_1^2}{2!}\mu_5^2\left(\frac{1}{\mu_4} + 2te^{\mu_4 t} - \frac{1}{\mu_4}e^{2\mu_4 t}\right). \tag{51}$$

Equation (51) constitutes the second approximation. Thus far, then

$$X_1(t) = X_{11}(t) + X_{12}(t)$$

$$= \mu_5(1 - e^{\mu_4 t}) - \frac{\mu_1\mu_5^2\alpha_1^2}{2!}\left(\frac{1}{\mu_4} + 2te^{\mu_4 t} - \frac{1}{\mu_4}e^{2\mu_4 t}\right) \tag{52}$$

From Eq. (45) the following is obtained by substituting Eq. (49) and (51)

$$\left(\frac{d}{dt} - \mu_4\right)X_{13}(t) = \frac{\mu_2\alpha_1^3}{3!}\mu_5^3(1 - e^{\mu_4 t})^3 - \frac{\mu_1^2\mu_5^2\alpha_1^4}{2!}(1 - e^{\mu_4 t})\left(\frac{1}{\mu_4} + 2te^{\mu_4 t} - \frac{1}{\mu_4}e^{2\mu_4 t}\right). \tag{53}$$

Multiplying through by $e^{-\mu_4 t}$ and collecting terms Eq. (53) becomes

$$\frac{d}{dt}\left(X_{13}e^{-\mu_4 t}\right) = \frac{\mu_2\alpha_1^3\mu_5^3}{3!}\left(e^{-\mu_4 t} - 3 + 3e^{\mu_4 t} - e^{2\mu_4 t}\right)$$

$$- \frac{\mu_1^2\mu_5^3\alpha_1^4}{2!\mu_4}\left[e^{-\mu_4 t} + (2\mu_4 t - 1) - (2\mu_4 t + 1)e^{\mu_4 t} + e^{2\mu_4 t}\right] \tag{54}$$

Integration of Eq. (54) results in

$$X_{13}(t)e^{-\mu_4 t} = \frac{\mu_2\alpha_1^3\mu_5^3}{3!}\left(-\frac{e^{-\mu_4 t}}{\mu_4} - 3t + \frac{3}{\mu_4}e^{\mu_4 t} - \frac{1}{2\mu_4}e^{2\mu_4 t}\right)$$
$$- \frac{\mu_1^2\mu_5^3\alpha_1^4}{2\mu_4}\left[-\frac{e^{-\mu_4 t}}{\mu_4} + \mu_4 t^2 - t - 2\mu_4\cdot\frac{e^{\mu_4 t}}{\mu_4^2}(\mu_4 t - 1)\right.$$
$$\left. - \frac{e^{\mu_4 t}}{\mu_4} + \frac{1}{\mu_4}e^{2\mu_4 t}\right] + c_3 \qquad (55)$$

If the initial condition $X_{13}(0) = 0$, then

$$c_3 = -\frac{\mu_1^2\mu_5^3\alpha_1^4}{2\mu_4^2} - \frac{\mu_2\alpha_1^3\mu_5^3}{4\mu_4}$$

Thus

$$X_{13}(t) = \frac{\mu_2\alpha_1^3\mu_5^3}{3!}\left(-\frac{3}{2}e^{\mu_4 t} - \frac{1}{\mu_4} - 3te^{\mu_4 t} + \frac{3}{\mu_4}e^{2\mu_4 t} - \frac{1}{2\mu_4}e^{3\mu_4 t}\right)$$
$$- \frac{\mu_1^2\mu_5^3\alpha_1^4}{2\mu_4}\left[+\frac{1}{\mu_4}e^{\mu_4 t} - \frac{1}{\mu_4} + \mu_4 t^2 e^{\mu_4 t} - te^{\mu_4 t}\right.$$
$$\left. - 2\frac{e^{2\mu_4 t}}{\mu_4}(\mu_4 t - 1) - \frac{e^{2\mu_4 t}}{\mu_4 t} + \frac{e^{3\mu_4 t}}{\mu_4}\right] \qquad (56)$$

Equation (56) constitutes the third approximation and the solution is now

$$X_1(t) = X_{11}(t) + X_{12}(t) + X_{13}(t) \qquad (57)$$

The process can be continued indefinitely. Although involved, the procedure is straightforward.

Referring now to Eq. (35), integration of this expression

with respect to t yields

$$X(t) = X_1(t) + K_1 \int_0^t \sinh \alpha_1 X_1 \, dt.$$

Now

$$\sinh \alpha_1 X_1 = \alpha_1 X_1 + \frac{\alpha_1^3 X_1^3}{3!} + \frac{\alpha_1^5 X_1^5}{5!} + \ldots .$$

$$= \alpha_1 (X_{11} + X_{12} + X_{13}) + \frac{\alpha_1^3}{3!}(X_{11}+X_{12}X_{13})^3$$

$$+ \frac{\alpha_1^5}{5!}(X_{11} + X_{12} + X_{13})^5 + \ldots . \qquad (58)$$

Suppose that only the first two terms of this expansion are retained. Then

$$X(t) = X_1(t)+K_1\alpha_1\int_0^t (X_{11}+X_{12}+X_{13})dt + K_1 \frac{\alpha_1^3}{3!}\int_0^t (X_{11}+X_{12}+X_{13})^3 dt \qquad (59)$$

The calculation is again tedious, but can be carried out by anyone acquainted with the calculus.

Equations 48 through 57 are given only as examples of the method. The boundary conditions employed, however, are not satisfactory as a solution of the problem of Fig. 3. Suitable initial conditions are $X_1(0) = X_{10}$, $X_2(0) = X_{20}$ and $X_{10} = X_{20}$ = the deflection which would occur in the springs as a result of F_o if the dash pots were rigid.

Non-linear Maxwell and Voigt Units in Series with Two Masses

The model considered in this section is shown in Fig. 3 and is of the same form as that discussed in the first section except that the elements of the model are non-linear. For the same reasons given in the previous section the non-linear behavior of the springs and dashpots will be assumed to be represented by hyperbolic sine functions as follows:

$$X_1 = b_1 \sinh f_1/a_1 \quad \text{for spring 1,} \tag{60}$$

$$X_2 = b_2 \sinh f_2/a_2 \quad \text{for spring 2,} \tag{61}$$

$$\dot{X}_2 - \dot{X}_1 = K_1 \sinh f_3/\beta_1 \quad \text{for dashpot 1,} \tag{62}$$

$$\dot{X}_3 - \dot{X}_2 = K_2 \sinh f_4/\beta_2 \quad \text{for dashpot 2,} \tag{63}$$

where b_1, b_2, a_1, a_2, are constants of the springs and K_1, K_2, β_1, β_2 are constants of the dashpots.

By forming the inverse of Eq. (60-63) the forces may be determined and used in forming the equations of motion as follows:

$$a_1 \sinh^{-1} X_1/b_1 - \beta_1 \sinh^{-1}(\dot{X}_2-\dot{X}_1)/K_1 = 0 \tag{64}$$

$$a_2 \sinh^{-1}(X_3-X_2)/b_2 + \beta_2 \sinh^{-1}(\dot{X}_3-\dot{X}_2)/K_2 - \beta_1 \sinh^{-1}(\dot{X}_2-\dot{X}_1)/K_1 = m_1\ddot{X}_2 \tag{65}$$

$$F(t) - a_2 \sinh^{-1}(X_3-X_2)/b_2 - \beta_2 \sinh^{-1}(\dot{X}_3-\dot{X}_2)/K_2 = M_2\ddot{X}_3 \tag{66}$$

Substituting Eq. (64) in (65) and (65) in (66) the following results:

$$F(t) = m_2\ddot{X}_3 + m_1\ddot{X}_2 + a_1 \sinh^{-1} X_1/b_1 \tag{67}$$

from which $X_1 = b_1 \sinh (F(t) - m_2\ddot{X}_3 - m_1\ddot{X}_2)/a_1$ (68)

Let $m_2 = m_1 = 0$, which amounts to assuming that the accelerations are small enough to be neglected. Then X_1 is known.

$$X_1 = b_1 \sinh F(t)/a_1 \tag{69}$$

Also $$\dot{X}_1 = \dot{F}(t)\frac{b_1}{a_1} \cosh F(t)/a. \tag{70}$$

Substituting Eq. (65) in (66):

$$F(t) = m_2\ddot{X}_3 + m_1\ddot{X}_2 + \beta_1 \sinh^{-1}(\dot{X}_2 - \dot{X}_1)/K_1 \tag{71}$$

Then substituting $\dot{X}_1$ from Eq. (66) and setting $m_2 = m_1 = 0$

$$F(t) = \beta_1 \sinh^{-1}(\dot{X}_2 - \dot{F}(t)\frac{b_1}{a_1} \cosh F(t)/a_1)/K_1 \tag{72}$$

or $$\dot{X}_2 = K_1 \sinh \frac{F(t)}{\beta_1} + \dot{F}(t)\frac{b_1}{a_1} \cosh \frac{F(t)}{a_1}.$$

Then X_2 can be determined as a function of $F(t)$

$$X_2 = K_1\int_o^t \sinh \frac{F(t)}{\beta_1}\, dt + \frac{b_1}{a_1}\int_o^t \dot{F}(t) \cosh \frac{F(t)}{a_1}\, dt \tag{73}$$

Substituting $\dot{X}_2$ and X_2 in Eq. (66):

$$F(t) = a_2 \sinh^{-1}(X_3 - \int_o^t \left[K_1 \sinh \frac{F(t)}{\beta_1} + \dot{F}(t)\frac{b_1}{a_1} \cosh \frac{F(t)}{a_1}\right] dt)/b_1$$

$$+ \beta_2 \sinh^{-1}(\dot{X}_3 - K_1 \sinh \frac{F(t)}{\beta_1} - \dot{F}(t)\frac{b_1}{a_1} \cosh\frac{F(t)}{a_1})/K_2 \tag{74}$$

For creep $F(t) = F_o$, a constant for $t > 0$. Thus $\dot{F}(t) = 0$.

Then Eq. (74) becomes

$$F_o = a_2 \sinh^{-1}(X_3 - tK_1 \sinh F_o/\beta_1)/b_1 + \beta_2 \sinh^{-1}(\dot{X}_3 - K_1 \sinh F_o/\beta_1)/K_2 \qquad (75)$$

The solution of this differential equation will yield the creep deformation X_3 as a function of time t at a constant force F_o.

For relaxation $X_3 = X_o$, a constant, for $t > 0$. Thus $\dot{X}_3 = 0$.

Then Eq. (74) becomes

$$F(t) = a_2 \sinh^{-1}\left\{X_o - \int_o^t \left[K_1 \sinh \frac{F(t)}{\beta_1} + \dot{F}(t)\frac{b_1}{a_1}\cosh\frac{F(t)}{a_1}\right] dt\right\}/b_1 + \beta_2 \sinh^{-1}\left\{-K_1 \sinh\frac{F(t)}{\beta_1} - \dot{F}(t)\frac{b_1}{a_1}\cosh\frac{F(t)}{a_1}\right\}/K_2 \qquad (76)$$

The solution of this equation will yield the force F(t) as a function of time t at a constant deformation X_o of the model.

An approximate solution of Eq. (75) may be obtained as follows:

From equation (75)

$$\text{Sinh}^{-1}(\dot{X}_3 - K_1 \sinh F_o/\beta_1)/K_2 = F_o/\beta_2 - a_2/\beta_2 \sinh^{-1}(X_3 - tK_1 \sinh F_o/\beta_1)/b_1 \qquad (77)$$

or

$$(\dot{X}_3 - K_1 \sinh F_o/\beta_1)/K_2 = \sinh(F_o/\beta_2 - a_2/\beta_2 \sinh^{-1}(X_3 - tK_1 \sinh F_o/\beta_1)/b_1 \qquad (78)$$

Expanding the hyperbolic sine in the right hand side of (78) and substituting in (78)

$$\dot{X}_3 = K_1\alpha_1 + K_2\alpha_2 \cosh\left[a_2/\beta_2 \sinh^{-1}(X_3 - tK_1\alpha_1)/b_1\right] - K_2\alpha_2 \sinh\left[a_2/\beta_2 \sinh^{-1}(X_3 - tK_1\alpha_1)/b_1\right] \qquad (79)$$

where $\alpha_1 = \sinh F_o/\beta_1$, $\alpha_2 = \sinh F_o/\beta_2$ and $\alpha_3 = \cosh F_o/\beta_2$.

Let $(X_3 - tK_1\alpha_1)/b_1 = Z_3$; then $\dot{X}_3 = b_1\dot{Z}_3 + K_1\alpha_1$

and (79) becomes

$$\dot{Z}_3 = K_2\alpha_2/b_1 \cosh\left[a_2/\beta_2 \sinh^{-1}Z_3\right] - K_2\alpha_3/b_1 \sinh\left[a_2/\beta_2 \sinh^{-1} Z_3\right]. \qquad (80)$$

Using the series expansion of the inverse hyperbolic functions and dropping terms above the fourth order equation (80) is found

to be

$$\dot{Z}_3 = K_2\alpha_2/b_1 \cosh\left[a_2/\beta_2(Z_3 - \frac{Z_3^3}{6}\right] - K_2\alpha_2/b_1 \sinh\left[a_2/\beta_2(Z_3 - \frac{Z_3^3}{6})\right] \tag{81}$$

Also using the series expansion of the hyperbolic functions:

$$\cosh\left[a_2/\beta_2(Z_3 - \frac{Z_3^3}{6})\right] =$$

$$1 + \frac{a_2^2/\beta_2^2}{2!} Z_3^2 + (\frac{a_2^4/\beta_2^4}{4!} - \frac{a_2^2/\beta_2^2}{3!})Z_3^4 + (\frac{a_2^2/\beta_2^2}{72} - \frac{a_2^4/\beta_2^4}{36})Z_3^6$$

$$+ \frac{a_2^4/\beta_2^4}{144} Z_3^8 - \frac{a_2^4/\beta_2^4}{1296} Z_3^{10} + \frac{a_2^4/\beta_2^4}{31104} Z_3^{12}. \tag{82}$$

and

$$\sinh\left[a_2/b_2(Z_3 - \frac{Z_3^3}{6})\right] = a_2/\beta_2(Z_3 - \frac{Z_3^3}{6})$$

$$+ \frac{a_2^3/\beta_2^3}{3!}(Z_3^3 - \frac{Z_3^5}{2} + \frac{Z_3^7}{12} - \frac{Z_3^9}{216}) \tag{83}$$

Substituting (82) and (83) in equation (81), dropping terms above the fourth order, and transposing, (81) becomes

$$\dot{Z}_3 + K_2\alpha_2/b_1(a_2/\beta_2)Z_3 - K_2\alpha_2/b_1(\frac{a_2^2/\beta_2^2}{2!})Z_3^2$$

$$+ K_2\alpha_2/b_1(\frac{a_2^3/\beta_2^3}{3!} - \frac{a_2/\beta_2}{6})Z_3^3$$

$$- K_2\alpha_2/b_1(\frac{a_2^4/\beta_2^4}{4!} - \frac{a_2^2/\beta_2^2}{3!})Z_3^4 + \ldots = K_2\alpha_2/b_1 \tag{84}$$

Equation (84) is now in a form to which the method of reversion[3] can be applied. To simplify the computations let g_1, g_2, g_3 and g_4 be the coefficients of Z_3, Z_3^2, Z_3^3 and Z_3^4

respectively, and let $K_2\alpha_2/b_1 = B$.

Then Eq. (84) becomes

$$\dot{Z}_3 + g_1 Z_3 + g_2 Z_3^2 + g_3 Z_3^3 + g_4 Z_3^4 = B. \tag{85}$$

This expression may be solved in the same manner outlined on page 12 for the solution of Eq. 42.

The boundary conditions which may be applied to solve this problem for creep, i.e. $F(t) = F_o$ = constant, are:

$$X_1(0) = X_2(0) = X_3(0) = b_1 \sinh F_o/a_1 \text{ and}$$

$$\dot{X}_2(0) = \dot{X}_3(0) = 0. \tag{86}$$

For stress relaxation, i.e., $X_3(t) = X_{30}$ = constant, the boundary conditions which may be employed are:

$$X_1(0) = X_2(0) = X_{30}, \quad F(0) = a_1 \sinh^{-1} X_{30}/b_1, \text{ and } \dot{X}_2(0) = 0.$$

REFERENCES

1. W. N. Findley, "Derivation of a Stress-Strain Equation from Creep Data for Plastics," Proc. First National Congress of Applied Mechanics, 1952, p. 595-602.
2. W. N. Findley, C. H. Adams, and W. J Worley, "The Effect of Temperature on the Creep of Two Laminated Plastics as Interpreted by the Hyperbolic sine Law and Activation Energy Theory," Proceedings, A.S.T.M., Vol. 48, 1948, pp. 1217-1239.
3. A. C. Sim, "A Generalization of Reversion Formulae with their Application to Non-linear Differential Equations," Philosophical Magazine, Series 7, Vol. 42, 1951, Part 1, p. 228-238.

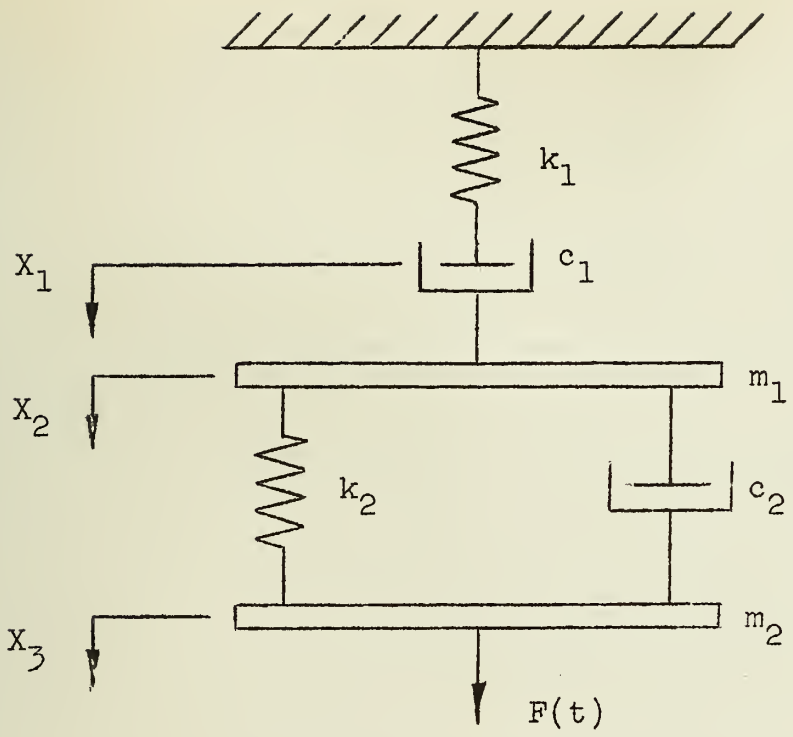

Fig. 1 Linear Maxwell and Voigt Units in Series with Two Masses.

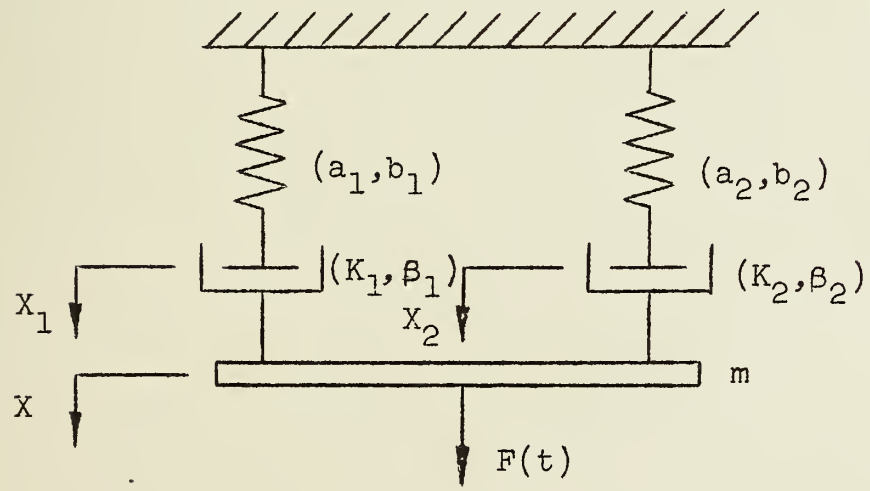

Fig. 2 Two Nonlinear Maxwell Units in Parallel Coupled by a Mass

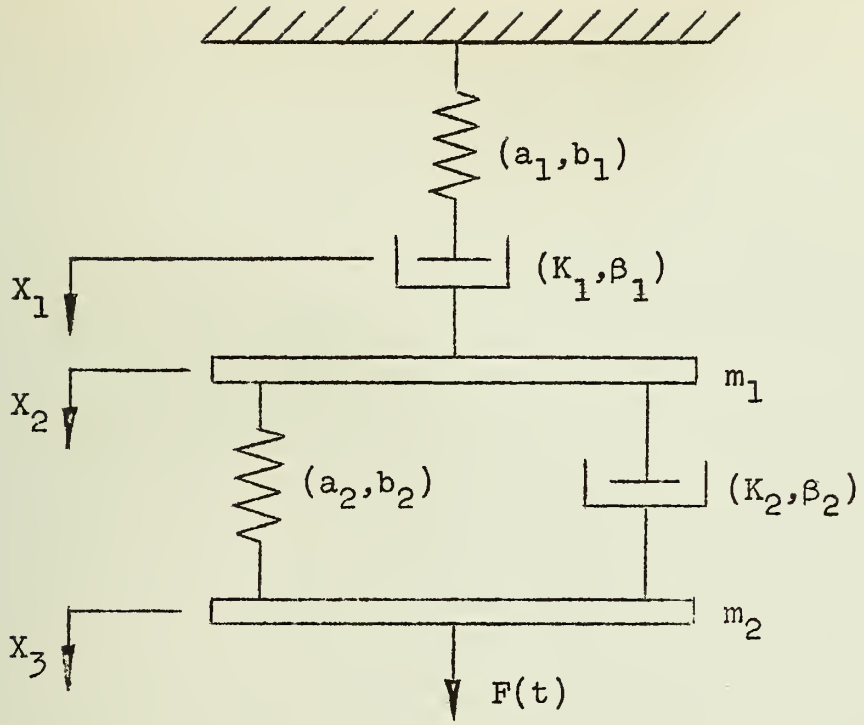

Fig. 3 Nonlinear Maxwell and Voigt Units in Series with Two Masses.

PREDICTION OF CREEP IN BENDING FROM TENSION CREEP DATA WHEN CREEP COEFFICIENTS ARE UNEQUAL

by

W. N. Findley, J. J. Poczatek,
and P. N. Mathur

A Research Project of the
DEPARTMENT OF THEORETICAL AND APPLIED MECHANICS
UNIVERSITY OF ILLINOIS

Sponsored by
PICATINNY ARSENAL, ORDNANCE CORPS
DEPARTMENT OF THE ARMY
Contract No. DA-11-022-ORD-401, Project No. TB4-721
Interim Report No. 3

Urbana, Illinois

[redacted]

February, 1954

DISTRIBUTION LIST

INTERIM AND FINAL REPORTS

Contract No. DA-11-022-ORD-401 Project No. TB4-721

Commanding Officer
Attn: Technical Division (2)
R and D Contract Section
Picatinny Arsenal
Dover, New Jersey

Commanding Officer
Attn: Library
Picatinny Arsenal
Dover, New Jersey

Chicago Ordnance District
Attn: R and D Branch
209 West Jackson Boulevard
Chicago 6, Illinois

Chief of Ordnance
Attn: ORDTB (10)
Department of the Army
Washington 25, D. C.

Chief of Ordnance
Attn: ORDTX-AR
Department of the Army
Washington 25, D. C.

Chief of Ordnance
Attn: ORDTA
Department of the Army
Washington 25, D. C.

Chief of Ordnance
Attn: ORDTR
Department of the Army
Washington 25, D. C.

Chief of Ordnance
Attn: ORDTS
Department of the Army
Washington 25, D. C.

Chief of Ordnance
Attn: ORDTT
Department of the Army
Washington 25, D. C.

Chief of Ordnance
Attn: ORDTU
Department of the Army
Washington 25, D. C.

Chief of Ordnance
Attn: ORDIX (2)
Department of the Army
Washington 25, D. C.

Chief of Ordnance
Attn: ORDFX (2)
Department of the Army
Washington 25, D. C.

Department of the Navy
Office of Naval Research
Attn: Code 423
Washington 25, D. C.

Department of the Navy
Bureau of Aeronautics
Airborne Equipment Division
Materials Branch
Washington 25, D. C.

Signal Corps Engineering Laboratory
Squier Signal Laboratory
Materials Section
Attn: Mr. Luis Reiss
Fort Monmouth, New Jersey

Chemical Corps
Attn: Mr. T. P. Steinmetz
Technical Command
Army Chemical Center, Md.

Commanding General
U. S. Air Force (2)
Air Material Command
Engineering Division
Materials Laboratory
Attn: Mr. Robert T. Schwartz, WCRTS
Mr. Peterson, WCRTE
Wright-Patterson Air Base, Ohio

Department of the Navy
Attn: Mr. H. A. Perry
Naval Ordnance Laboratory
8050 Georgia Avenue
Silver Springs, Maryland

Director of Naval Research
Attn: Technical Information Officer
Washington 25, D.C.

Department of the Navy
Bureau of Ships (2)
Research and Development
Material Development Division
Attn: Mr. J. B. Alfors, Code 346
Mr. J. G. Kuenzel, Code 345
Washington 25, D. C.

Department of the Navy
Attn: Code Re 1
Bureau of Ordnance
Research and Development Division
Materials and Handling Branch
Washington 25, D. C.

Engineer Center
Engineer Research and Development
Laboratories
Attn: Mr. Philip Mitton
Materials Branch
Fort Belvoir, Virginia

Office of the Quartermaster General
Research and Development Division
Attn: Dr. Warren Stubblebine
Chemical and Plastics Section
Washington, D. C.

Department of Commerce
Attn: Mr. Frank W. Reinhart
National Bureau of Standards
Romm 4022, Industrial Building
Washington 25, D. C.

Department of the Navy
Attn: Mr. M. N. DeNeale
Naval Gun Factory
Metallurgical and Testing Branch
M and 8th Streets, S. E.
Washington 25, D. C.

Office of Ordnance Research
Box CM
Duke Station
Durham, North Carolina

Commanding Officer
Attn: Technical Division (2)
Detroit Arsenal
28251 Van Dyke
Centerline, Michigan

Commanding Officer
Attn: Technical Division (2)
Aberdeen Proving Ground, Md.

Commanding Officer
Attn: Technical Division
White Sands Proving Ground
Las Cruces, New Mexico

Commanding Officer
Attn: Technical Division
Redstone Arsenal
Huntsville, Alabama

Commanding Officer
Attn: Technical Division (2)
Frankford Arsenal
Bridesburgh Station
Philadelphia 37, Pennsylvania

Commanding Officer
Attn: Technical Division
Picatinny Arsenal
Dover, New Jersey

Commanding Officer
Attn: Technical Division
Rock Island Arsenal
Rock Island, Illinois

Commanding Officer
Attn: Technical Division
Springfield Armory
Springfield 1, Massachusetts

Commanding Officer
Attn: Technical Division
Watertown Arsenal
Watertown 72, Massachusetts

Commanding Officer
Attn: Technical Division
Watervliet Arsenal
Watervliet, New York

Aerojet Engineering Corp.
Azusa, California
Attn: Dr. Paul J. Blatz

Allegany Ballistics Lab.
Cumberland, Maryland
Attn: Mr. Harry Winnerling

Naval Ordnance Test Station
Code 4021
Inyokern, China Lake, Calif.
Attn: Mr. D. D. Ordahl

Naval Powder Factory
Indian Head, Maryland
Attn: Mr. A. S. Johnson

Thiokol Corp., Redstone Div.
Huntsville, Alabama
Attn: Mr. W. I. Dale, Jr.

Chief Superintendent
C.A.R.D.E. N-8-3-5
P.O. Box 1427
Quebec, Que, Canada
Attn: Mr. I. R. Cameron

INTERIM REPORT NO. 3

on a research project entitled
STUDY OF RELATIONSHIP BETWEEN
TIME SENSITIVE MECHANICAL
PROPERTIES OF PLASTICS

Project Supervisor, W. N. Findley

PREDICTION OF CREEP IN BENDING FROM TENSION CREEP DATA WHEN CREEP COEFFICIENT ARE UNEQUAL

W. N. Findley
Research Associate Professor

J. J. Poczatek
Research Assistant
(Now with American Machine
and Foundry Co.)

P. N. Mathur
Research Assistant

DEPARTMENT OF THEORETICAL AND APPLIED MECHANICS
UNIVERSITY OF ILLINOIS

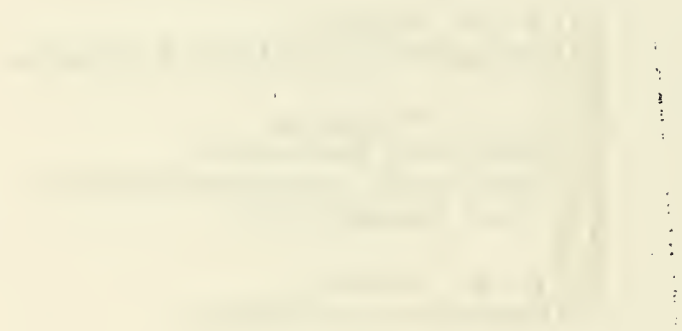

SUMMARY

The method of predicting creep in bending from data on creep in tension previously described has been extended to the prediction of creep in bending when the creep in tension and compression are unequal and when the time-dependent and time-independent stress functions are unequal. It was shown that the stress distribution and position of the neutral axis in a beam changed with time when the creep in tension and compression were unequal; and the stress distribution changed with time when the time-dependent and time-independent stress functions were unequal.

Computed creep deflections were compared with available data on canvas laminate and polystyrene, with good results for the former and fair results for the latter.

CONCLUSIONS

It has been shown that creep and stress distribution in bending can be predicted from tension and compression creep data. However, the available test data are inadequate to provide an accurate check of the theory.

ACKNOWLEDGEMENTS

This project was conducted in the Department of Theoretical and Applied Mechanics as part of the work of the Engineering Experiment Station of the University of Illinois in cooperation with Picatinny Arsenal, Ordnance Corps, Department of the Army.

The authors are grateful to B. K. Ghandhi, W. A. Hagemeyer, G. Khosla and H. G. Russel for assistance in the computations and preparation of illustrations.

INTRODUCTION

When a material is subjected to a constant stress the time-dependent portion of the resulting strain imposed on it is referred to as creep. Although creep behavior of materials under various states of stress is both of practical and theoretical interest, most creep data reported in the literature have been obtained with simple tensile loading. In the design of many industrial products one of the more simple cases of complex stresses encountered is bending. The purpose of the present investigation was to develop a theory correlating the creep behavior in bending with creep in tension and compression.

In a previous paper (1)* the existing literature related to this problem was reviewed and a method for predicting creep in bending from the creep data in tension was derived. In the previous paper the creep behavior of the material was assumed to be equal in tension and compression and the coefficients of the time-dependent and time-independent terms of the stress function were considered equal. The theoretical equations obtained from this analysis were compared with experimental data obtained from a canvas laminate with good success. The method was also applied to the case of creep under a nonuniform bending moment.

An earlier paper by Marin (2) which has not been referred to in recent papers was discovered since preparation

---

* Numbers in parentheses refer to the list of references appended to this paper.

of our first paper on this subject. In the paper by Marin creep was assumed to be described by a power function of time and the stress functions in the time-dependent and time-independent terms were also assumed to be power functions. The predictions of Marin's analysis were tested against creep data from four aluminum alloy beams with errors of 13, 22, 24 and 28 per cent, respectively. The application of the analysis to statically indeterminate structures was also described.

The present paper extends the analysis to include bending of materials which have unequal creep in tension and compression and which exhibit unequal coefficients of the time-dependent and time-independent terms. Both of these conditions make the solution of the problem much more difficult.

BENDING WITH UNEQUAL CREEP IN TENSION AND COMPRESSION

Derivation:

Some materials evidently have unequal creep behavior in tension and compression (3). The derivation of creep relations for bending from unequal relations for tension and compression creep is complicated by the lack of symmetry which probably causes the stress distribution and position of the neutral axis to change with time.

In previous papers (4, 5, 6) the creep curves obtained from a canvas laminate tested at different constant stresses in tension were found to be closely described by an

equation of the form

$$\epsilon = \epsilon_o + mt^n = (\epsilon_o' + m't^n) \sinh \sigma/\sigma_o \qquad (1)$$

where ϵ is the strain; t is the time under a constant stress, σ; ϵ_o', m', n and σ_o are constants whose values depend on the material and temperature; and ϵ_o and m are functions of stress.

The stress dependence in this relation is of the same form as that in the activation energy theory of creep as advanced by Kauzmann (7). It has also been shown (6) that an equation for the stress-strain curve obtained from a constant strain rate tension test could be derived from equation (1) and that the resulting equation was in close agreement with the experimental data. It should be noted that the time-dependent term $\epsilon_o = \epsilon_o' \sinh \sigma/\sigma_o$ in equation (1) expresses the instantaneous strain, i.e., the strain at time zero, and that it does not represent linear elasticity except when σ_o is large compared to σ.

Equation (1) accurately represents the creep data of some materials under conditions of constant stress. It probably does not, however, accurately describe creep under varying stress. Thus, if the stress distribution in the beam changes during creep, as described by Popov (8) and Fried (9) some inaccuracy may be introduced by the use of this equation unless the material obeys the time-hardening law (10) which is probably not the case.

If the constants in the equation for tension are all different from those for compression the creep equations may be written

$$\epsilon_T = (\epsilon_{oT}' + m'_T t^{n_T}) \sinh \sigma_T/\sigma_{oT} \qquad (2)$$

$$\epsilon_s = (\epsilon_{os}' + m'_s t^{n_s}) \sinh \sigma_s/\sigma_{os} \qquad (3)$$

where the subscripts T and s denote tension and compression respectively.

To determine the bending creep relation the conditions of equilibrium and geometry must be satisfied. From the observation that plane sections remain plane in a beam subjected to a uniformly or nearly uniformly distributed bending moment the following well-known geometrical relations are obtained:

$$\epsilon_s = \frac{y_s}{\rho}; \quad \epsilon_T = \frac{y_T}{\rho} \qquad (4)$$

where y_T and y_s are the normal distances from the neutral axis to any point in the tension or compression side of the beam, respectively, ϵ_T and ϵ_s are the corresponding strains and ρ is the radius of curvature of the neutral axis. The neutral axis is at some undetermined distance c from the extreme "fiber" on the tension face of the beam.

The fact that plane sections in a beam subjected to pure bending remain plane has been demonstrated for plastically bent beams by Nadai (11) and for creep of lead beams by MacCullough (12). Also, consideration of compatibility of

strains in the different "fibers" of a beam of great length, bent by a constant bending moment into the arc of a circle, suggests that plane sections must remain plane at all points along the beam which are remote from the ends. If this were not so, different "fibers" would be markedly displaced relative to each other at points at a distance from the center of the beam.

The conditions of equilibrium for a beam are expressed by the following equations when the accelerations involved in the creep are so small as to be negligible--which is usually the case:

$$\int_{c-h}^{c} \sigma dA = 0 \qquad (5)$$

$$\int_{c-h}^{c} \sigma y dA = M \qquad (6)$$

where A is the cross-sectional area of the beam, h is the depth of the beam and c is the distance from the neutral axis to the tension face of the beam.

Solving for σ_T and σ_s in equations (2) and (3) and substituting equations (4) for ϵ_s and ϵ_T the following equations are obtained.

$$\sigma_T = \sigma_{oT} \sinh^{-1} \frac{y_T/\rho}{\epsilon'_{oT} + m'_T t^{n_T}} = \sigma_{oT} \sinh^{-1} \frac{N_T}{\rho} y_T \qquad (7)$$

$$\sigma_s = \sigma_{os} \sinh^{-1} \frac{y_s/\rho}{\epsilon'_{os} + m'_s t^{n_T}} = \sigma_{os} \sinh^{-1} \frac{N_s}{\rho} y_s \qquad (8)$$

where the symbols

$$N_T = \frac{1}{\epsilon'_{oT} + m'_T t^{n_T}} \text{ ; and } N_s = \frac{1}{\epsilon'_{os} + m'_s t^{n_s}}$$

have been introduced.

For a beam of rectangular cross-section of width b, dA = bdy. Making this subsitution equations (5) and (6) become:

$$b\int_{-(h-c)}^{0} \sigma_T dy + b\int_{0}^{c} \sigma_s dy = 0 \qquad (9)$$

and

$$M = b\int_{-(h-c)}^{0} \sigma_T y_T dy + b\int_{0}^{c} \sigma_s y_s dy \qquad (10)$$

Substituting for σ_T and σ_s from equations (7) and (8) into equation (9), and integrating, the resulting expression becomes:

$$\frac{\sigma_{oT}}{N_T}\left\{1 + \frac{N_T}{\rho}(h - c) \sinh^{-1} \frac{N_T}{\rho}(h - c) - \sqrt{1 + \left[\frac{N_T}{\rho}(h - c)\right]^2}\right. =$$

$$\left.\frac{\sigma_{os}}{N_s}\left\{1 + \frac{N_s}{\rho} c \sinh^{-1} \frac{N_s}{\rho} c - \sqrt{1 + (\frac{N_s}{\rho} c)^2}\right\}\right. . \qquad (11)$$

Substituting for σ_T and σ_s from equations (7) and (8) into equation (10) and integrating

$$M = \frac{b\sigma_{oT}\rho^2}{4(N_T)^2}\left\{\left[2\frac{N_T^2}{\rho^2}(h-c)^2 + 1\right]\sinh^{-1}\frac{N_T}{\rho}(h-c) - \frac{N_T}{\rho}(h-c)\sqrt{1+\left[\frac{N_T}{\rho}(h-c)\right]^2}\right\} + \frac{b\sigma_{os}\rho^2}{4(N_s)^2}\left\{\left[2\left(\frac{N_s}{\rho}c\right)^2 + 1\right]\sinh^{-1}\frac{N_s}{\rho}c - \frac{N_s}{\rho}c\sqrt{1+\left[\frac{N_s}{\rho}c\right]^2}\right\} \quad (12)$$

For a given constant bending moment M applied for a given time t to a given beam, equations (11) and (12) are simultaneous equations in two unknowns, the location of the neutral axis c and the radius of curvature ρ. Values of ρ and c may be obtained by trial.

For a beam of constant bending moment the deflection at mid-span may then be obtained from the well known geometrical relation:

$$z = \frac{\ell^2}{8\rho} \quad (13)$$

where Z is the deflection at the center relative to the ends of a span of a beam of length ℓ subjected to a uniform bending moment.

The stress distribution may be obtained from the value of c and equations (7) and (8).

Since N_s and N_T are functions of time the radius of curvature ρ will change with time. Since N_s and N_T are unequal functions of time it is evident that the ratios $\frac{N_s}{\rho}$ and $\frac{N_T}{\rho}$ cannot both remain constant and independent of time. Hence, from equation (11) it follows that c must vary with time.

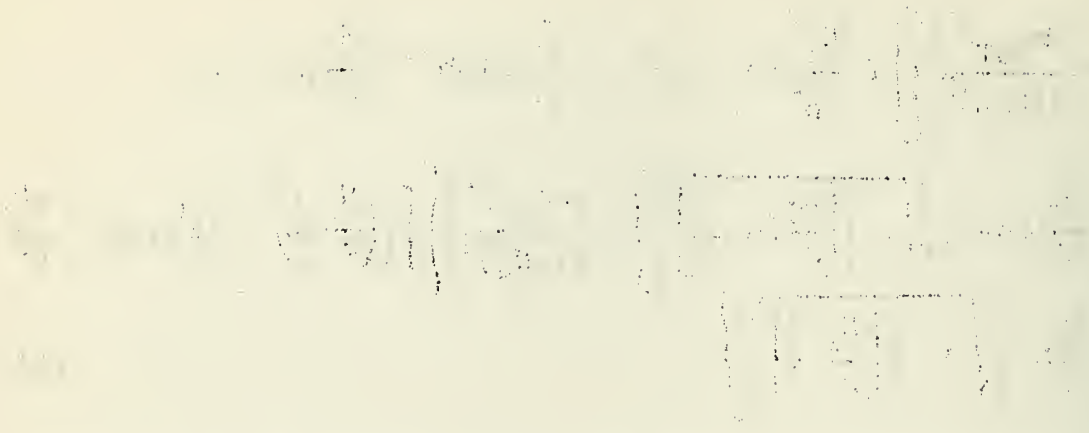

Since the ratios $\frac{N_s}{\rho}$ and $\frac{N_T}{\rho}$ change with time the stress distribution must change with time. This follows from equations (7) and (8). Not only does the stress distribution change with time because of the time dependence of the above ratios but because the position of the neutral axis changes with time and this affects the values of y_T and y_s in equations (7) and (8).

Equation (1) may accurately describe the relationship between strain, stress and time only for constant stress or stresses which change only slightly. Hence, if the change in stress distribution described above causes large changes in stresses during creep then the above derivation will not yield accurate results.

It is easily verified that equations (11) and (12) reduce to equations (16) and (18) in the previous paper (1) when tension and compression creep are equal. This verification is accomplished by substituting the following in equations (11) and (12):

$$\sigma_{oT} = \sigma_{os} = \sigma_o; \quad N_T = N_s = N\rho; \quad h - c = c.$$

Illustration:

Equations (11) and (12) have been solved for the particular problem of a beam of canvas laminate in which the creep in tension and compression can be described by relations of the form of equations (2) and (3). And the constants for creep in tension were the same as employed for the canvas

laminate analyzed in the previous report (1);

$$\epsilon_{oT} = m'_T = 0.001875$$

$$\sigma_{oT} = 4000 \text{ psi}$$

$$n_T = 0.1183$$

while the constants for creep in compression were arbitrarily chosen to be 20 per cent higher than those for tension creep;

$$\epsilon_{os} = m'_S = 0.002250$$

$$\sigma_{os} = 4800 \text{ psi}$$

$$n_s = 0.14196$$

To solve equations (11) and (12) for the purpose of determining the deflection-time relation in bending the values of N_S and T_T were computed for a particular set of values of time t. Then the constant coefficients in the equations were computed. Graphical techniques for solving the simultaneous equations were tried but were found to lack the necessary precision.

A numerical procedure was employed in which $N_T(h-c)/\rho$, and $N_S c/\rho$ were used as variables. Likely values of these variables were inserted in equation (11) and the value of the left hand side and the right hand side of the equation were computed. Then the values of both variables were plotted as ordinates versus the value of the right-or left hand side of the equation. Thus any number of pairs of values which would satisfy equation (11) could be read from these curves. Pairs of these values were then substituted in equation (12) and

the bending moment was computed. This process was repeated until the computed bending moment matched the required value with sufficient accuracy.

From the values of the above variables which satisfied equations (11) and (12) the values of ρ and c were computed, and from ρ the deflection was computed by means of equation (13). The deflection-time relation for a bending moment of 679 inch-pounds determined in this way is shown in Fig. 1 together with the corresponding experimental bending creep curve and the theoretical creep curve for equal creep in tension and compression.

The following observation was of interest: In spite of the fact that the assumed creep in compression varied from 20 per cent greater than in tension at t = 0 to 33 per cent greater than in tension at 880 hours for the same stress, the computed creep in bending was nearly the same over the time interval considered as that computed for a beam in which the creep in compression was the same as that in tension.

The position of the neutral axis was found to vary with time from one side of the center line to the other as shown in Fig. 2.

The distribution of stress across the beam was computed at two different values of time from equations (7) and (8), and was plotted for a time of zero and of 880 hr. in Fig. 3a. It was observed that the change in stress distribution was relatively small--less than 2 per cent in 880 hours at the extreme fiber.

In order to better illustrate the change which occurred in the stress distribution the difference between the computed stress distribution and the equivalent linear stress distribution was determined for three values of time and is shown in Fig. 3b. It was found that a high degree of precision was required in the computations to insure accurate results in the stress distribution.

BENDING WITH UNEQUAL TIME DEPENDENT AND INDEPENDENT STRESS FUNCTIONS

Derivation:

The creep behavior of some materials is accurately represented by a more general form of equation (1) in which the constants in the stress function are different for the time-independent and time-dependent terms as follows:

$$\epsilon = \epsilon_o' \sinh \sigma/\sigma_\epsilon + m' t^n \sinh \sigma/\sigma_m \qquad (14)$$

When the tension and compression creep behaviors are identical and are single-valued functions of stress and time as described by equation (14) for constant stresses or small changes in stress, the creep in bending can be expressed by equations derived in the following manner:

Equation (14) may be written as follows by dividing by ϵ_o'.

$$e = \sinh x + T \sinh ax \qquad (15)$$

where

$$e = \epsilon/\epsilon_o' \; ; \quad T = \frac{m' t^n}{\epsilon_o'} \; ; \quad a = \sigma_\epsilon/\sigma_m \text{ and } x = \sigma/\sigma_\epsilon. \qquad (16)$$

For a straight beam of rectangular cross section in which the creep equations in tension and compression are

identical the neutral axis can be shown to be at half the depth of the beam. Thus from statics the bending moment M in a beam of width b and depth h is related to the stress σ by the following equation:

$$M = \int_{-c}^{c} b\sigma y dy = b \int_{-c}^{c} \sigma_{\epsilon}\, xy\, dy \qquad (17)$$

where

c = half the beam depth, and

y = distance measured from the neutral axis in a direction perpendicular to the neutral axis.

From the geometry of strains as expressed by equation (4) and the creep relation, equation (15), the following was obtained:

$$y = \rho\epsilon = \rho\epsilon_o{}^{b} = \rho\epsilon_o'(\sinh x + T \sinh ax). \qquad (18)$$

Differentiating equation (18) at constant ρ and T

$$dy = \rho\epsilon_o' (\cosh x\, dx + aT \cosh ax\, dx) \qquad (19)$$

Substituting equations (18) and (19) into equation (17) for any given time t, (and corresponding T and ρ) and expanding

$$M = b\sigma_{\epsilon}(\rho\epsilon_o')^2 \left\{ \int_{-x_1}^{x_1} x \sinh x \cosh x\, dx + aT \int_{-x_1}^{x_1} x \sinh x \cosh ax\, dx + T \int_{-x_1}^{x_1} x \sinh ax \cosh x\, dx + aT^2 \int_{-x_1}^{x_1} x \sinh ax \cosh ax\, dx \right\} \qquad (20)$$

where the limits of x correspond to the limits of y; that is, x_1 is the stress at y = c and $-x_1$ is the stress at y = -c.

Performing the integration as indicated in equation (20), the resulting equation for radius of curvature ρ as a function of bending moment M and stress at the extreme "fiber" $\sigma_1 = \sigma_\epsilon x_1$ was

$$M = \frac{b\sigma_\epsilon(\epsilon_o')^2\rho^2}{2}\left\{\left[(2\sinh^2 x_1 + 1)x_1 - \sinh x_1 \cosh x_1\right]\right.$$
$$+ \frac{T^2}{a}\left[(2\sinh^2 ax_1 + 1)ax_1 - \sinh ax_1 \cosh ax_1\right]$$
$$\left. + 4T\left[x_1 \sinh x_1 \sinh ax_1 - \frac{1}{(a^2 - 1)}(a \sinh x_1 \cosh ax_1 - \cosh x_1 \sinh ax_1)\right]\right\} \qquad (21)$$

Solving equation (18) for $1/\rho$ when y = c and $x = x_1$ the following is obtained:

$$\frac{1}{\rho} = \frac{\epsilon_o'}{c}(\sinh x_1 + T \sinh ax_1). \qquad (22)$$

These two independent relations, (21) and (22), can be solved simultaneously at any given time $t = t_1$ (or $T = T_1$) for the extreme fiber stress function x_1 and the radius of curvature ρ. The deflection for a beam having uniform bending moment may then be obtained from equation (13).

If the ratio $a = \sigma_\epsilon/\sigma_m$ is allowed to equal unity, equation (14) reduces to equation (1). Consequently, equation (21) should reduce to equation (18) of reference (1). Performing the indicated substitution and solving for M

$$M = \frac{b\sigma_o(\rho\epsilon_o')^2}{2}\left\{(1 + T^2)\left[(2 \sinh^2 x_1 + 1)\, x_1 - \sinh x_1 \cosh x_1\right]\right.$$
$$\left. + T\left[x_1 \sinh^2 x_1 - \lim_{a \to 1} \left(\frac{1}{a^2 - 1}\right)(a \sinh x_1 \cosh a x_1 \right.\right.$$
$$\left.\left. - \cosh x_1 \sinh a x_1)\right]\right\} \qquad (23)$$

Taking the limit and making use of equation (14) of reference (1) equation (23) was found to reduce to equation (18) of reference (1).

The simultaneous equations (21) and (22) may be solved by substituting equation (22) for ρ in equation (21), expanding and collecting terms in T. The following quadratic equation in T results:

$$T^2\left\{(2M/bc^2\sigma_\epsilon)\sinh^2 a x_1 - x_1(1 + 2 \sinh^2 a x_1)\right.$$
$$+ (1/a) \cosh a x_1 \sinh a x_1 + T\left\{\left[(4M/bc^2 - 4x_1\right] \sinh a x_1 \sinh x_1\right.$$
$$\left. - \left[4/(a^2 - 1)\right] \sinh a x_1 \cosh x_1 + \left[4a/(a^2 - 1)\right] \cosh a x_1 \sinh x_1\right\}$$
$$\left. + \left\{\sinh x_1 \cosh x_1 + (2M/bc^2\sigma_\epsilon)\sinh^2 x_1 - x_1(1 + 2 \sinh^2 x_1)\right\} = 0\right.$$

(24)

Equation (24) is then evaluated for the given value of M and several reasonable values of x_1 by using the quadratic formula. The solution of the quadratic formula gives the time function T corresponding to each chosen stress function x_1. From the value of T the time t was determined from equation (16). The curvature $1/\rho$ was determined from equation (22) by substituting T and x_1. Then by utilizing equation (13) the deflection z was was determined for the same value of time.

The above procedure is straight forward but involves a great deal of labor and requires a large number of significant figures in the computations.

From the values of x_1 at different times the change in extreme fiber stress may be determined as a function of time by use of the last relation in equations (16). Also at any given value of time and corresponding values of T and ρ the stress distribution can be computed from equation (18). Because the creep functions were assumed to be the same in tension and compression the neutral axis does not change position with time.

Illustration:

Creep data were available for tension (13, 14) and bending (13) of polystyrene. The two sets of tension creep data were both made on polystyrene of the same description from the same manufacturer. One set of tension creep data did not have enough self consistency to permit evaluating the constants of the creep equation, but by combining the two sets of data this became possible--though with limited accuracy.

It was found that equation (1) could not adequately describe the data so equation (14) was tried with the results shown in Fig. 4. The corresponding values of the constants in equation (14) were found to be as follows:

$$\epsilon_o' = 4.3077 \times 10^{-2}$$
$$\sigma_\epsilon = 20{,}000 \text{ psi}$$
$$m' = 4.098 \times 10^{-6}$$
$$\sigma_m = 700 \text{ psi}$$
$$n = 0.475$$

These values were obtained largely by trial. The data did not yield readily to rational procedures of evaluating the constants such as used previously (4, 6). Utilizing these values of the constants and the procedure outlined above, the creep in bending was computed for a beam of the dimensions employed in the tests of reference (13) and a bending moment of 553 in. lb. The results of these computations are shown in Fig. 5 together with test data reported in reference (13).

Also shown in Fig. 5 is the change in the stress at the extreme fiber with time. The computed stress at the extreme fiber decreased 10 per cent in 1000 hours and decreased 12.4 per cent in 3200 hours. Since the bending moment remained constant the stress distribution changed.

The agreement between the theoretical and experimental creep deflections was not as good as would be desired although the shape of the curve was satisfactorily predicted from 100 to 1000 hr. Possible reasons for the lack of better agreement may be among the following: (a) Creep of the polystyrene tested in bending and part of the tension tests may not have been accurately described by the constants selected for the creep equation. Some of the tension creep curves for this material showed similar departures from the theory in both tension and bending tests; (b) crazing was observed to occur in tension creep and on the tension side of the beams; (c) the data in the first 100 hours of creep in bending appear to be questionable; (d) creep in tension

and compression may not have been the same; and (e) the change in stress distribution with time caused the stress on a given fiber to change during creep instead of remaining constant as assumed by the use of equation (14).

REFERENCES

1. W. N. Findley and J. J. Poczatek, "A Relation between Creep in Tension, Creep in Bending and Tension Tests," Interim Report No. 1, Picatinny Arsenal Contract No. DA-11-022-ORD-401, August 1953; also "Prediction of Creep-Deflection and Stress Distribution in Beams from Creep in Tension," Journal of Applied Mechanics, (in press).

2. Joseph Marin, "Mechanics of Creep for Structural Analysis," Proc. Am. Soc. of Civil Engineers, May 1942, p. 719.

3. J. Marin, Y. H. Pao, and G. E. Cuff, "Creep Properties of Lucite and Plexiglass for Tension, Compression, Bending, and Torsion," Trans. A.S.M.E., Vol. 73, 1951, pp. 705-719.

4. W. N. Findley, "Creep Characterisitcs of Plastics," 1944 Symposium on Plastics, A.S.T.M., 1944, p. 18.

5. W. N. Findley and W. J. Worley, "Mechanical Properties of Five Laminated Plastics," NACA, Tech. Note 1560, August 1948.

6. W. N. Findley, "Derivation of a Stress-Strain Equation from Creep Data for Plastics," Proc. First U. S. National Congress of Applied Mechanics, June 11-16, 1951, p. 595.

7. W. Kauzmann, "Flow of Solid Metals from the Standpoint of the Chemical Rate Theory," Trans. American Inst. of Mining and Metallurgical Engineering, Institute of Metals Division, Vol. 143, 1941, p. 57.

8. E. P. Popov, "Bending of Beams with Creep," Jour. of App. Physics, Vol. 20, 1949, p. 251-256.

9. B. Fried, Some Observations on Photoelastic Materials Stressed Beyond the Elastic Limit, S.E.S.A., Vol. VIII, No. 2, 1951, p. 143.

10. I. Roberts, "Prediction of Relaxation of Metals from Creep Data," Proceedings A.S.T.M., Vol. 51, 1951, p. 811.

11. A. Nadai, "Plasticity," The McGraw Hill Book Co., Inc., 1935, p. 121.

12. G. H. MacCullough, "An Experimental and Analytical Investigation of Creep in Bending," Trans. A.S.M.E., Vol. 55, 1933, p. APM 56-9-55.

13. J. Marin and G. Cuff, "Creep-Time Relations for Polystyrene under Tension, Bending, and Torsion," Proceedings A.S.T.M., Vol. 49, 1949, p. 1158-1174.

14. W. N. Findley, "Comments on Creep and Damping Properties of Polystyrene," Jour. of Applied Physics, Vol. 21, No. 3, May 1950, p. 258.

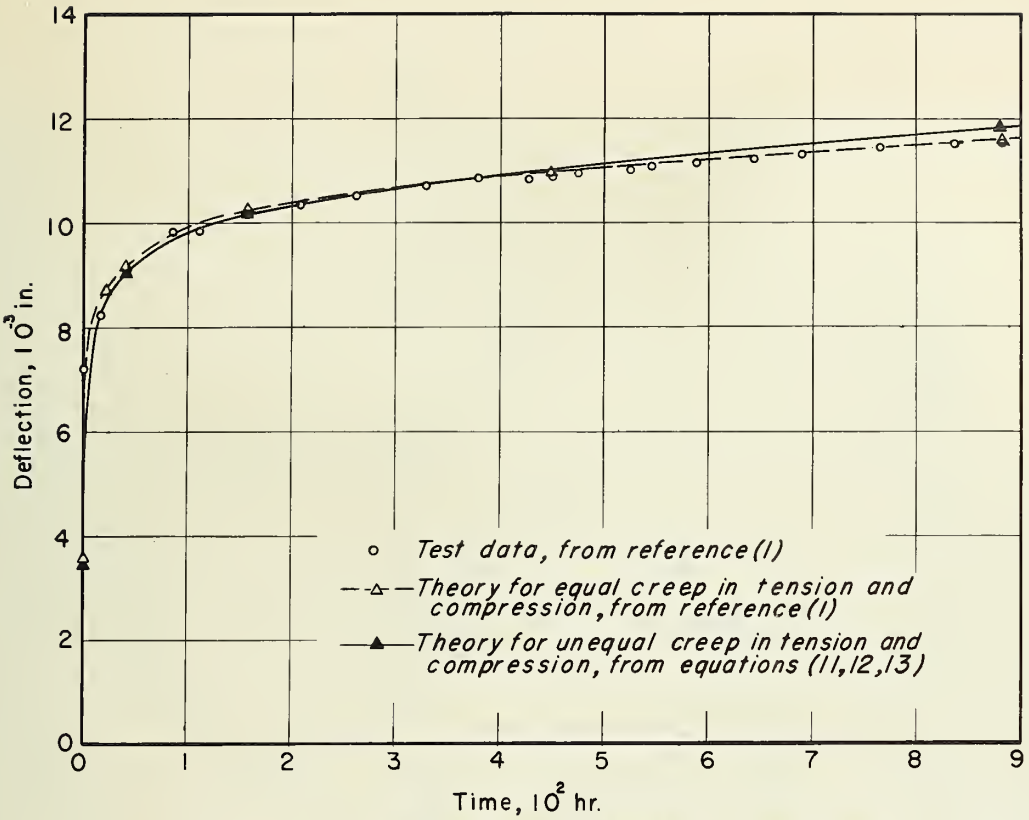

FIG. 1 DEFLECTION—TIME RELATION IN BENDING CREEP FROM DIFFERENT THEORIES, FOR CANVAS LAMINATE AT 77°F. AND BENDING MOMENT OF 679 IN.-LB.

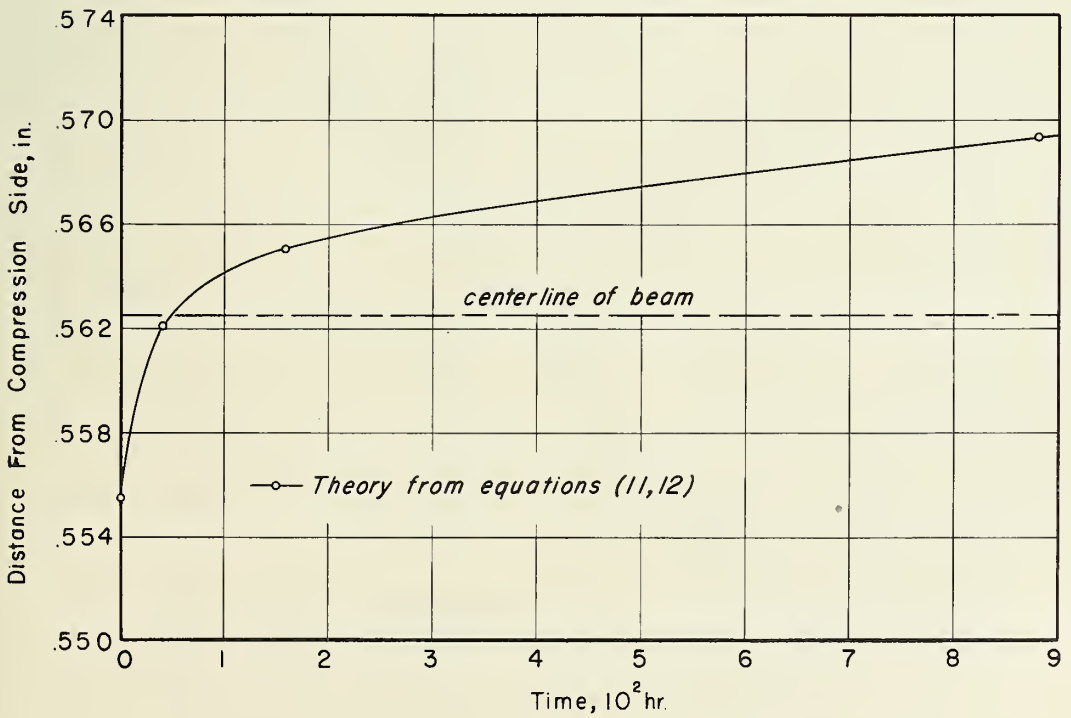

FIG. 2 LOCATION OF NEUTRAL AXIS DURING CREEP IN BENDING WHEN TENSION AND COMPRESSION CREEP ARE UNEQUAL, FOR CANVAS LAMINATE AT 77°F. AND BENDING MOMENT OF 679 IN.-LB.

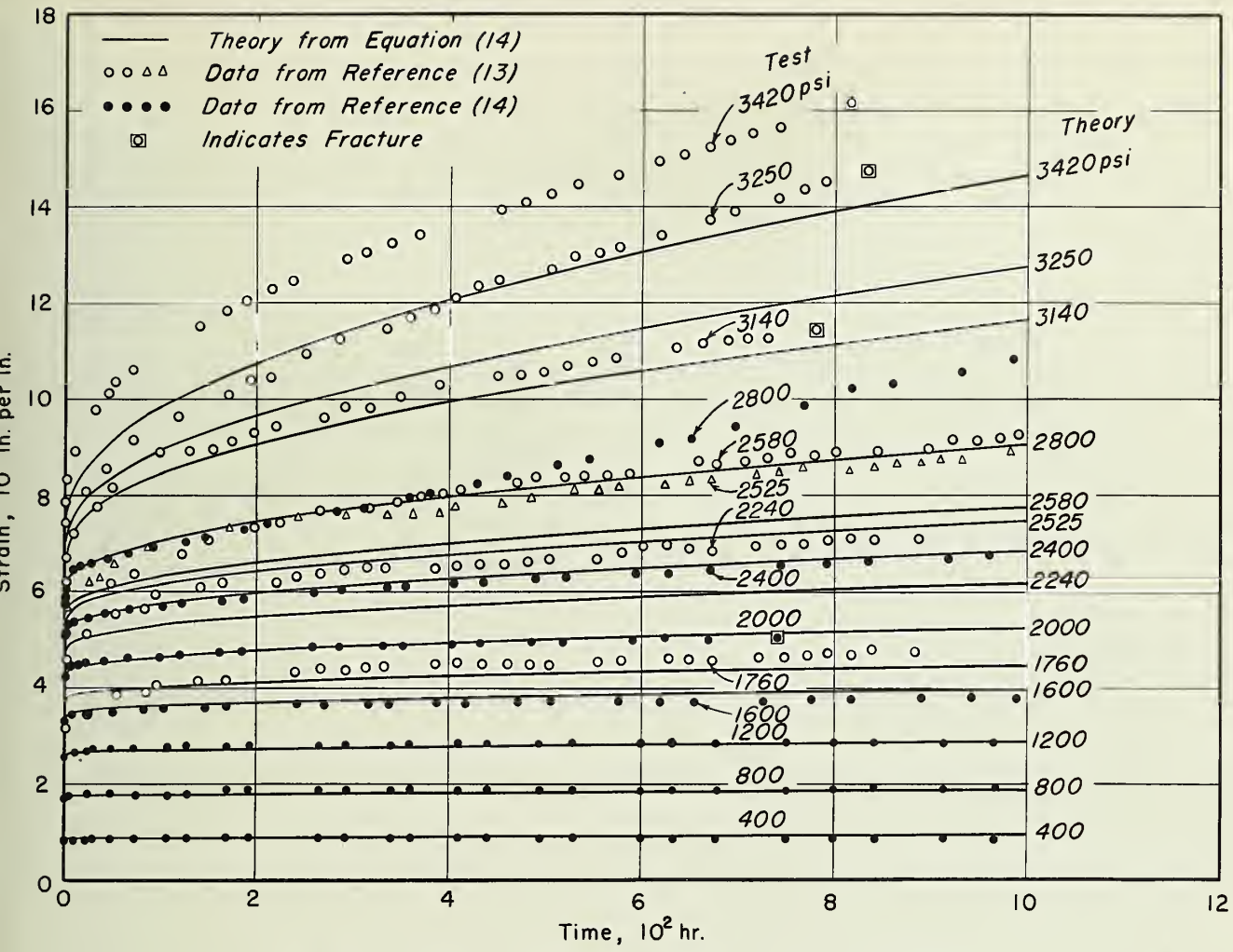

FIG. 4 CREEP TESTS IN TENSION AT DIFFERENT STRESSES FOR POLYSTYRENE AT 77F.

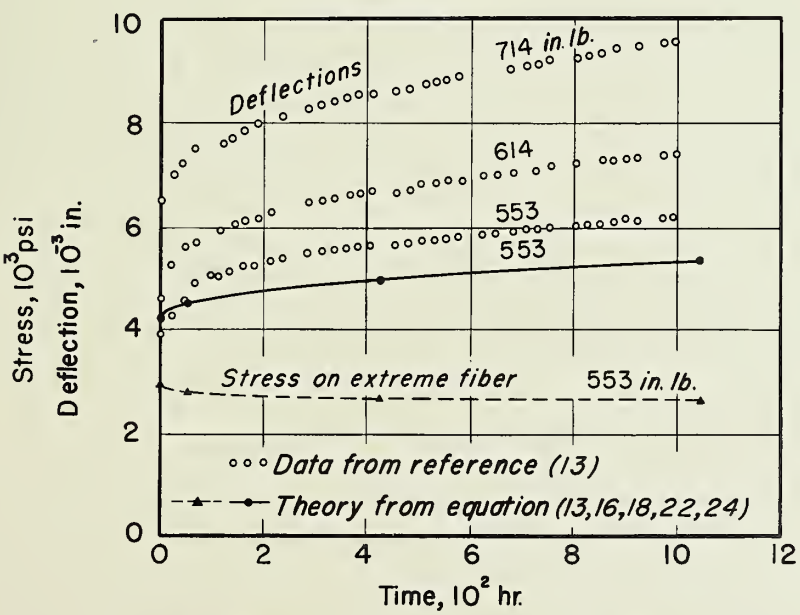

FIG. 5 CREEP TESTS IN BENDING AT DIFFERENT BENDING MOMENTS FOR POLYSTYRENE AT 77°F.

AN EQUATION FOR TENSION CREEP OF THREE UNFILLED THERMOPLASTICS

by

W. N. Findley and Gautam Khosla

A Research Project of the
DEPARTMENT OF THEORETICAL AND APPLIED MECHANICS
UNIVERSITY OF ILLINOIS

Sponsored by
PICATINNY ARSENAL, ORDNANCE CORPS
DEPARTMENT OF THE ARMY

Interim Report No. 4
on
The Relationship Between Time Sensitive
Mechanical Properties of Plastics

Contract No. DA-11-022-ORD-401, Project No. TB4-721

Urbana, Illinois
April, 1954

Interim Report No. 4

on a research project entitled
Study of Relationships Between
Time Sensitive Mechanical
Properties of Plastics

Project Supervisor: W. N. Findley

An Equation for Tension Creep of Three Unfilled Thermoplastics

W. N. Findley
Research Associate Professor of
Theoretical and Applied Mechanics
University of Illinois

Gautam Khosla
Research Assistant in
Theoretical and Applied Mechanics
University of Illinois

Department of Theoretical and Applied Mechanics
University of Illinois

SUMMARY

Results of creep tests of the following plastics are reported: (a) polyethylene

(b) Polychlorotrifluoroethylene (Kel-F), crystalline, and

(c) polyvinyl chloride (Geon 404), annealed.

Each of the plastics was loaded in tension creep at several different values of stress. Creep tests were performed at a temperature of 77°F and a relative humidity of 50%.

Creep strains observed in these tests were compared with those obtained theoretically by assuming a creep equation of the form:

$$\epsilon = \epsilon_o' \sinh \frac{\sigma}{\sigma_\epsilon} + m' t^n \sinh \frac{\sigma}{\sigma_m}$$

where ϵ = strain, σ = stress, t = time and n, ϵ_o', σ_ϵ, m', and σ_m are constants.

It is shown that the experimental creep curves are very well described by the above creep equation.

CONCLUSIONS

It was observed that a creep equation of the form

$$\epsilon = \epsilon_o' \sinh \frac{\sigma}{\sigma_\epsilon} + m' t^n \sinh \frac{\sigma}{\sigma_m}$$

where ϵ_o', σ_ϵ, m', σ_m and n are constants, described the experimental creep data for the three plastics very well.

The rate of creep at 500 hours and the percentage increase in strain from 20 seconds to 500 hours was the greatest for Polyethylene and the least for Kel-F (crystalline). However, the total creep at 500 hours was the greatest for Kel-F (crystalline) and the least for Geon-404 (annealed).

Crazing of Kel-F (crystalline) occurred at the highest stress of $\sigma = 3600$ psi., so that the total creep, creep rate and percentage increase in creep were unusually high at this stress. Further study in this connection is warranted.

DISTRIBUTION LIST

INTERIM AND FINAL REPORTS

Contract No. DA-11-022-ORD-401 Project No. TB4-721

Commanding Officer
Attn: Technical Division (2)
R and D Contract Section
Picatinny Arsenal
Dover, New Jersey

Commanding Officer
Attn: Library
Picatinny Arsenal
Dover, New Jersey

Chicago Ordnance District
Attn: R and D Branch
209 West Jackson Boulevard
Chicago 6, Illinois

Chief of Ordnance
Attn: ORDTB (10)
Department of the Army
Washington 25, D. C.

Chief of Ordnance
Attn: ORDTX-AR
Department of the Army
Washington 25, D. C.

Chief of Ordnance
Attn: ORDTA
Department of the Army
Washington 25, D. C.

Chief of Ordnance
Attn: ORDTR
Department of the Army
Washington 25, D. C.

Chief of Ordnance
Attn: ORDTS
Department of the Army
Washington 25, D. C.

Chief of Ordnance
Attn: ORDTT
Department of the Army
Washington 25, D. C.

Chief of Ordnance
Attn: ORDTU
Department of the Army
Washington 25, D. C.

Chief of Ordnance
Attn: ORDIX (2)
Department of the Army
Washington 25, D. C.

Chief of Ordnance
Attn: ORDFX (2)
Department of the Army
Washington 25, D. C.

Department of the Navy
Office of Naval Research
Attn: Code 423
Washington 25, D. C.

Department of the Navy
Bureau of Aeronautics
Airborne Equipment Division
Materials Branch
Washington 25, D. C.

Signal Corps Engineering Laboratory
Squier Signal Laboratory
Materials Section
Attn: Mr. Luis Reiss
Fort Monmouth, New Jersey

Chemical Corps
Attn: Mr. T. P. Steinmetz
Technical Command
Army Chemical Center, Md.

Commanding General
U. S. Air Force (2)
Air Material Command
Engineering Division
Materials Laboratory
Attn: Mr. Robert T. Schwartz, WCRTS
Mr. Peterson, WCRTE
Wright-Patterson Air Base, Ohio

Department of the Navy
Attn: Mr. H. A. Perry
Naval Ordnance Laboratory
8050 Georgia Avenue
Silver Springs, Maryland

Director of Naval Research
Attn: Technical Information Officer
Washington 25, D.C.

Department of the Navy
Bureau of Ships (2)
Research and Development
Material Development Division
Attn: Mr. J. B. Alfors, Code 346
Mr. J. G. Kuenzel, Code 345
Washington 25, D. C.

Department of the Navy
Attn: Code Re 1
Bureau of Ordnance
Research and Development Division
Materials and Handling Branch
Washington 25, D. C.

Engineer Center
Engineer Research and Development
Laboratories
Attn: Mr. Philip Mitton
Materials Branch
Fort Belvoir, Virginia

Office of the Quartermaster General
Research and Development Division
Attn: Dr. Warren Stubblebine
Chemical and Plastics Section
Washington, D. C.

Department of Commerce
Attn: Mr. Frank W. Reinhart
National Bureau of Standards
Romm 4022, Industrial Building
Washington 25, D. C.

Department of the Navy
Attn: Mr. M. N. DeNeale
Naval Gun Factory
Metallurgical and Testing Branch
M and 8th Streets, S. E.
Washington 25, D. C.

Office of Ordnance Research
Box CM
Duke Station
Durham, North Carolina

Commanding Officer
Attn: Technical Division (2)
Detroit Arsenal
28251 Van Dyke
Centerline, Michigan

Commanding Officer
Attn: Technical Division (2)
Aberdeen Proving Ground, Md.

Commanding Officer
Attn: Technical Division
White Sands Proving Ground
Las Cruces, New Mexico

Commanding Officer
Attn: Technical Division
Redstone Arsenal
Huntsville, Alabama

Commanding Officer
Attn: Technical Division (2)
Frankford Arsenal
Bridesburgh Station
Philadelphia 37, Pennsylvania

Commanding Officer
Attn: Technical Division
Picatinny Arsenal
Dover, New Jersey

Commanding Officer
Attn: Technical Division
Rock Island Arsenal
Rock Island, Illinois

Commanding Officer
Attn: J. L. Bluhm, Laboratory
Springfield Armory
Springfield 1, Massachusetts

Commanding Officer
Attn: Technical Division
Watertown Arsenal
Watertown 72, Massachusetts

Commanding Officer
Attn: Technical Division
Watervliet Arsenal
Watervliet, New York

Aerojet Engineering Corp.
Azusa, California
Attn: Dr. Paul J. Blatz

Allegany Ballistics Lab.
Cumberland, Maryland
Attn: Mr. Harry Winnerling

Naval Ordnance Test Station
Code 4021
Inyokern, China Lake, Calif.
Attn: Mr. D. D. Ordahl

Naval Powder Factory
Indian Head, Maryland
Attn: Mr. A. S. Johnson

Thiokol Corp., Redstone Div.
Huntsville, Alabama
Attn: Mr. W. I. Dale, Jr.

Chief Superintendent
C.A.R.D.E. N-8-3-5
P.O. Box 1427
Quebec, Que, Canada
Attn: Mr. I. R. Cameron

ACKNOWLEDGMENT

This is a portion of a project which was conducted in the Department of Theoretical and Applied Mechanics, as a part of the work of the Engineering Experiment Station of the University of Illinois, in cooperation with Picatinny Arsenal, Ordnance Corps, Department of the Army.

The authors are indebted to R. G. Carlier, B. K. Ghandhi and W. J. Worley for observation of data, to D. M. Sen for checking of results, and to B. G. Hering for preparation of illustrations.

The gift of the sample of polyethylene by the Plax Corporation and the sample of Kel-F by the M. W. Kellogg Company are gratefully acknowledged. Also, the cooperation of the B. F. Goodrich Chemical Company and Nixon Nitration Works in preparing a special sample of Geon 404 is appreciated.

AN EQUATION FOR TENSION CREEP OF THREE UNFILLED THERMOPLASTICS

Introduction

Efforts to express creep behavior by a mathematical expression have been attempted by various authors. Creep strain at constant load has been described by both linear and non-linear functions of time.

For the plastics under consideration, creep strain is a non-linear function of time, as, at no stage of the creep curve was the creep rate constant. A few of the investigations in which creep has been observed to be a non-linear function of time are given below:

Leaderman[1]* expressed creep of Bakelite under torsion as:

$$\epsilon = A \cdot \log t + B \cdot t + C \qquad (1)$$

where ϵ = creep strain, t = time and A, B, and C are constants which are functions of stress and of the material.

The same type of equation has been used by Telfair, Carswell and Nason[2] for phenolic plastics and later by Lyons[3] for tire cords.

Cottrel and Aytekin[4] used a modification of the Andrade equation for single crystals:

$$\epsilon = \epsilon_o + At^{1/3} + Bt \qquad (2)$$

where ϵ = shear strain at time t, ϵ_o = instantaneous shear strain, and A and B are constants.

---

* Superior numbers in parentheses refer to the references at the end of this paper.

Pao and Marin[5] used the following expression for creep:

$$\epsilon = A + B(1-e^{-ct}) + Dt \tag{3}$$

where again constants A, B, c and D are functions of stress and of the material.

For the present tests, however, the following creep equation[6,7,8] was employed:

$$\epsilon = \epsilon_o + mt^n \tag{4}$$

where n is a constant, while ϵ_o and m are hyperbolic sine functions of stress σ and are expressed by

$$\begin{aligned} \epsilon_o &= \epsilon_o' \sinh \frac{\sigma}{\sigma_\epsilon} \\ m &= m' \sinh \frac{\sigma}{\sigma_m} \end{aligned} \tag{5}$$

where ϵ_o', m', σ_ϵ and σ_m are constants of the material.

Writing Eq. 4 in the final form by the help of Eq. 5:

$$\epsilon = \epsilon_o' \sinh \frac{\sigma}{\sigma_\epsilon} + m't^n \sinh \frac{\sigma}{\sigma_m} \tag{6}$$

Eq. 6 has been used to describe the creep of polyethylene, Kel-F (crystalline) and Geon-404 (annealed) in this report and shows a good agreement with the experimental results.

Materials

Polyethylene was obtained in the form of a compression molded sheet 9/16" thick from Plax Corporation, Con. The molding powder used in fabricating the sheet of polyethylene was

Bakelite DE 2400, having a melt index of about 1.2 decigrams/ minute with an extrapolated number-average molecular weight of approximately 22,000. There were no additives or anti-oxidants employed.

The molding powder was preheated for 25 minutes at a pressure of 5 psi. The pressure was then raised to approximately 30 psi. for 4 minutes and then left in the press for about 30 minutes with water at 60°F running through the cooling platens. It was reported that such a thick sheet probably contained a large proportion of the crystalline phase.

Kel-F (polychlorotrifluoroethylene) of grade 300 was obtained in sheets of 1/8 in. thickness from the M. W. Kellogg Co. This grade was unplasticized and represents the highest molecular weight in the form of molding powder. The high density molding powder had a compression ratio of 2 to 1. The sheets were compression molded under a pressure of 2500 to 3000 psi. and at a temperature of 480 to 500°F. The crystalline form of Kel-F was obtained after pressing by dropping the temperature quickly by means of steam to 450°F then cooling to room temperature in the press. It required 6 to 8 hours to cool.

Geon 404 (polyvinyl chloride) was obtained as a sheet 9/16 inch thick from the Nixon Nitration Works. The formulation was designated VX-108 Natural and contained no plasticizer, 3.3% dibutal-tin-diborate as a stabilizer, and 0.5% stearic acid as a lubricant. The ingredients were mixed and blended at 280°F and calendered into sheets 0.02 in. thick on rolls having a temperature of 300°F. About 28 of these sheets were laminated

together in a hydraulic press to form the final sheet and remove most of the residual strain resulting from the calendering. The sheets were subjected to a pressure of 280 psi. at 315°F for about 30 min. and then cooled rapidly in the press.

Before the test specimens were formed the material was given a second anneal by heating it in an electric oven at 275°F for 15 min. The anneal was observed to cause a shrinkage of 5.7% in width and an expansion of 1.6% in length measured at the surface of the sheet.

Specimens

A milling cutter was used to cut the creep specimens from the original sheet. For polyethylene and Geon-404 the flat side of the specimen was perpendicular to the plane of the sheet, while for Kel-F it was in the same plane. All reduced sections and radii at the ends were formed on a shaper. All the specimens were finished by sanding with No. 0 emery cloth. The dimensions of the specimens are given in Fig. 1.

Apparatus and Test Procedure

The equipment used for conducting the creep tests was the same as reported previously[9] for creep tests of five laminated plastics.

Creep specimens for each plastic were tested simultaneously under a constant tension load at several different values of stress. The values of stress chosen were evenly spaced from zero to a maximum value. One specimen of each plastic was tested at a stress of zero in order to determine the magnitude

of the shrinkage which might occur due to gradual changes in moisture content or other time dependent phenomena, such as aging.

All creep tests were conducted at a constant temperature of $77^{\circ} \pm 1^{\circ}F$ and a constant relative humidity of 50 ± 2 percent for the entire 500 hours of the test. After noting the initial extensometer reading just prior to application of the load, readings of strain and time were taken at the following time intervals: 20 seconds, then 1, 2, 3, 5, 7, 10, 12, 15, 18, 30, 42 minutes, then 1, 2, 3, 5, 7, 15, 18 hours, and then every 24 hours to about 500 hours.

Further information about the apparatus and test procedure is given in reference (9).

Results

The creep curves of polyethylene are shown in Fig. 1. For each of the stresses σ = 75, 150, 225 and 300 psi, two test specimens were used. In order to make correction for changes in relative humidity and temperature, an additional specimen at zero stress was used as a control.

The creep curves of Kel-F (crystalline) and Geon-404 (annealed) were obtained in a similar manner, i.e. using four different stresses and a total of nine test specimens for each of the plastics.

Evaluation of Creep Constants

In order to describe the experimental creep curves by Eq. 6, it was necessary to evaluate the constants n, ϵ_o', σ_o, m_o' and σ_m for each of the plastics by using the corresponding experimental creep curves.

The following procedure was employed for all the creep curves of a given material: Rearranging Eq. 4 and taking logarithms of both sides:

$$\log(\epsilon - \epsilon_o) = \log m + n \log t \qquad (7)$$

Eq. 7 represents a straight line with $\log (\epsilon-\epsilon_o)$ as ordinate and log t as abscissa. Thus a particular value of ϵ_o was selected, such that when $\log (\epsilon-\epsilon_o)$ was plotted against log t, the creep data fell on a straight line. The ordinate of this straight line at t = 1 hour provided the value of m while the slope of the straight line yielded the value of n.

Values of ϵ_o' and m' were obtained by the use of Eq. 5. Appropriate values of σ_ϵ and σ_m were chosen so that ϵ_o vs $\sinh \frac{\sigma}{\sigma_\epsilon}$ and m vs. $\sinh \frac{\sigma}{\sigma_m}$ were straight lines. The slopes of these lines, then, yielded the values of constants ϵ_o' and m', respectively.

The procedure for evaluation of these constants is illustrated for polyethylene. If strains ϵ and time t shown in Fig. 1 are plotted on a log-log graph, the data fall on a curve which is convex downwards. In order to straighten this curve the proper choice of ϵ_o was made such that when $\log (\epsilon-\epsilon_o)$ was plotted against log t, the data were on a straight line.

The data for each different stress were treated in this manner and are shown as straight lines in Fig. 2. The slopes of these lines are the same and yield the value of n, while the value of m was read at t = 1 hr. It was observed that both m and ϵ_o increased with increase of stress σ. Similar diagrams for Kel-F (crystalline) and Geon-404 (annealed) are given in Fig. 3 and Fig. 4. The fact that the data are nearly on a straight line indicates agreement with the data.

For evaluating constants ϵ_o', σ_ϵ, m' and σ_m, of polyethylene, reference may be made to Fig. 5. Appropriate values of σ_ϵ and σ_m were chosen so that ϵ_o vs $\sinh \frac{\sigma}{\sigma_\epsilon}$ and m vs $\sinh \frac{\sigma}{\sigma_m}$ yielded straight lines. In order to increase the accuracy of these constants, proper scales for the two axes were chosen so that the straight lines made approximately a 45^o inclination with the axes. The slopes of these lines yielded the values of constants ϵ_o' and m'. Similar diagrams for Kel-F (crystalline) and Geon-404 (annealed) are given in Fig. 6 and Fig. 7. The values of the constants of Eq. 6 are given in Table I for the three plastics. It was observed that for Kel-F (crystalline) the value of n at the highest stress σ = 3600 psi. was much greater than for the lower stresses. A much higher total creep and rate of creep was also observed at this stress. This fact is shown in Fig. 3 where the slope n of the straight-line corresponding to stress σ = 3600 psi is much more than the constant slopes of the other lines at lower stresses.

At this highest stress, a noticeable amount of crazing occurred in Kel-F (crystalline) which probably changed the

structure of the material and may have produced the increase in creep. The stress at which crazing started was determined from a supplementary creep test in which the stress was increased at intervals from 2700 to 3000 to 3300 to 3600 psi. Crazing started after 19 hours at 3300 psi.

The values of strain ϵ computed from Eq. 6 are plotted in Fig. 1 for Polyethylene. These theoretical data show a good comparison with the observed data for all the constant stresses employed. At the highest stress of σ = 300 psi the theoretical values seem to be slightly higher than the observed ones for the interval of time t = 0 to t = 250 hours. This discrepancy may be due to a certain amount of compromise required in selecting the constants, see Fig. 2 and 5, or to errors in observation of the experimental creep curves.

The theoretical values of strain ϵ from Eq. 6 were computed also for Kel-F (crystalline) and Geon-404 (annealed). For these plastics, also, an equally good comparison with the observed data was noticed except for the highest stress σ = 3600 psi for Kel-F (crystalline).

20-Second Elastic Strains

The extent of strain in a plastic after it has been under a constant load for 20 seconds is designated as 20-second

elastic strain. The word "elastic" is justified, because the contribution of the time-dependent strain to the total strain is negligible for such a short interval of time. The 20-second elastic strains of the plastics were found for each of the several constant stresses by plotting the experimental strain ϵ against time t on log-log paper up to a time of one hour. The value of the 20-second strain was then read for a time of 20 seconds from the straight line which resulted from this plotting.

The total strain (elastic plus plastic) at 500 hours for a given stress σ can be read from the creep curves such as Fig. 1. The elastic strain at 20 seconds and the total strain at 500 hours for different stresses are plotted in Fig. 8 for all three of the plastics. It was observed that the appearance of these curves was similar to stress-strain curves in tension.

The tangent moduli of elasticity obtained by measuring the slopes of these curves at about zero stress is shown in Table II. A comparison of the moduli of elasticity obtained from the 20-second elastic strains of the creep curves, with those obtained by a static tension test at the same temperature and relative humidity would be desirable.

However, the values of the moduli of elasticity obtained from the 20-second elastic strain can be compared with those computed by a stress-strain relation for static tension from the creep Eq. 6. This relation was presented in a previous paper[10] in the following form:

$$\epsilon = \epsilon_o' \sinh \frac{\sigma}{\sigma_\epsilon} + \left\{ \frac{m'n}{V} \sinh \frac{\sigma}{\sigma_m} \right\}^{\frac{n}{1-n}} \cdot m' \sinh \frac{\sigma}{\sigma_m} \qquad (8)$$

The constants ϵ_o', σ_ϵ, m', σ_m and n in Eq. 8 are the same as in the creep Eq. 6, while V expresses the strain rate of the tension test curve.

The tangent modulus of elasticity, E, was obtained from Eq. 8 by taking the derivative with respect to stress, as follows:

$$\frac{1}{E} = \frac{\partial \epsilon}{\partial \sigma} = \frac{\epsilon_o'}{\sigma_\epsilon} \cosh \frac{\sigma}{\sigma_\epsilon} + \left(\frac{n}{V} \sinh \frac{\sigma}{\sigma_m} \right)^{\frac{n}{1-n}} \cdot \frac{(m')^{\frac{1}{1-n}}}{(1-n)\sigma_m} \cosh \frac{\sigma}{\sigma_m} \qquad (9)$$

At stress $\sigma = 0$, Eq. 9 yielded the relation

$$E = \frac{\sigma_\epsilon}{\epsilon_o'} \qquad (10)$$

The evaluation of E from Eq. 10 involved the determination of the constants σ_ϵ and ϵ_o'. These constants are given in Table I. The values of the tangent modulus E evaluated theoretically from Eq. 10 together with those obtained by

measuring the slopes of the curves for the 20-second elastic strain in Fig. 8 are given in Table II. A fairly good comparison between the two sets of values was observed.

It was observed that the value computed from Eq. 10 was higher for each material than that measured from the slopes of the curves in Fig. 8. This is in accord with the predictions of Eq. 9 as described in reference (10) In this reference it was shown that the tangent modulus predicted by Eq. 9 decreased rapidly with increase in stress for stresses near zero. Since the slopes measured from Fig. 8 were interpolated from stress values substantially above the origin the values of the moduli should have been less than predicted by Eq. 10, as observed.

Creepocity

Equation (4) for creep can be used to evaluate the percentage increase in strain for a given time interval (called creepocity). See reference (9). The percentage increase in strain, ϕ_1 from $t = 0$ to $t = t_1$ is given by

$$\phi_1 = \frac{(\epsilon_o + mt^n) - \epsilon_o}{\epsilon_o} \times 100 = \frac{m}{\epsilon_o}(100t_1^n) = \frac{m}{\epsilon_o}\psi_1 \qquad (11)$$

where

$$\psi_1 = 100t_1^n \qquad (12)$$

when $m = \epsilon_o \cdot \phi_1$ is independent of stress[9]. But when $m = m' \sinh \frac{\sigma}{\sigma_m}$ and $\epsilon_o = \epsilon_o' \sinh \frac{\sigma}{\sigma_\epsilon}$, ϕ_1 is a function of stress σ as well as time t_1, while ψ_1 is independent of stress and dependent on time t_1 alone. ϕ_1 was found to be nearly

independent of stress for five plastic laminates[9]. The "creepocity" of a plastic, when independent of stress, serves as one measure of its serviceability under conditions of creep. For the materials tested in this investigation, however, the creepocity Φ_1 was a function of stress since ϵ_o did not equal m.

If the percentage increase in strain is determined from t_1 = 20 sec. to t_2 = 500 hrs., Φ is expressed as:

$$\Phi = \left\{ \frac{m/\epsilon_o}{1 + \frac{m}{\epsilon_o} t_1^n} \times 100 \right\} (t_2^n - t_1^n) \qquad (15)$$

The values of Φ determined from the experimental data and given in Table II appear to show no systematic increase with increase of stress for a given plastic. The reasons for this are probably that Φ is not very sensitive to changes in stress, and insufficient accuracy in determining the strains experimentally. However, it was noticed from Table II that the average values of Φ obtained theoretically by use of Eq. 15 compare well with the average value obtained from the experimental data, except for polyethylene.

It was observed that the average value of Φ was highest for polyethylene and lowest for Kel-F (crystalline) which means that the time-sensitivity of polyethylene was the greatest while that for Kel-F was the least.

Rate of Creep

The rate of creep V, at a specified time, was obtained from Eq. 4 or Eq. 6 by taking the derivative of strain ϵ with respect to time t:

$$V = \frac{\partial \epsilon}{\partial t} = mnt^{n-1} = (m'nt^{n-1})\sinh \frac{\sigma}{\sigma_m} \qquad (16)$$

The rate of creep at 500 hours was evaluated by using Eq. 16 and the constants m', σ_m and n which are given in Table I. The results are shown in Table II and are plotted with respect to stress σ for each of the plastics in Fig. 9.

For a given stress, the highest rate of creep was observed for polyethylene and lowest for Kel-F (crystalline).

REFERENCES

1. H. Leaderman, "Creep, Elastic Hysteresis, and Damping, in Bakelite Under Torsion", Trans. A.S.M E., Vol. 61, p. A79, June, 1939.

2. D. Telfair, T. S. Carswell and H. K. Nason, "Creep Properties of Molded Phenolic Plastics," Modern Plastics, Vol. 21, No. 6, pp. 137-144, 174 and 176, February 1944.

3. W. J. Lyons, "General Relations of Flow in Solids and Their Application to the Plastic Behavior of Tire Cords," Journal of Applied Physics, Vol. 17, p. 472, 1946.

4. A. H. Cottrel and V. Aytekin, "Andrade's Creep Law and the Flow of Zinc Crystals," Nature, Vol. 160, p. 328, 1947.

5. Y. Pao and J. Marin, "Deflections and Stresses in Beams Subjected to Bending and Creep," Trans. A.S.M.E., Vol. 74, pp. 478-484, December 1952.

6. R. G. Strum, C. Dumont, and F. M. Howell, "A method of Analyzing Creep Data," Journal of Applied Mechanics, Vol. 3, No. 2, p. A62, June 1939.

7. W. N. Findley, C. H. Adams and W. J. Worley, "The effect of Temperature on the Creep of Two Laminated Plastics as Interpreted by the Hyperbolic-Sine Law and Activation Energy Theory," Proceedings, A.S.T.M , Vol. 48, p. 1217, 1948.

8. W. N. Findley, "Creep Characteristics of Plastics," 1944 Symposium on Plastics, A.S.T.M., p. 18, 1944.

9. W. N. Findley and W. J. Worley, "Mechanical Properties of Five Laminated Plastics," NACA Tech. Note 1560, August, 1948.

10 W. N. Findley, "Derivation of a Stress-Strain Equation from Creep Data for Plastics," Proceedings of the First U.S. National Congress of Applied Mechanics, Chicago, Illinois, p. 595, June 11-16, 1951.

TABLE I. CONSTANTS OF CREEP EQUATION FOR THREE PLASTICS

MATERIAL	n	ϵ'_o, percent	m', percent	σ_ϵ, psi	σ_m, psi
Polyethylene	0.0890	1.350	0.397	400	185
Kel-F (Crystalline)	0.0872*	0.810	0.099	2600	1475
Geon-404 (Annealed)	0.3109	1.150	0.018	6000	2100

* For stresses σ = 900, 1800, 2700 psi, n = 0.0872 while for σ = 3600 psi, n = 0.185.

TABLE II. ANALYSIS OF CREEP DATA

MATERIAL	Stress σ, psi	20-sec. Elastic Strain, ϵ_o, Percent	Mod. of Elasticity E_o from 20-sec. Strain Curves, psi.	Mod. of Elasticity from Theory, $E_o = \frac{\sigma_o}{\epsilon_o'}$, psi.	Total Creep at 500 hrs., percent	Rate of Creep V at 500 hrs., From Theory, 10^{-8} in./in.hr.	Percent Increase in Strain from 20 sec. to 500 hrs. ϕ (exptl.) percent	ϕ (theo.) percent
Polyethylene	75	0.290	0.025×10^6	0.0296×10^6	0.573	51.17	97.6	51.14
	150	0.627			1.163	110.89	85.4	53.41
	225	1.029			1.892	189.08	83.8	57.17
	300	1.500			2.735	298.77	82.6	62.30
						AVERAGE	87.3	56.00
Kel-F (Crystalline)	900	0.345	0.274×10^6	0.321×10^6	0.393	19.25	13.9	21.28
	1800	0.706			0.862	45.91	22.1	23.56
	2700	1.163			1.544	90.19	32.7	27.34
	3600	1.697			3.245	169.32	91.1*	32.63
						AVERAGE	22.9	26.20
Geon-404 (Annealed)	1000	0.170	0.501×10^6	0.521×10^6	0.224	38.35	31.2	30.68
	2000	0.374			0.521	85.57	39.0	32.24
	3000	0.648			0.855	152.54	32.0	39.29
	4000	0.827			1.302	254.78	57.4	47.56
						AVERAGE	39.9	37.69

* Last value excluded from average because of crazing.

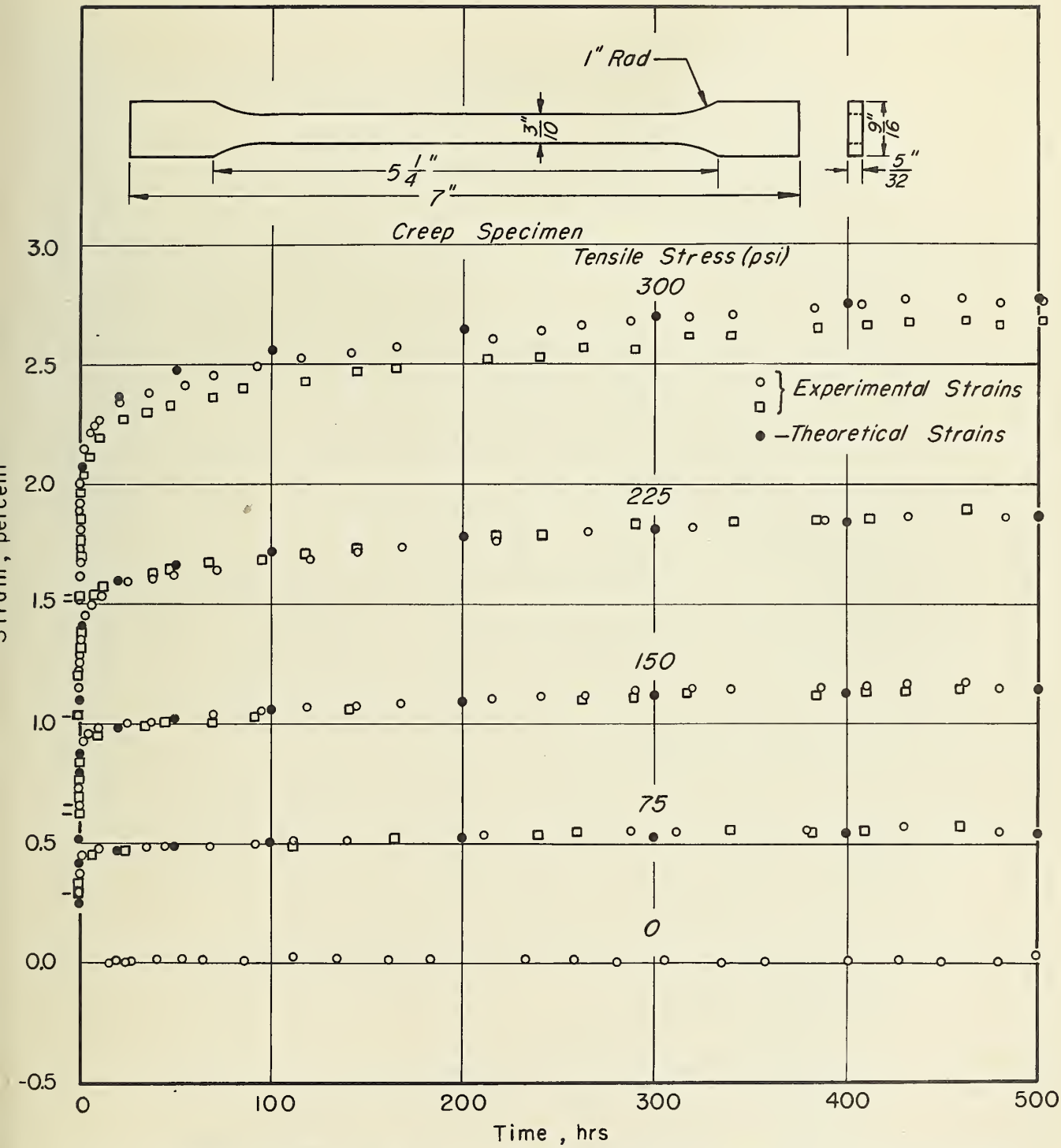

FIG. 1. CREEP AGAINST TIME FOR TENSION CREEP TESTS OF POLYETHYLENE FOR 500 HOURS AT CONSTANT LOAD. TEMPERATURE, 77°F ; RELATIVE HUMIDITY, 50 PERCENT. FIRST TEST POINT FOR EACH SPECIMEN IN A SERIES OF CREEP TESTS IS INDICATED BY A SHORT DASH LINE.

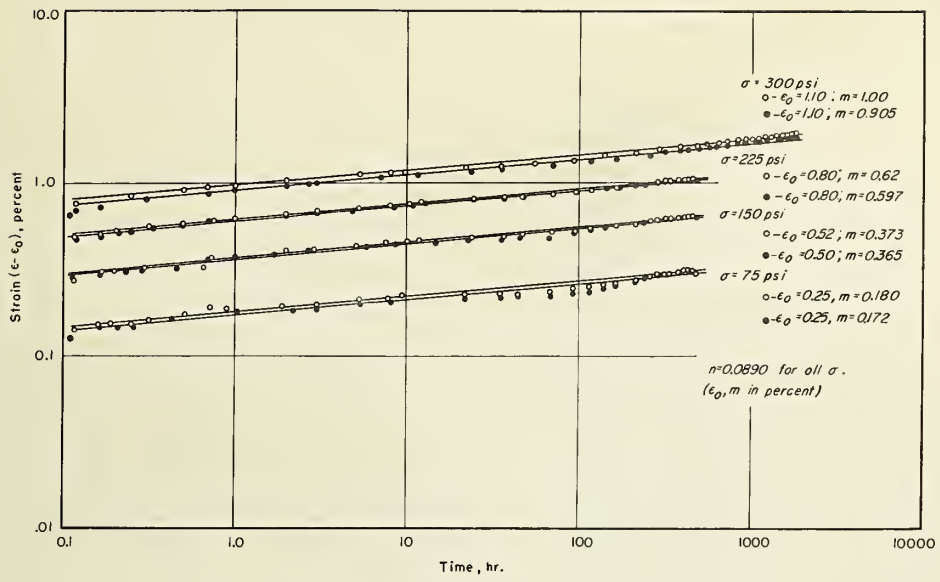

FIG 2. EVALUATION OF CONSTANTS ϵ_0, m, AND n FOR POLYETHYLENE.

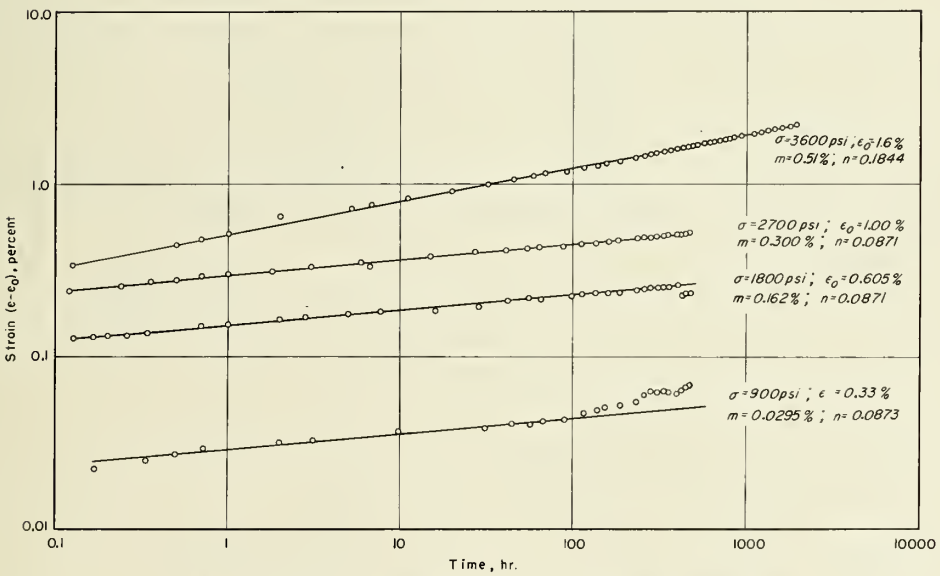

FIG 3. EVALUATION OF CONSTANTS ϵ_0, m, AND n FOR KEL-F (CRYSTALLINE)

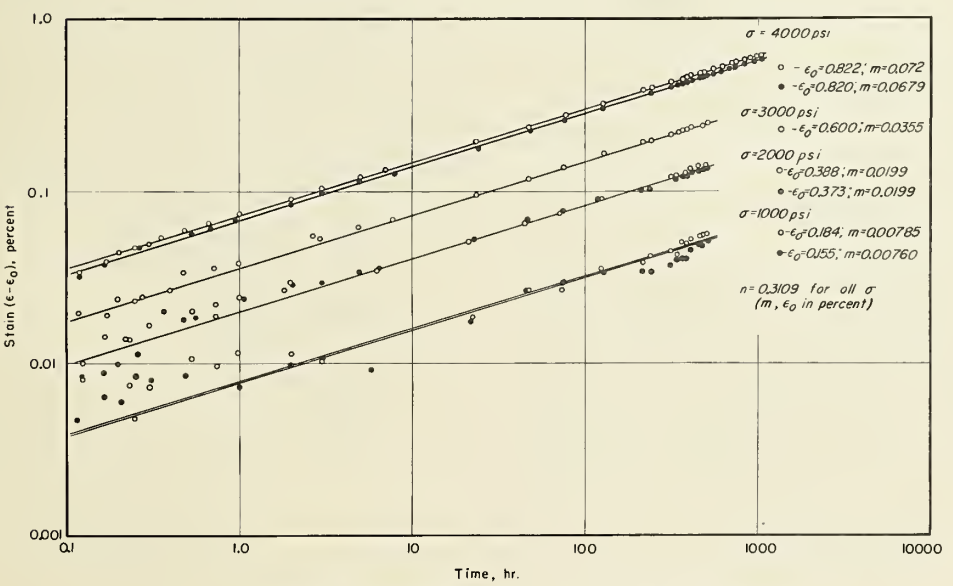

FIG 4 EVALUATION OF CONSTANTS ϵ_0, m, AND n FOR GEON-404 (ANNEALED).

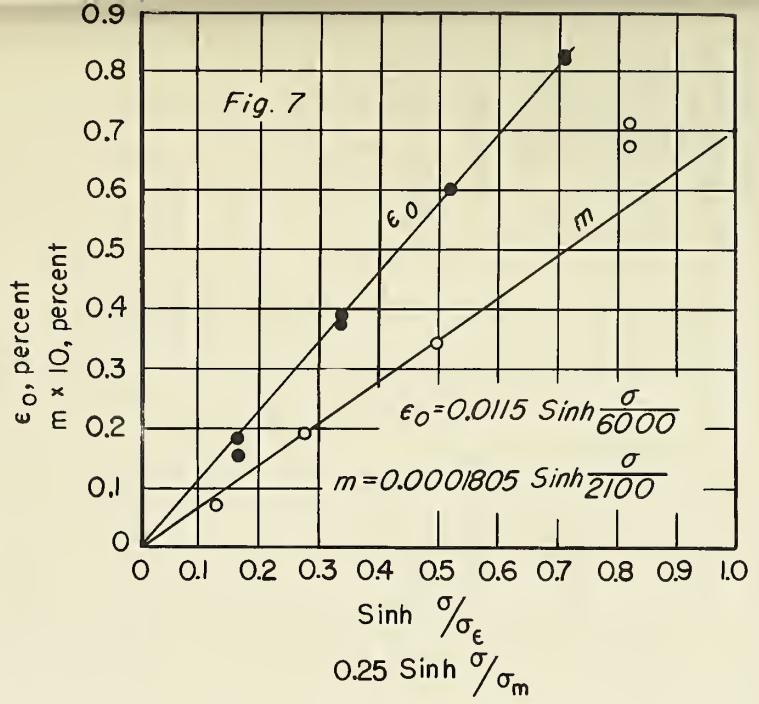

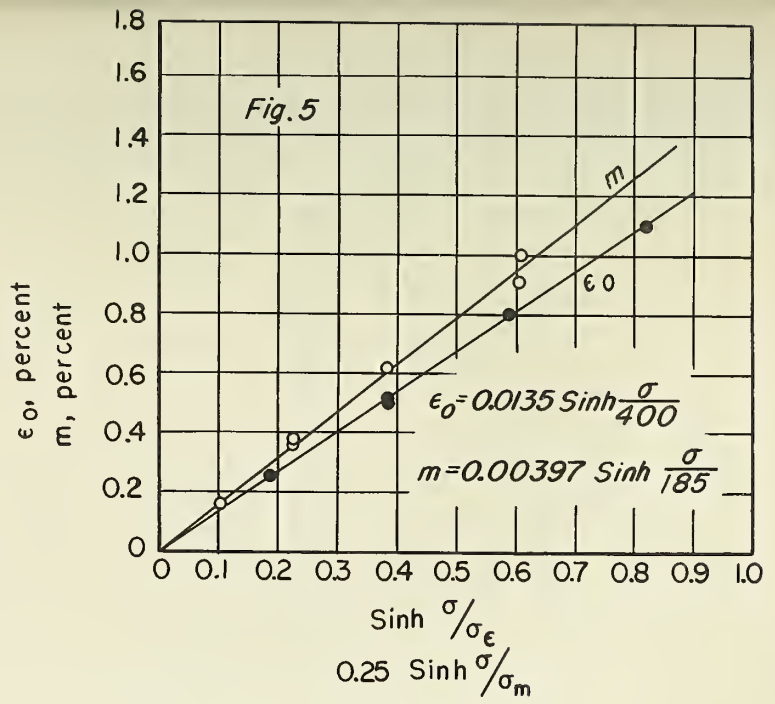

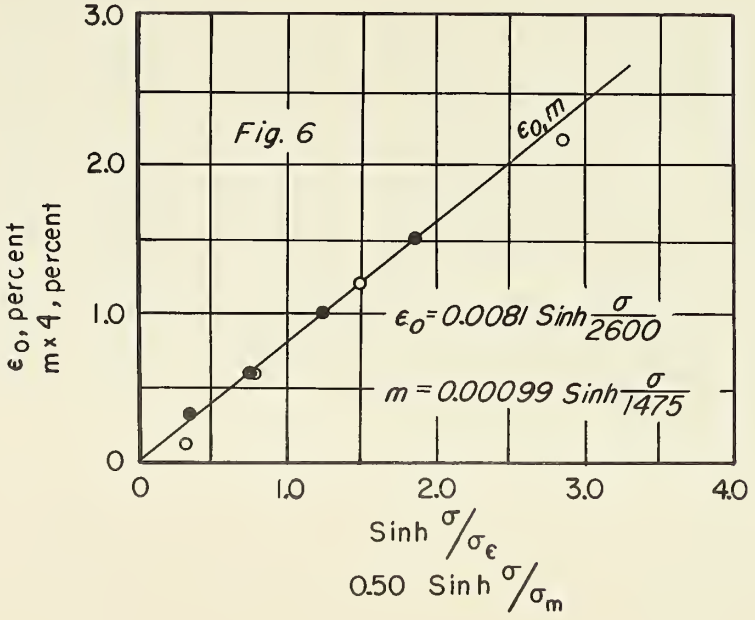

FIG. (5, 6, 7) EVALUATION OF CONSTANTS σ_ϵ, σ_m, ϵ_o' AND m' FOR POLYETHYLENE, KEL-F (CRYSTALLINE), AND GEON-404 (ANNEALED), RESPECTIVELY.

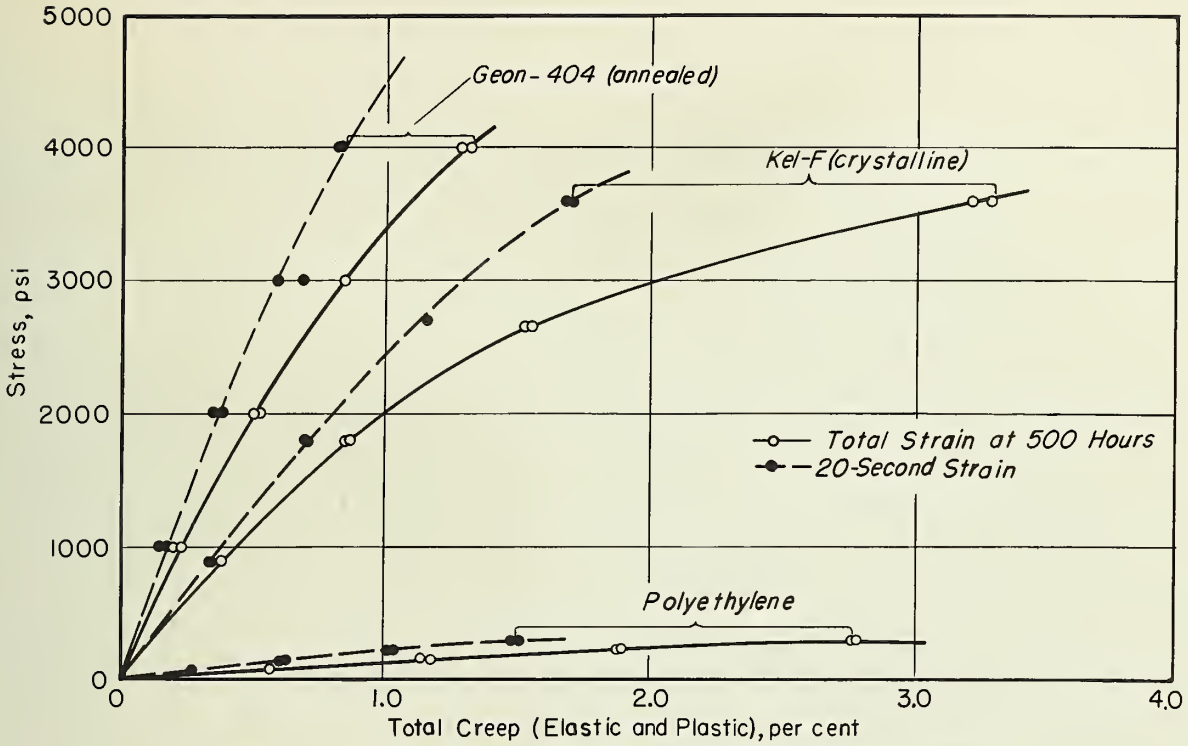

FIG. 8:–EFFECT OF STRESS ON 20-SECOND ELASTIC STRAIN AND ON TOTAL CREEP AT 500 HOURS FOR THREE PLASTICS.

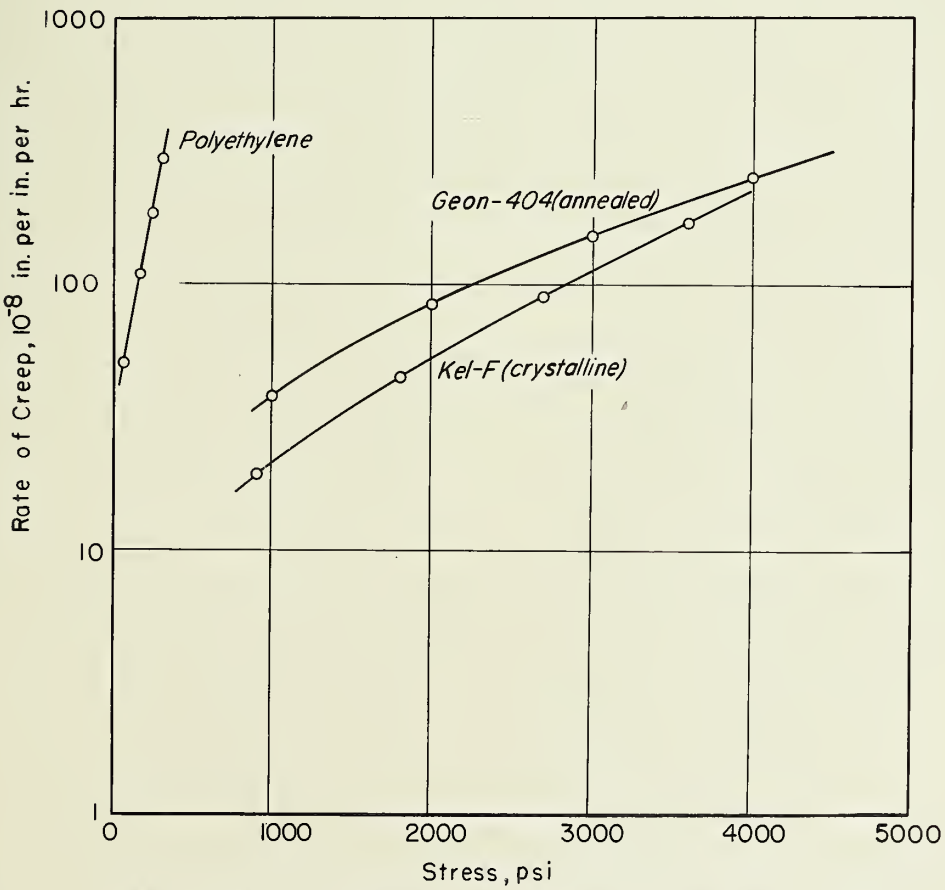

FIG. 9 RATE OF CREEP AT 500 HOURS AGAINST STRESS FOR THE THREE PLASTICS AS COMPUTED FROM EQUATION 16.

EFFECT OF CRYSTALLINITY AND CRAZING, AGING, AND RESIDUAL STRESS ON CREEP OF KEL-F, CANVAS LAMINATE, AND GEON RESPECTIVELY

by
William N. Findley

A Research Project of the
Department of Theoretical and Applied Mechanics
University of Illinois

Sponsored by
Picatinny Arsenal, Ordnance Corps
Department of the Army

Interim Report No. 7
on
The Relationship Between Time Sensitive
Mechanical Properties of Plastics

Contract No. DA-11-022-ORD-401, Project No.TB 4-721

Urbana, Illinois
May, 1954

Interim Report No. 7

on a research project entitled
Study of Relationship Between
Time Sensitive Mechanical
Properties of Plastics

Project Supervisor, W. N. Findley

EFFECT OF CRYSTALLINITY AND CRAZING, AGING, AND RESIDUAL STRESS ON CREEP OF KEL-F, CANVAS LAMINATE, AND GEON RESPECTIVELY

by

William N. Findley

Research Associate Professor

Department of Theoretical and Applied Mechanics

University of Illinois

EFFECT OF CRYSTALLINITY AND CRAZING, AGING, AND RESIDUAL STRESS ON CREEP OF KEL-F, CANVAS LAMINATE, AND GEON RESPECTIVELY

by William N. Findley[1]

SUMMARY

Results of tension creep tests at 77° F and 50 percent relative humidity are presented which show the effect of the following variables:

(a) the degree of crystallization of monochlorotrifluorethylene (Kel-F)

(b) residual stresses remaining after fabrication of sheets of polyvinylchloride (Geon 404) and

(c) aging of grade-C canvas laminate at 77° F and 50 percent relative humidity.

The Kel-F was tested in the amorphous, fully crystalline and intermediate (commerical) state. The effect of residual stresses was shown by tests of samples of Geon 404 before and after an anneal at 275° F which resulted in shrinkage of the material. The canvas laminate was tested in creep before and after aging at constant temperature and humidity for about ten years.

---

[1] University of Illinois

CONCLUSIONS

1. Creep of Kel-F was markedly influenced by crystallinity. The most crystalline material was the most resistant to creep.
2. Crazing of Kel-F was found to result from creep. At the same stress the amorphous sample showed some crazing, intermediate samples showed none, and the crystalline sample crazed.
3. Creep produced crazing in the crystalline Kel-F in 19 hr. at 2210 psi, and at 3600 psi considerable crazing was present.
4. When crazing occurred the creep strains were much larger than without crazing.
5. Residual tensile stresses in Geon 404 resulted in greater creep.
6. Aging of grade-C canvas laminate produced a substantial reduction in creep.

DISTRIBUTION LIST

INTERIM AND FINAL REPORTS

Contract No. DA-11-022-ORD-401 Project No. TB4-721

Commanding Officer
Attn: Technical Division (2)
R and D Contract Section
Picatinny Arsenal
Dover, New Jersey

Commanding Officer
Attn: Library
Picatinny Arsenal
Dover, New Jersey

Chicago Ordnance District
Attn: R and D Branch
209 West Jackson Boulevard
Chicago 6, Illinois

Chief of Ordnance
Attn: ORDTB (10)
Department of the Army
Washington 25, D. C.

Chief of Ordnance
Attn: ORDTX-AR
Department of the Army
Washington 25, D. C.

Chief of Ordnance
Attn: ORDTA
Department of the Army
Washington 25, D. C.

Chief of Ordnance
Attn: ORDTR
Department of the Army
Washington 25, D. C.

Chief of Ordnance
Attn: ORDTS
Department of the Army
Washington 25, D. C.

Chief of Ordnance
Attn: ORDTT
Department of the Army
Washington 25, D. C.

Chief of Ordnance
Attn: ORDTU
Department of the Army
Washington 25, D. C.

Chief of Ordnance
Attn: ORDIX (2)
Department of the Army
Washington 25, D. C.

Chief of Ordnance
Attn: ORDFX (2)
Department of the Army
Washington 25, D. C.

Department of the Navy
Office of Naval Research
Attn: Code 423
Washington 25, D. C.

Department of the Navy
Bureau of Aeronautics
Airborne Equipment Division
Materials Branch
Washington 25, D. C.

Signal Corps Engineering Laboratory
Squier Signal Laboratory
Materials Section
Attn: Mr. Luis Reiss
Fort Monmouth, New Jersey

Chemical Corps
Attn: Mr. T. P. Steinmetz
Technical Command
Army Chemical Center, Md.

Commanding General
U. S. Air Force (2)
Air Material Command
Engineering Division
Materials Laboratory
Attn: Mr. Robert T. Schwartz, WCRTS
Mr. Peterson, WCRTE
Wright-Patterson Air Base, Ohio

Department of the Navy
Attn: Mr. H. A. Perry
Naval Ordnance Laboratory
8050 Georgia Avenue
Silver Springs, Maryland

Director of Naval Research
Attn: Technical Information Officer
Washington 25, D.C.

Department of the Navy
Bureau of Ships (2)
Research and Development
Material Development Division
Attn: Mr. J. B. Alfors, Code 346
Mr. J. G. Kuenzel, Code 345
Washington 25, D. C.

Department of the Navy
Attn: Code Re 1
Bureau of Ordnance
Research and Development Division
Materials and Handling Branch
Washington 25, D. C.

Engineer Center
Engineer Research and Development
Laboratories
Attn: Mr. Philip Mitton
Materials Branch
Fort Belvoir, Virginia

Office of the Quartermaster General
Research and Development Division
Attn: Dr. Warren Stubblebine
Chemical and Plastics Section
Washington, D. C.

Department of Commerce
Attn: Mr. Frank W. Reinhart
National Bureau of Standards
Romm 4022, Industrial Building
Washington 25, D. C.

Department of the Navy
Attn: Mr. M. N. DeNeale
Naval Gun Factory
Metallurgical and Testing Branch
M and 8th Streets, S. E.
Washington 25, D. C.

Office of Ordnance Research
Box CM
Duke Station
Durham, North Carolina

Commanding Officer
Attn: Technical Division (2)
Detroit Arsenal
28251 Van Dyke
Centerline, Michigan

Commanding Officer
Attn: Technical Division (2)
Aberdeen Proving Ground, Md.

Commanding Officer
Attn: Technical Division
White Sands Proving Ground
Las Cruces, New Mexico

Commanding Officer
Attn: Technical Division
Redstone Arsenal
Huntsville, Alabama

Commanding Officer
Attn: Technical Division (2)
Frankford Arsenal
Bridesburgh Station
Philadelphia 37, Pennsylvania

Commanding Officer
Attn: Technical Division
Picatinny Arsenal
Dover, New Jersey

Commanding Officer
Attn: Technical Division
Rock Island Arsenal
Rock Island, Illinois

Commanding Officer
Attn: J. L. Bluhm, Laboratory
Springfield Armory
Springfield 1, Massachusetts

Commanding Officer
Attn: Technical Division
Watertown Arsenal
Watertown 72, Massachusetts

Commanding Officer
Attn: Technical Division
Watervliet Arsenal
Watervliet, New York

Aerojet Engineering Corp.
Azusa, California
Attn: Dr. Paul J. Blatz

Allegany Ballistics Lab.
Cumberland, Maryland
Attn: Mr. Harry Winnerling

Naval Ordnance Test Station
Code 4021
Inyokern, China Lake, Calif.
Attn: Mr. D. D. Ordahl

Naval Powder Factory
Indian Head, Maryland
Attn: Mr. A. S. Johnson

Thiokol Corp., Redstone Div.
Huntsville, Alabama
Attn: Mr. W. I. Dale, Jr.

Chief Superintendent
C.A.R.D.E. N-8-3-5
P.O. Box 1427
Quebec, Que, Canada
Attn: Mr. I. R. Cameron

Armed Service Technical
Information Agency
Document Service Center
Knott Building
Dayton 2, Ohio

ACKNOWLEDGMENT

This work was performed in the Department of Theoretical and Applied Mechanics as a part of the work of the Engineering Experiment Station of the University of Illinois, in cooperation with Picatinny Arsenal, Ordnance Corps, Department of the Army.

The author wishes to acknowledge the assistance of R. G. Carlier, B. K. Ghandhi, H. S. Harper, R. G. Hering, G. Khosla, and D. M. Sen in performing the tests and preparing the data.

The gift of samples of Kel-F by the M. W. Kellogg Company and the samples of canvas laminate by the Synthane Corporation are gratefully acknowledged. The cooperation of the B. F. Goodrich Chemical Company and the Nixon Nitration Works in preparing a special sample of Geon 404 is appreciated.

INTRODUCTION

The effect of different degrees of crystallinity, residual stress and aging on creep of materials has not received wide attention. The only work on these topics for plastics which has been reported, as far as is known, are a study of the effect of aging on creep of cellulose acetate (1)[2] and a creep test method for determining the cracking sensitivity of polythelene polymers (2).

Of course, most engineering materials are not available with a wide range in degree of crystallinity. Metals, for example, are largely crystalline and contain only minute but important regions of amorphous material at the grain boundaries. Changes in structure with time are found in other engineering materials besides plastics at certain temperatures, such as steels at high temperatures. Residual stresses may be found in many applications of many materials. Usually residual stresses are relatively low in magnitude at temperatures where creep becomes significant in many engineering materials such as high temperature steels.

The effect of residual stresses in plastics has often been observed. Means of reducing these stresses and the theory and measurement of residual stresses for plastics have been considered by some investigators. Crazing of

---

[2] Numbers in parenthesis refer to the list of references appearing at the end of this paper.

plastics has been the subject of several investigations. For linear polymers, crazing has been described as a mechanical separation of polymer chains or groups of chains under the action of tensile stress, and starts in a region where the polymer chains are oriented at right angles to the tensile stress. References to these topics are given in a feature article in Applied Mechanics Reviews (3).

MATERIALS

Kel - F (monochlorotrifluoroethylene) of grade 300 was obtained in sheets of 1/8 in. thickness from the M. W. Kellogg Co. This grade was unplasticized and represents the highest molecular weight in the form of molding powder. The high density molding powder had a compression ratio of 2 to 1. The sheets were compression molded under a pressure of 2500 to 3000 psi. and at a temperature of 480 to 500° F. Immediately after pressing a sheet was quenched in water to produce the amorphous sample. Another sample was cooled between platens which had cold water circulating through them to produce the material with intermediate crystallinity (commercial practice). The crystalline form was obtained after pressing by dropping the temperature quickly by means of steam to 450° F, then cooling to room temperature in the press. It required 6 to 8 hours to cool.

The grade-C canvas laminate employed in these tests was the same from which test specimens were obtained for previous tests (4). A detailed description of the material is given in reference (4).

Geon 404 (polyvinyl chloride) was obtained as a sheet 9/16 inches thick from the Nixon Nitration Works. The formulation was designated VX-108 Natural and contained no plasticizer, 3.3 percent dibutal-tin diborate as a stabilizer and 0.5 percent stearic acid as a lubricant. The ingredients were mixed and blended at 280° F and calendered into sheets 0.02 in. thick on rolls having a temperature of 300° F. About 28 of these sheets were laminated together in a hydraulic press to form the final sheet and remove most of the residual strain resulting from the calendering. The sheets were subjected to a pressure of 280 psi at 315° F for about 30 min. and then cooled rapidly in the press.

SPECIMENS AND TEST PROCEDURE

The specimens and procedure employed for the creep tests were the same as previously described (4) except that the specimens for creep tests of Kel - F and Geon 404 had 4-inch gage length and the specimens of Kel - F were the thickness of the sheet instead of 5/32 in. thick.

RESULTS AND INTERPRETATION

Figure 1 shows the results of the creep tests of Kel - F in three different degrees of crystallization. It was observed that the greatest creep occurred in the amorphous and the least in the crystalline. Both the time-independent (elastic) strains and creep strains were much larger in the amorphous. The total strain at a stress of 2700 psi after 500 hours under a constant load was 3.3, 2.8, and 1.5 percent for the amorphous, intermediate, and crystalline respectively. Recovery following creep of the amorphous and intermediate samples is also shown in Fig. 1.

Creep of the crystalline material is shown for four different stresses in Fig. 1. It was observed that creep at the stress of 3600 psi was much greater than would be expected from the creep of the crystalline material at lower stresses.

Examination of the specimens disclosed that crazing occurred in the crystalline material at the stress of 3600 psi. It was not known whether crazing occurred in the lower stresses. Crazing was not observed in the material of intermediate crystallinity, but slight crazing was observed on one side of the amorphous sample.

This suggests that the larger creep in the sample tested at 3600 psi was probably due to the combination of

crazing plus creep. In order to determine at what stress crazing started in the crystalline material, a creep test was performed in which the stress was increased at intervals from 1610 to 1910 to 2210 to 2510 psi. It was found that no crazing occurred until about 19 hours after the load was increased to 2210 psi. At this time the strain increased from 1.06 to 1.27 per cent. From this time on, a count was taken of the number of transverse crazing marks per inch. In one inch the number of marks increased in succeeding 24 hour periods from 7 to 15 to 125 to 130.

Results of two creep tests of Geon 404 at 4000 psi are shown in Fig. 2, together with recovery following removal of load. One of these specimens was prepared from the sheet of material as received from the molder. The other specimen was prepared from the same sheet with the same orientation, after the sheet of material had been annealed to remove residual stresses. The material was annealed by placing it on a glass plate and heating in an electric oven at 275° F for 15 minutes and cooling slowly. Measurement of reference marks on the surface before and after the annealing indicated a shrinkage of 5.1 and 0.8 percent lengthwise and crosswise respectively of the original sheet (and direction of the calendaring). Greater shrinkage at the center of the sheet than at the surface was indicated by the concave appearance of the edges of the sheet.

As shown in Fig. 2 the as-received sample showed more creep than the annealed sample, about 1.48 and 1.39 percent creep respectively. Apparently the tensile residual stresses locked in the sample made the material more susceptible to the action producing creep.

Creep tests at two different stresses are shown in Fig.3 for a grade-C canvas laminate. The two tests shown at each stress were tested with an elapse of time of about 10 years between tests. When tested in August 1943 the laminate was about one month old. It has been stored at a constant temperature of 77° F and 50 percent relative humidity continuously since that time except during machining of specimens.

The results shown in Fig. 3 indicate that the creep resistance has improved with age. The creep at 500 hours was reduced with age from 1.17 to 0.99 percent at 5700 psi and 0.42 to 0.37 percent at 2850 psi.

REFERENCES

1. W. N. Findley, "Mechanical Tests of Cellulose Acetate-Part II on Creep", Proc. A.S.T.M. Vol. 42, p. 914, 1942.
2. W. C. Ellis and J. D. Cummings, "Creep Test Method for Determining Cracking Sensitivity of Polyethylene Polymers", A.S.T.M. Bulletin No. 178, p. Dec. 1951.
3. W. N. Findley, "Plastics: Their Mechanical Behavior and Testing", Applied Mechanics Reviews, Feb., 1953 pp 49-53.
4. W. N. Findley and W. J. Worley, "Mechanical Properties of Five Laminated Plastics", Tech. Note No. 1560, Natl. Adv. Committee for Aeronautics, Aug., 1948.

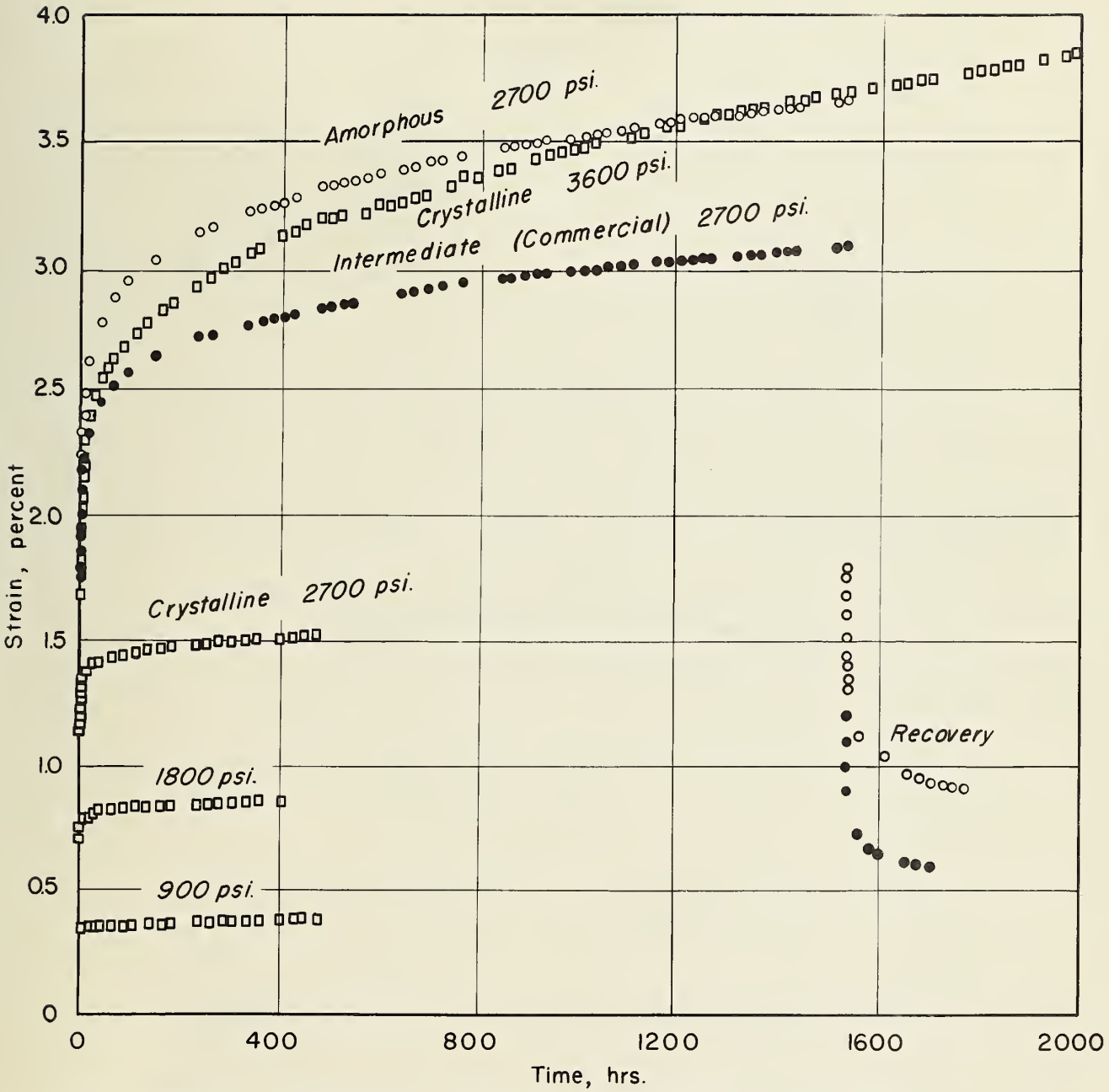

FIG. 1. CREEP CURVES FOR KEL-F AT DIFFERENT STRESSES AND THREE DIFFERENT DEGREES OF CRYSTALLIZATION; TEMPERATURE 77° F, RELATIVE HUMIDITY 50%

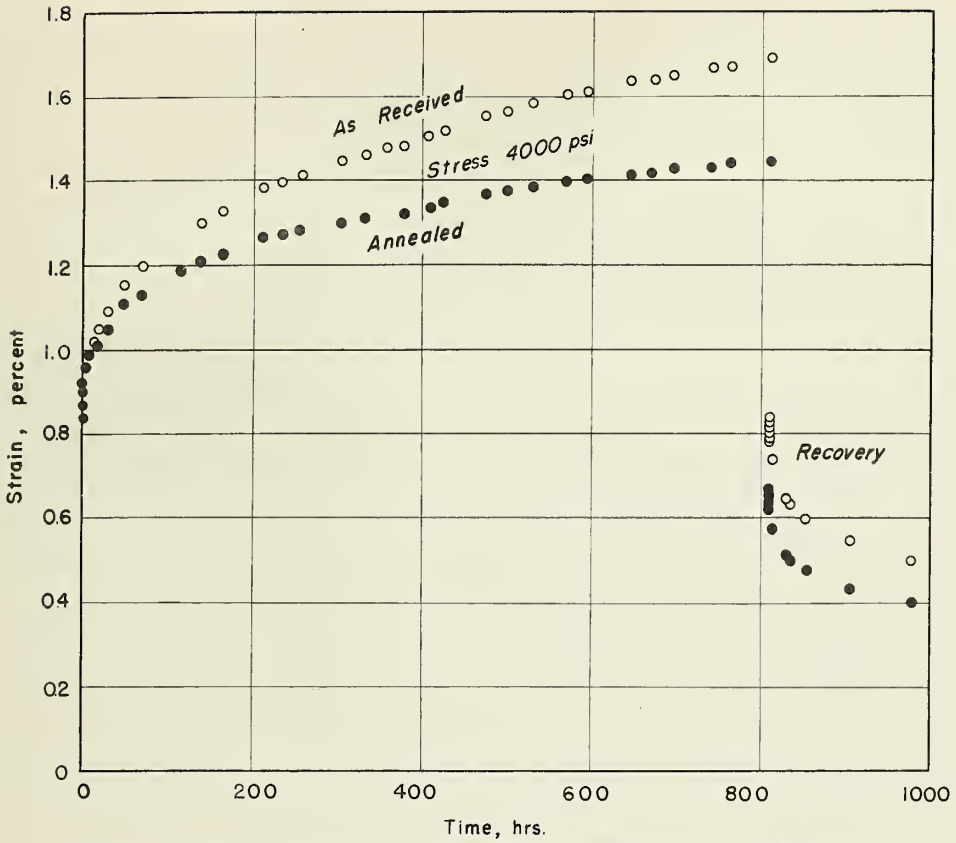

FIG. 2. CREEP CURVES FOR GEON 404 BEFORE AND AFTER ANNEALING TO REMOVE RESIDUAL STRESSES; TEMPERATURE 77°F, RELATIVE HUMIDITY 50%

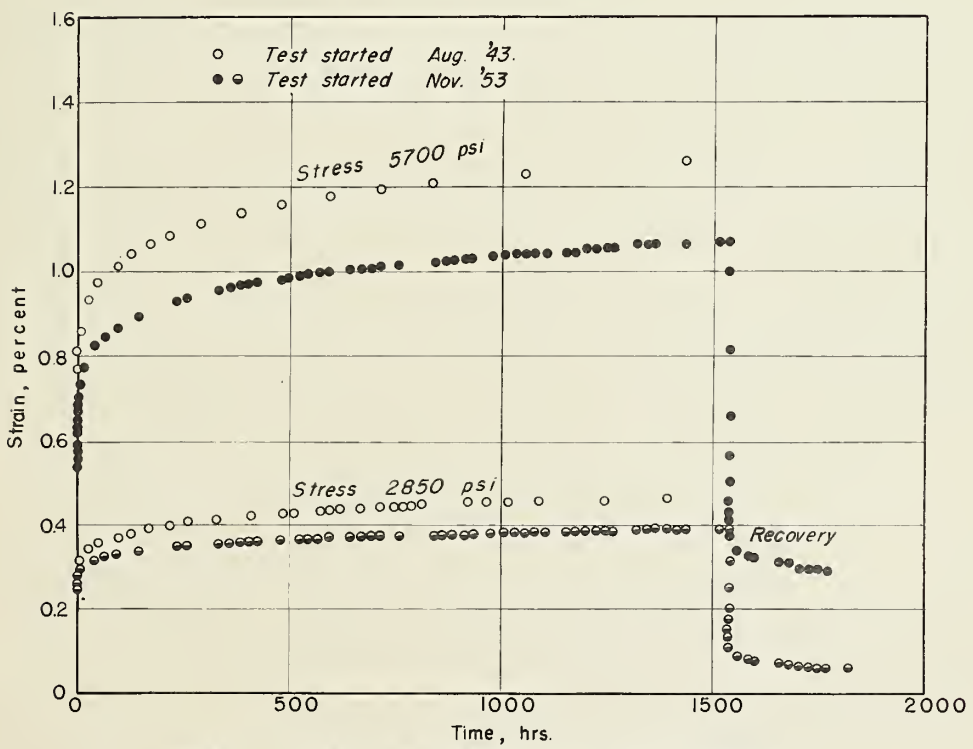

FIG. 3 CREEP CURVES FOR GRADE C CANVAS LAMINATE TEMPERATURE 77°F, RELATIVE HUMIDITY 50%